

Modelling of response scenarios of Tien Shan glacierised catchments to climate change

A thesis submitted
to the School of Forest Science and Resource Management
Sustainable Resource Management Program
in partial fulfilments of the requirements for the degree of
Master of Science

by

Thomas Nesgaard, B.Sc.

Advisor: Dr. Annette Menzel

November, 2004
Technische Universität München

Contents

Contents	I
Content of Figures	II
Content of Tables	IV
Acknowledgments	V
Abstract	1
1. Introduction	2
1.1 Problem	2
1.2 Aim	4
1.3 Benefit	4
2. Study Area	5
2.1 Geographical location, political setting of the Tien Shan	5
2.2 Climate of the Tien Shan	6
3. Observed and expected climate change	11
3.1 Observed	11
3.2 Scenarios	11
4. Methodology and data	13
4.1 Procedure of model application	13
4.1.1 Placing of the HBV3 ETH9 and OEZ model within the wider model context	13
4.1.2 Applying the HBV model	15
4.1.3 Applying the OEZ model	19
4.2 Comparison of models	23
4.3 Data Series and data preparation	24
4.4 Plausibility tests of Calibration	27
4.4.1 Goodness of fit for HBV calibration	27
4.4.2 Goodness of fit for OEZ calibration	28
4.5 Validation	34
4.5.1 Validation of HBV calibration for Abramov	34
4.5.2 Validation of OEZ calibration for Abramov	34
5. Results and Discussion	36
5.1 Simulation of current conditions	36
5.2 Simulation of future scenarios	39
5.2.1 Logical progression of OEZ runoff curve change	39
5.2.2 Comparison of HBV and OEZ runoff scenarios for 50% glaciation remaining	42
5.2.3 Comparison of HBV and OEZ runoff scenarios for 0% glaciation remaining	45
5.2.4 Summary	48
6. Conclusion	50
References	52

Content of Figures

Fig 1.1	Map of hydrological significance of mountains to surrounding lowlands (Viviroli, 2001)	3
Fig 2.1:	Location and climate zones of the catchments being studied within the Tien Shan	5
Fig 2.2.1	Oigaing catchment: area-elevation and aspect distribution of total and glaciated areas	7
Fig 2.2.2	Ala Archa catchment: area-elevation and aspect distribution of total and glaciated areas	7
Fig 2.2.3	Abramov catchment: area-elevation and aspect distribution of total and glaciated areas	7
Fig 2.2.4	Oigaing catchment: mean temperature, precipitation and runoff	8
Fig 2.2.5	Ala Archa catchment: mean temperature, precipitation and runoff	8
Fig 2.2.6	Abramov catchment: mean temperature, precipitation and runoff	8
Fig 4.1.1	Placing of HBV and OEZ models within wider model context	13
Fig 4.1.2	Structure of the HBV model	15
Fig 4.4.3	Oigaing: OEZ Accumulation / ablation curves & specific mass balance for calibration (CO ₂ x 1)	30
Fig 4.4.4	Ala Archa: OEZ Accumulation / ablation curves & specific mass balance for calibration (CO ₂ x 1)	30
Fig 4.4.5	Abramov: OEZ Accumulation / ablation curves & specific mass balance for calibration (CO ₂ x 1)	30
Fig 4.4.6	Map of mass balance regions of the Tien Shan as defined by ELA	32
Fig 5.1.2	Oigaing current climate: Comparison HBV & OEZ runoff simulations to meas. monthly means	38
Fig 5.1.3	Ala Archa current climate: Comparison HBV & OEZ runoff simulations to meas. monthly means	38
Fig 5.1.4	Abramov current climate: Comparison HBV & OEZ runoff simulations to meas. monthly means	38
Fig 5.2.1	Oigaing: OEZ progression of runoff curves as glaciated area is reduced	39
Fig 5.2.2	Ala Archa: OEZ progression of runoff curves as glaciated area is reduced	40
Fig 5.2.3	Abramov: OEZ progression of runoff curves as glaciated area is reduced	41
Fig 5.2.4	Oigaing: HBV & OEZ Runoff scenarios for CO ₂ x 2, 50% of current glaciation remaining	42
Fig 5.2.5	Ala Archa: HBV & OEZ Runoff scenarios for CO ₂ x 2, 50% of current glaciation remaining	44
Fig 5.2.6	Abramov: HBV & OEZ Runoff scenarios for CO ₂ x 2, 50% of current glaciation remaining	44
Fig 5.2.7	Oigaing: HBV & OEZ Runoff scenarios for CO ₂ x 2, 0% glaciation	45

Fig 5.2.8	Ala Archa: HBV & OEZ Runoff scenarios for CO2 x 2, 0% glaciation	46
Fig 5.2.9	Abramov: HBV & OEZ Runoff scenarios for CO2 x 2, 0% glaciation	47
Fig A1	Oigaing reference meteorological station: full precipitation series (data source: CADB)	55
Fig A2	Oigaing reference meteorological station: full temperature series (data source: CADB)	55
Fig A3	Ala Archa reference meteorological station: full precipitation series (data source: CADB)	56
Fig A4	Ala Archa reference meteorological station: full temperature series (data source: CADB)	56
Fig A5	Abramov reference meteorological station: full precipitation series (data source: Abramov Glacier Data Reference Book)	57
Fig A6	Abramov reference meteorological station: full temperature series (data source: Abramov Glacier Data Reference Book)	57
Fig D1	Effect of redistribution factor on runoff Scenarios	64
Fig D2	Sensitivity of OEZ scenario for Abramov with complete loss of glaciation to groundwater readjustment	64
Fig F1	Oigaing: Meteorological context of HBV & OEZ runoff curves	66
Fig F3	Ala Archa: Meteorological context of HBV & OEZ runoff curves	67
Fig F5	Abramov: Meteorological context of HBV & OEZ runoff curves	68
Fig G1	Oigaing: Meteorological context of HBV & OEZ runoff curves	69
Fig G3	Ala Archa: Meteorological context of HBV & OEZ runoff curves	70
Fig G5	Abramov: Meteorological context of HBV & OEZ runoff curves	71

Content of Tables

Table 2.2.7	Comparison of selected hydrometeorological features using full data series means	9
Table 3.2.1	GCM Temperature & Precipitation change predictions for CO ₂ x 2 for part of Tien Shan	11
Table 3.2.2	“GISS” GCM results for ΔT and ΔP for CO ₂ x 2	12
Table 4.3.1	Available data	24
Table 4.4.1	Nash-Sutcliffe coefficient (R^2) values for HBV simulation of measured runoff	27
Table 4.4.2	Degree-day factors (mm w.e. K ⁻¹ d ⁻¹) resulting from OEZ calibrations	28
Table 4.4.6	Effect of redistribution factor on ELA and AAR	31
Table 4.5.1	Comparison of R^2 values for Abramov calibration and validation	34
Table 4.5.2	Discrepancies between measured and simulated runoff in mm for calibrations and validations	35
Table 4.5.3	Mean measured temperature and precipitation values for OEZ calibration compared to means for first and second validation decades, and the differences between them	35
Table 5.1.1	Annual water balance values produced by OEZ and HBV calibrations	37
Table B1	Input data	58
Table B2	Optimisation parameters	60
Table B3	Future scenario adaption and prediction power	61
Table C1	Degree-day factors (mm w.e. K ⁻¹ d ⁻¹) for Oigaing: HBV3 ETH9 matrix.	62
Table C2	Degree-day factors (mm w.e. K ⁻¹ d ⁻¹) for Ala Archa: HBV3 ETH9 matrix.	62
Table C3	Degree-day factors (mm w.e. K ⁻¹ d ⁻¹) for Abramov: HBV3 ETH9 matrix.	62
Table E1	Oigaing: OEZ Simulated monthly runoff (mm) for CO ₂ x 2 climate change, with 100%, 50% and 0% of current glaciation extent remaining	65
Table E2	Ala Archa: OEZ Simulated monthly runoff (mm) for CO ₂ x 2 climate change, with 100%, 50% and 0% of current glaciation extent remaining	65
Table E3	Abramov: OEZ Simulated monthly runoff (mm) for CO ₂ x 2 climate change, with 100%, 50% and 0% of current glaciation extent remaining	65
Table F2	Oigaing: Data displayed by Fig F1	66
Table F4	Ala Archa: Data displayed by Fig F3	67
Table F6	Abramov: Data displayed by Fig F5	68
Table G2	Oigaing: Data displayed by Fig G1	69
Table G4	Ala Archa: Data displayed by Fig G3	70
Table G6	Abramov: Data displayed by Fig F5	71

Acknowledgments

My first thanks go to Dr. Wilfried Hagg, who provided invaluable coaching throughout the progress of the thesis. Dr. Hagg did so in the framework of the DfG-funded project "Aral Sea" (BR1622/6). I wish to thank Dr. Ludwig Braun for making this thesis possible by providing guidance and encouragement from the beginning, and by making the resources of the Commission for Glaciology of the Bavarian Academy of Sciences available to me. I am grateful for important impulses from Dr. Annette Menzel and Prof. Dr. Michael Kuhn.

My heartfelt thanks go to my dear wife Carolin, for her patience and support throughout the course of this work. I am also indebted to my parents-in-law for their support during the final phase.

Abstract

The arid lowlands of Central Asia are highly dependent on the water supplied by the Tien Shan mountains. Snow and ice storage make large contributions to current runoff, particularly in summer. A runoff model with a monthly time-step was used to produce runoff scenarios for three glaciated catchments of the Tien Shan mountains for predicted climate change caused by the doubling of atmospheric CO₂, which is expected to take effect between 2050 and 2075. Scenario runs were produced for a 50% reduction of glaciation extent compared to current area, and for complete loss of glaciation. Results were compared to studies of runoff change for the same catchments carried out using a runoff model with a daily time-step. The application of the monthly time-step model was successful for two out of the three catchments. Agreement with results obtained using the daily time-step model was best for runs based on 50% glaciation loss, where both models predict an increase in spring and summer runoff compared to current levels. Scenarios for complete loss of glaciation predict an increase in spring runoff levels, followed by lower runoff levels for July and August. Model predictions differ concerning the degree of reduction of late summer runoff. These scenarios are sensitive to model simulation of basin precipitation, as well as to reduction of glaciation extent. The monthly time-step model is suitable for the study of runoff change in the Tien Shan, adding valuable insight to scenarios produced using the daily time-step model.

1. Introduction

1.1 Problem

Proper, sustainable water resource management is essential to human society. How best to achieve robust, sustainable management of water resources is a complex issue. Its success or failure is critical in regions where water supply already struggles to satisfy demand, and this is further heightened where predicted climate change is expected to affect water supply negatively. This may be either through reduction of volume, or change of timing and duration of availability throughout the year, or both. The arid lowlands around the Tien Shan mountains of Central Asia is one such region (Klötzli 1996).

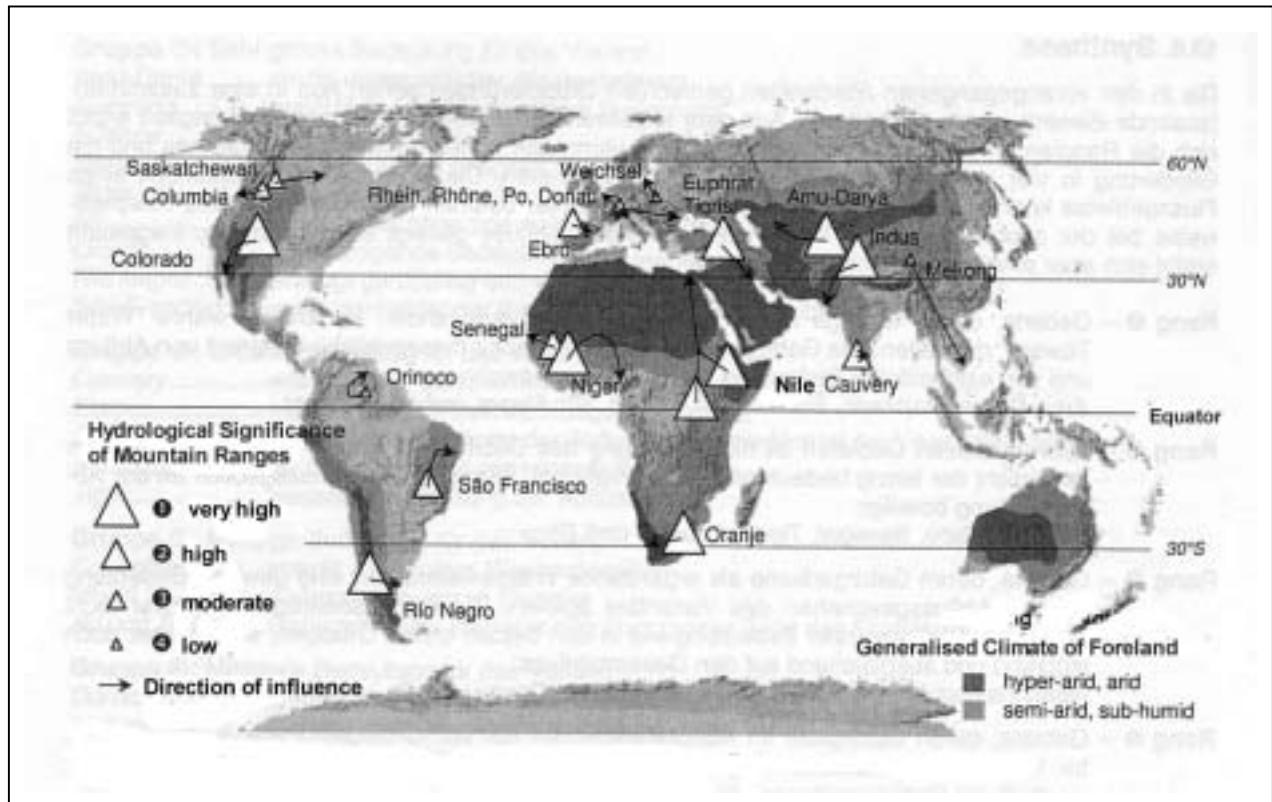
Present water supply from the Tien Shan to the surrounding lowlands, in terms of both volume, timing (intra-annual variability), and inter-annual consistency, is favourably influenced by the presence of glaciers.

However, the observed retreat of most Tien Shan glaciers since the little ice age (Chaohai and Tianding, 1992) is marked, and expected to continue as a result of the consequences of measured and predicted global warming. A significant reduction in, or complete loss of, water released from glaciers can be expected to further heighten water distribution conflicts which are already plaguing the region.

The complex political, social and economic aspects and problems of how the water currently available is used and distributed have been analysed and discussed in depth by Klötzli (1996).

The hydrological importance of the Central Asian mountains (Tien Shan, Pamir) for the surrounding lowlands, compared to other mountain chains, is illustrated by the map in *fig 1.1* below (*see triangle for "Amu-Darya"*).

Fig 1.1 Map of hydrological significance of mountains to surrounding lowlands (Viviroli, 2001)
 Note: The names of the rivers are in German, and have not been translated



1.2 Aim

This thesis deals exclusively with the estimation of the amount and timing of water available for use. Other aspects of water resource management, such as the collection, storage, use, and disposal of available water are not discussed here.

The aim is to compare and contrast results of two hydrological models - designed to enable “educated guesses” at how the availability of water from glacierised catchments of the Tien Shan mountains of Central Asia may change under climate conditions predicted for the doubling of CO₂ in the atmosphere, which is expected for 2050 – 2075 (KazNIIMOSK, 1999).

The first model, the HBV3 ETH9, is a linear reservoir model with a daily time-step. The model was developed at the Swedish Meteorological and Hydrological Institute (Bergström et al. 1973; Bergström, 1992). It was developed further at the ETH Zürich (Braun and Renner, 1992, Hottel et al., 1993), and again at the Commission for Glaciology of the Bavarian Academy of Sciences (KfG 1999). This model has already been applied to the three catchments which comprise the study area, by Hagg (2003), and Hagg et al. (2003). For the sake of readability, the model shall hereafter simply be referred to as the “HBV” model.

The second model, the OEZ model, is a water balance equation model with a monthly time-step. It was developed at the Institute for Meteorology and Geophysics of the University of Innsbruck (Kuhn et al., 1982; Kuhn and Pellett, 1989; Kuhn and Batlogg, 1998, 1999). I have applied this model to the three catchments in a way which permits comparison of runoff predictions of the two models.

1.3 Benefit

Attempting to predict how water availability will change in the future is important for the other aspects of water resource use: if availability changes (in particular if it lessens), how water is used, and possibly also how it is disposed of or re-used, may have to change. A significant and concentrated increase of runoff for a given period may also require changes in flood management.

The more timely the warning, the greater the chances are to prepare for such eventualities. The more a region struggles to meet water demand, as is the case with Central Asia, the more pressing the need for proper planning. The more models which are applied to a given issue, the better the picture of possible scenarios which need to be prepared for. This can be regarded as a start on an “ensemble” of models applied to the problem by hopefully enabling a new perspective on the HBV predictions of future runoff.

2. Study Area

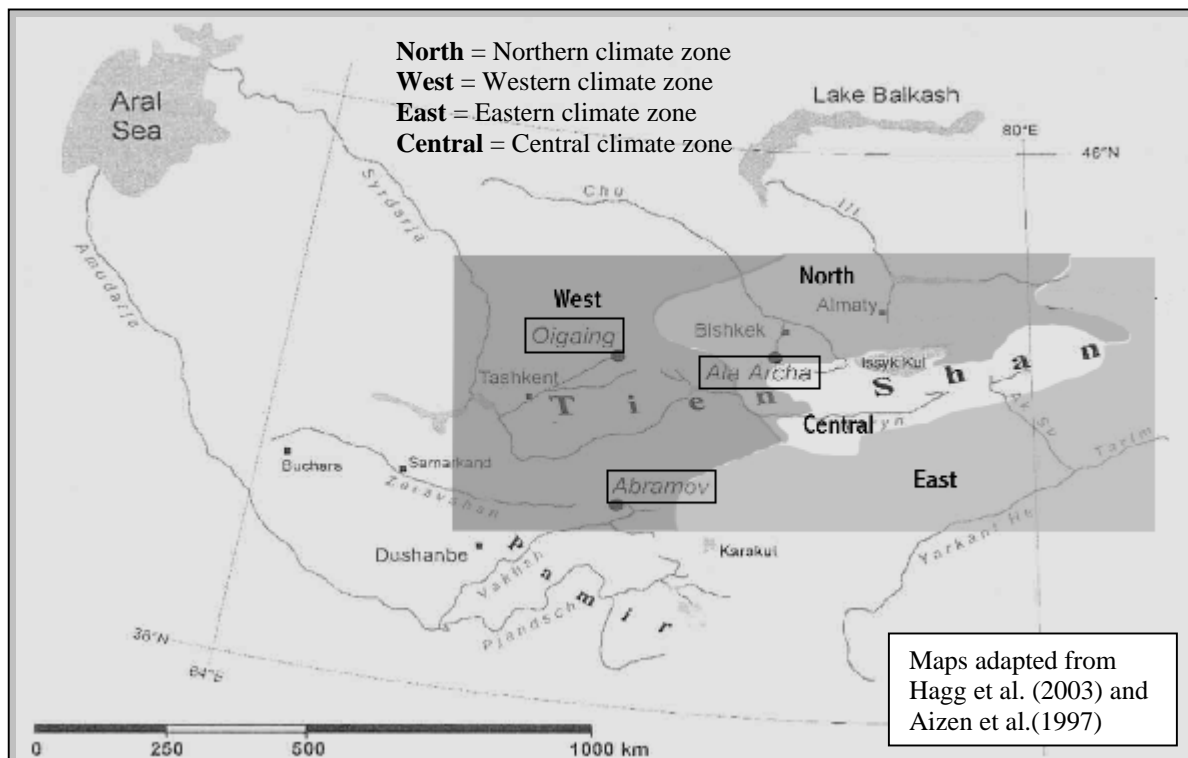
2.1 Geographical location, political setting of the Tien Shan

The Tien Shan mountains of central Asia stretch from 40°N to 50°N, and extend 2450 km from 67°E to 95°E (Chaohai and Tianding, 1992). The Tien Shan lie within the political boundaries of The People's Republic of China, Kazakhstan, Kyrgyzstan and Uzbekistan. The approximate number, area, and volume of glaciers are: 16 396, 16 427 km², 1369 km³, respectively (Chaohai and Tianding, 1992).

The map in *fig 2.1* below shows that the three catchments studied here lie in the North-central Tien Shan (Ala Archa), North-West Tien Shan (Oigaing) and Pamiro-Alay (Abramov). In the case of the latter, the range in which the catchment is situated is classed by some authors as part of the Pamir, which border the Tien Shan to the South, and by others as part of the Tien Shan. Climate zones are explained in section 2.2.

The three catchments being studied form parts of the Amu Darja (in the case of Abramov), Syr Darja (Oigaing) and Chu (Ala Archa) hydrological basins, all of which belong to the closed Aralo-Caspian basin, and whose lower boundary is formed by the Aral Sea. The Amu Darja and Syr Darja rivers are the major sources of water for the Aral Sea, and the drying up of the Aral Sea in the latter half of the 20th century is well publicised and the most widely known consequence of over-use of water resources stemming from the Tien Shan and the Pamir mountains of Central Asia.

Fig 2.1: Location and climate zones of the catchments being studied within the Tien Shan.



2.2 Climate of the Tien Shan

The climate of the Tien Shan can be generally described as continental, though the degree of continentality increases from a minimum in the North-West to a maximum in the East, and also increases southwards and towards the interior (Hagg, 2003; Aizen et al., 1997). Aizen et al. (1997) identify three main climate zones within the Tien Shan: West, North, and Central and East (see *fig 2.1* above). The western zone, encompassing both Oigaing and the Pamiro-Alay range in which Abramov is located, is only weakly affected by the Siberian anticyclone in winter, but moderately influenced by the southwestern cyclonic circulation that brings warm, moist air masses to the region. The region thus receives up to 50 mm of precipitation per month in autumn and winter. The precipitation maximum is in spring (March to June), with up to 80 mm precipitation falling per month (Aizen et al., 1997). Compared to Oigaing, Abramov is less affected by Atlantic air masses (Hagg et al., 2003), due to being further away from the edge of the mountains and so is deprived of some precipitation by the more peripheral ranges. The northern zone, in which the Ala Archa basin is located, is under strong influence of the Siberian anticyclone in winter, which decreases the quantity of winter precipitation. Maximum precipitation is observed in spring and summer, with up to 120 mm of precipitation per month (Aizen et al., 1997). The high ranges of the eastern and central zones of the Tien Shan prevent the entrance of moisture, and so winter precipitation is very low. Convection produces a precipitation maximum in summer, which can reach 130 mm per month. Thus as one moves from the North-West towards the East and South, total precipitation decreases, and this is most marked in winter (Hagg, 2003). For glaciers, this means that as one moves from the edges of the mountains to the interior, glacier winter balance makes a smaller contribution to annual mass balance, total accumulation and ablation are gradually reduced, and the mass exchange time increases (Chaohai and Tianding, 1992).

The climatic setting of each catchment is determined both by their location within the Tien Shan (see above), and also their aspect, elevation, elevation range, and area-elevation distribution. The thus determined temperature and precipitation patterns then dictate the hydrological nature of the catchment due to resultant glaciation and other factors such as groundwater bodies. *Figs 2.2.1 to 2.2.3* on page 7 below show the area-elevation distribution of the catchments, as well as the aspect distribution of the total and glaciated areas. *Figs 2.2.4 to 2.2.6* on page 8 show mean temperature, precipitation, and runoff as recorded in each of the catchments. The abbreviation "AGDRB" stands for "Abramov Glacier Data Reference Book" (1996), and "CADB" stands for "Central Asia Data Base". The means presented are for the periods used for water balance simulation by both models, which also correspond to the OEZ calibration period. In the case of precipitation and temperature data, the series used for modelling do not always correspond to the full data series available. For a comparison of the full data series means and those of the modelling period see *figs A1 to A6* in appendix A on pages 55 to 57.

Fig 2.2.1 Oigaiing catchment: area-elevation and aspect distribution of total and glaciated areas

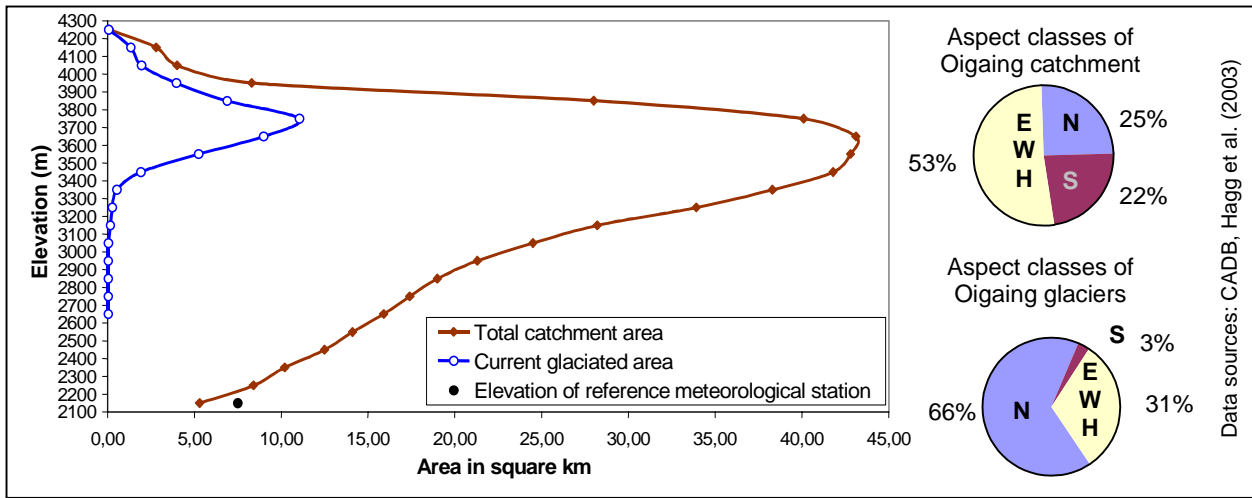


Fig 2.2.2 Ala Archa catchment: area-elevation and aspect distribution of total and glaciated areas

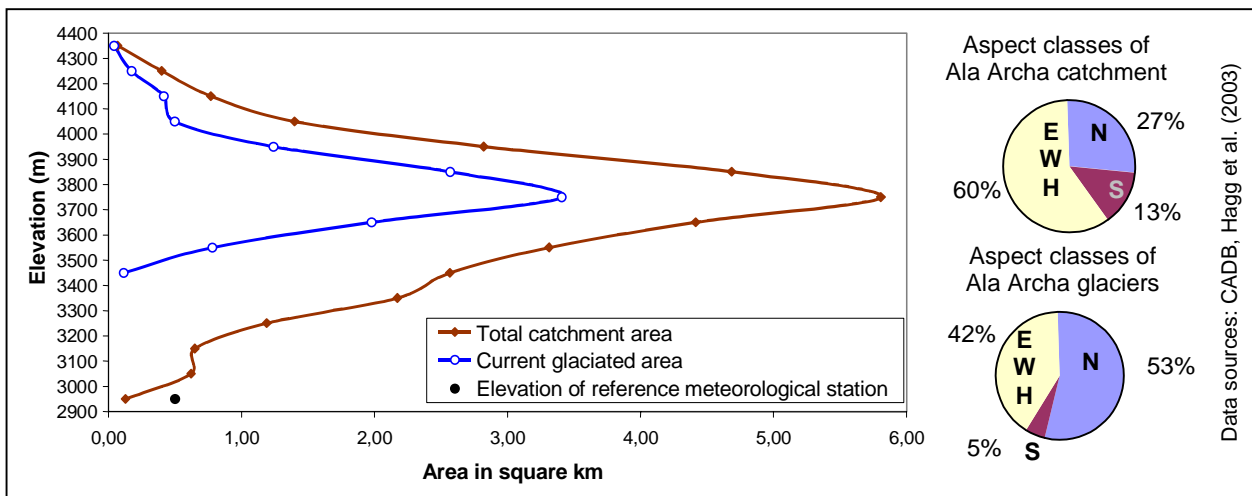


Fig 2.2.3 Abramov catchment: area-elevation and aspect distribution of total and glaciated areas

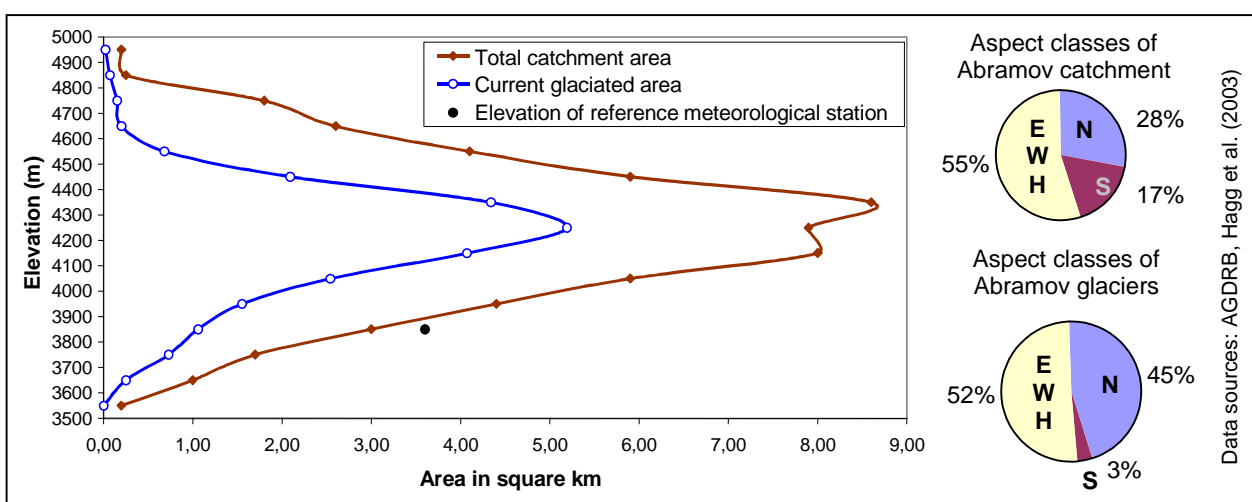


Fig 2.2.4 Oigang catchment: mean temperature, precipitation and runoff

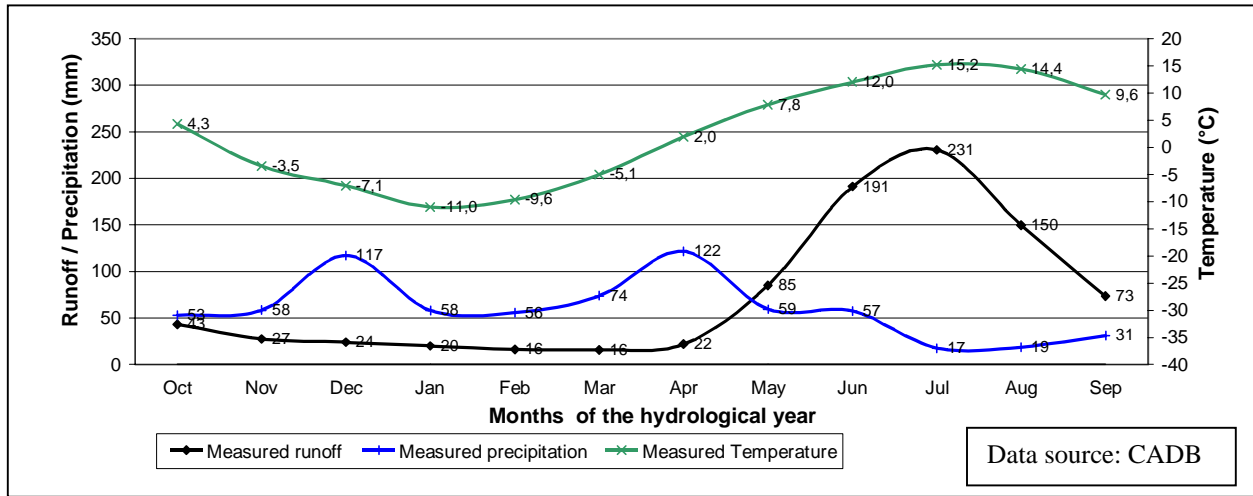


Fig 2.2.5 Ala Archa catchment: mean temperature, precipitation and runoff

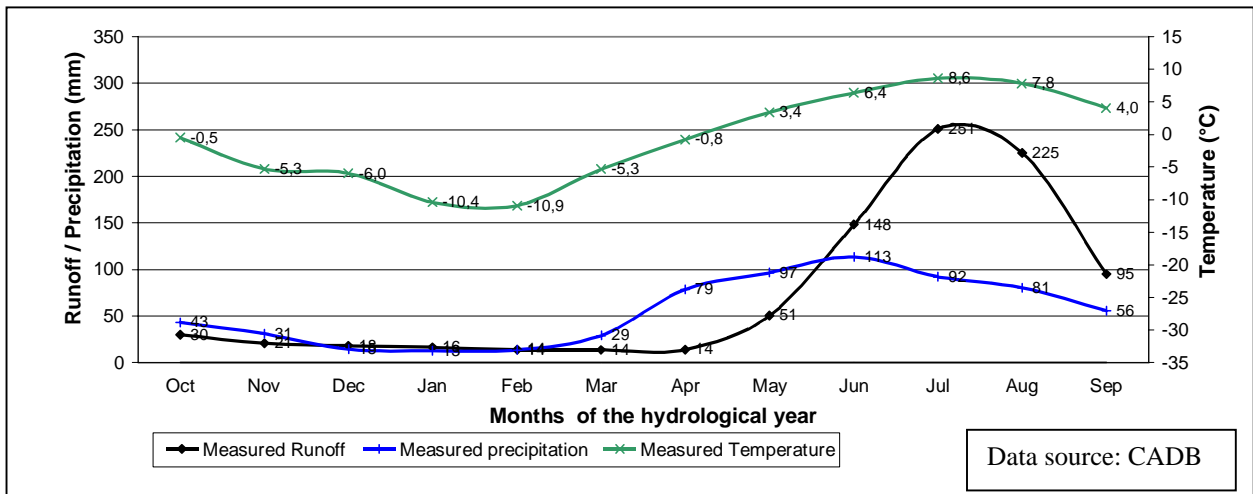


Fig 2.2.6 Abramov catchment: mean temperature, precipitation and runoff

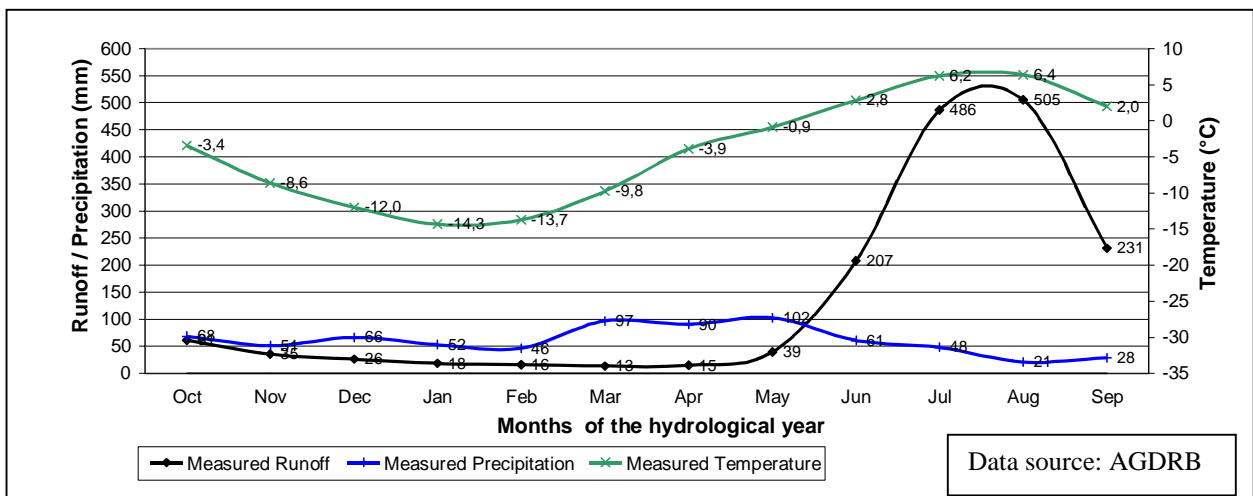


Table 2.2.7 Comparison of selected hydrometeorological features using full data series means

	Catchment (reference meteorological station altitude)		
	Oigaing (2140 m)	Ala Archa (2945 m)	Abramov (3837 m)
Topography			
Elevation range	2200 m	1500 m	1500 m
Min & max elevation	2100 m; 4300 m	2900 m; 4400 m	3500 m; 5000 m
Median elevation total area	3600 – 3700 m	3700 – 3800 m	4300 – 4400 m
Median elevation glaciers	3700 – 3800 m	3700 – 3800 m	4200 – 4300 m
Precipitation			
Minimum: timing	Jul, Aug, Sep	Dec, Jan, Feb	Aug, Sep
Maximum: timing	Dec & Apr	May, Jun	Mar, Apr, May
Annual Total	721 mm	710 mm	744 mm
Temperature			
Range of monthly mean	25,6°C	19,3°C	20,7°C
Months with mean above 0°C	Apr – Oct	May – Sep	Jun – Sep
Runoff			
Annual total	899 mm	897 mm	1653 mm
Peak: magnitude, timing	231 mm, Jul	251 mm, Jul	505 mm, Aug

As reflected by *Figs 2.2.1 to 2.2.6* and table 2.2.7, Oigaing's location in the NW Tien Shan makes it the least continental of the three. For example, Oigaing's mean precipitation for the mid-winter months from December to February is higher than that of both Ala Archa and Abramov (*see figs 2.2.4 to 2.2.6*), and December is in fact host to one of the precipitation maxima. This is in keeping with the fact that the NW Tien Shan are least affected by the Siberian anticyclone. Its precipitation maxima are in December and April, and the minimum in July, August and September. That Oigaing's temperature range is the greatest of the three records is due to the fact that the meteorological station is located at the lowest altitude and has the highest mean summer temperatures. Colder winter means than Ala Archa are most probably due to the influence of inversions. Current hydrometeorological behaviour can be classed as predominantly pluvo-nival, which is to be expected in the light of the large elevation range reaching down to 2100 m. The predominance of snowmelt can be seen in that, although like Ala Archa, peak runoff is typically recorded in July, the drop in runoff from July to August is noticeably steeper than for Ala Archa, where ice melt in August keeps the runoff curve high, with a marked drop in runoff only from August to September.

The Ala Archa basin lies in the central part of the Northern Tien Shan, and is thus located in the moderately humid belt of the Northern Tien Shan (Chaohai and Tianding, 1992). That the region receives less moisture than Oigaing, however, is indicated by the fact that the reference meteorological station records less mean annual precipitation at 2964 m than Oigaing at 2130 m. The growing influence of the Siberian anticyclone manifests itself in that during the winter half-year (October to April), Oigaing receives more than double the amount of precipitation Ala Archa does, whereas the opposite is true of the summer half-year (May to September). Ala Archa's precipitation maximum is in May and June, which is in keeping with the fact that as one moves from West to East along the northern periphery of the Tien Shan, the precipitation maximum shifts from

spring to summer as continentality increases (Aizen and Aizen, 1994). The precipitation minimum is typically during mid-winter (December, January, February). As mentioned above, compared to Oigaing with approximately 9% glaciation, Ala Archa with 33% glaciation has a runoff curve much more dominated by ice melt. Abramov's location away from the edge of the mountains is reflected by the fact that annual precipitation is similar to Oigaing's, but measured 1700 m higher up. The maximum during March to May and the marked minimum during August and September is typical of the western climate region. The runoff regime, like Ala Archa, is dominated by ice melt, but Abramov's annual and peak runoff values are approximately twice as high. This difference may partly be due to differences in basin precipitation, but raises also the question of whether Abramov's runoff as measured benefits from a greater contribution from glacier storage (i.e. greater negativity of mass balance) than Ala Archa (see *table 5.1.1 on page 37*).

3. Observed and expected climate change

3.1 Observed

The temperature and precipitation scenarios upon which the runoff scenarios of Hagg (2003), and therefore also of this study, are based, are taken from the following study:

KazNIIMOSK (1999): Climate change and a defence strategy against mudflows and snow avalanches. National report on the impact and adaptation assessment for the mountain region of South and Southeast Kazakhstan and the Kazakh part of the Caspian Sea coastal sector, Netherlands climate change studies assistance programme, Kazakhstan climate change study Vol. 1.

According to the KazNIIMOSK (1999) findings, observed mean annual temperature changes for the Tien Shan over the past 30 – 60 years, for which instrumental observation data are available, range from 0.1°C – 0.2°C per decade. Warming in November and December is significantly stronger, in the range of 0.3°C – 0.6°C per decade, and this is the main contributor to the warming observed for the whole winter season. No changes were observed for the summer season in most cases (KazNIIMOSK, 1999).

Recorded trends in precipitation are weak and not statistically significant, though mostly they are slightly negative, and slightly more marked in summer than in winter (KazNIIMOSK, 1999).

3.2 Scenarios

The KazNIIMOSK (1999) study considered the results of five General Circulation Models (GCMs) whose task it was to predict climate change for a doubling of the level of atmospheric CO₂ compared to current levels, which is expected to occur between 2050 and 2075. The GCMs used were the GFDL, GFDL-T, CCC, UKMO, and GISS models. The results relevant to this study are those for the mountains stations of the little Almatinka river basin, Almaty, BAL and Esik. *Table 3.2.1* below presents part of these GCM results, and is an adaptation of table A.3.2 of the KazNIIMOSK (1999) report.

Table 3.2.1: GCM Temperature & Precipitation change predictions for CO₂ x 2 for part of Tien Shan

	GFDL		GISS		UKMO		CCC		GFDL (10 dec.)	
	ΔT(°C)	ΔP(%)	ΔT(°C)	ΔP(%)	ΔT(°C)	ΔP(%)	ΔT(°C)	ΔP(%)	ΔT(°C)	ΔP(%)
Year	+3.7	+40	+4.2	+17	+5.9	-8	+7.1	-9	+4.8	-1
Summer	+4.2	+62	+3.9	+8	+7.2	-28	+6.9	-32	+5.4	-17
Winter	+3.2	+19	+4.5	+27	+4.7	+12	+7.4	+15	+4.2	+14

As *table 3.2.1* above shows, a significant increase in temperature is predicted by all five models, but changes in precipitation are inconclusive. This is in keeping with the fact that observed precipitation trends are not statistically significant.

Of these five, the GISS model was selected for the GCM-based scenario for analysis of climate change impact on snow cover and avalanche activity in the KazNIIMOSK (1999) study. The reasons were that the GISS model was best at describing current climate conditions, in that the difference between measured and simulated CO₂ x 1 temperature was close to 0, and the precipitation ratio was close to 1 for most months. In contrast, for example, the UKMO and CCC models produced temperatures for CO₂ x 1 which differed from those observed by 5°C and 23°C, respectively. The CCC and GFDL models produced precipitation ratios of 2 and 9, respectively (KazNIIMOSK, 1999). Selecting the model which is best able to replicate current conditions is based on the assumption that it will therefore also be best at producing future scenarios, though there is no guarantee that this is the case (KazNIIMOSK, 1999). It is also convenient that the GISS results do not lie at the extremities of predicted temperature and precipitation change. *Table 3.2.2* below shows the ΔT and ΔP values that the GISS model produces for each month of the year, and which have been used as input for climate change in both the OEZ and HBV models.

Table 3.2.2: "GISS" GCM results for ΔT and ΔP for CO₂ x 2

	Jan	Feb	Mar	Apr	May	Jun	Jul	Aug	Sep	Oct	Nov	Dec
$\Delta T(^{\circ}C)$	+4.2	+5.7	+3.6	+4.6	+3.1	+3.2	+3.4	+4.7	+4.4	+4.5	+3.4	+5.5
$\Delta P(\%)$	+42	+29	+13	+25	+21	+16	-6	-19	+17	+20	+3	+47

4. Methodology and data

4.1 Procedure of model application

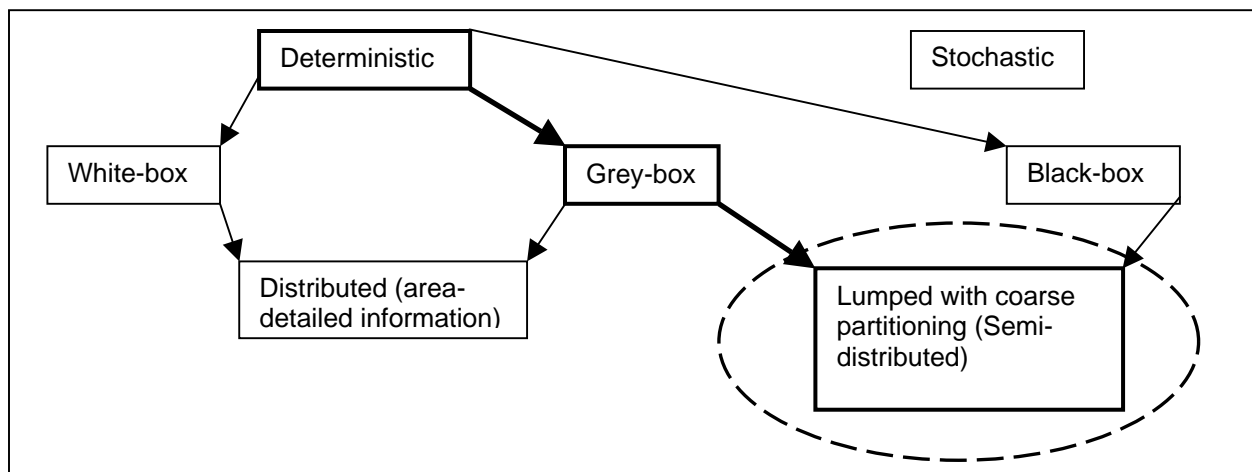
The reasons for adding the OEZ model to this study are twofold. As mentioned above, the greater the "ensemble" of models applied to a problem concerning future runoff, the better the picture of possible scenarios that can be made, and this is at least a beginning. The results of the OEZ model ought to provide a new perspective on those of the HBV model. Secondly, due to the fact that the OEZ model has a temporal resolution of monthly time-steps, as opposed to the daily time-step of the HBV model (in both cases concerning data input & model output), it was hoped that, should it perform convincingly, it may open up further Tien Shan catchments for study, which are not available for models requiring daily input data.

In this chapter, the methods for applying the models to the study of glacierised mountain catchments are described in section 4.1. The models are compared and contrasted in section 4.2 (*tables B1 to B3* in appendix B on pages 58 to 61 present this information in tabular form). In sections 4.3 to 4.6, aspects of the procedures of model application to the Tien Shan catchments which are relevant to the runoff scenarios are presented and discussed.

4.1.1 Placing of the HBV3 ETH9 and OEZ model within the wider model context

As *fig 4.1.1* below shows, both the HBV model and OEZ models belong to the same sub-group of models. These models are classed as grey-box, or conceptual, because they describe hydrological processes with simplified and combined physical formulae (Bergström, 1991).

Fig 4.1.1 Placing of HBV and OEZ models within wider model context



Conceptual models are most appropriate for the task because:

- (a) It is both cumbersome and expensive to set up a dense enough network of measurements to enable the use of hydrodynamic models (also called “physical”, i.e. those driven by fundamental laws). Such dense measurement networks are rarely, if ever, available, and for this reason hydrodynamic models have limited application potential at catchment scale.
- (b) Black box models are of no interest / use, because their inner workings bear no relation to reality. It is desirable / advantageous that, for example, the values for snow water equivalent in the models reflect the real world situation.

They are lumped with coarse vertical spatial partitioning, also known as semi-distributed, which is appropriate for the following reasons:

- (a) Vertical distribution is essential, as elevation is a key factor in the interaction of temperature and precipitation, and resultant storage and release of water.
- (b) Horizontal variation of runoff within the catchments is not considered in this study, only net runoff (output), as this is what is relevant for predictions of runoff scenarios under future climates – with a view to water availability for the populations of the Tien Shan and surrounding lowlands.

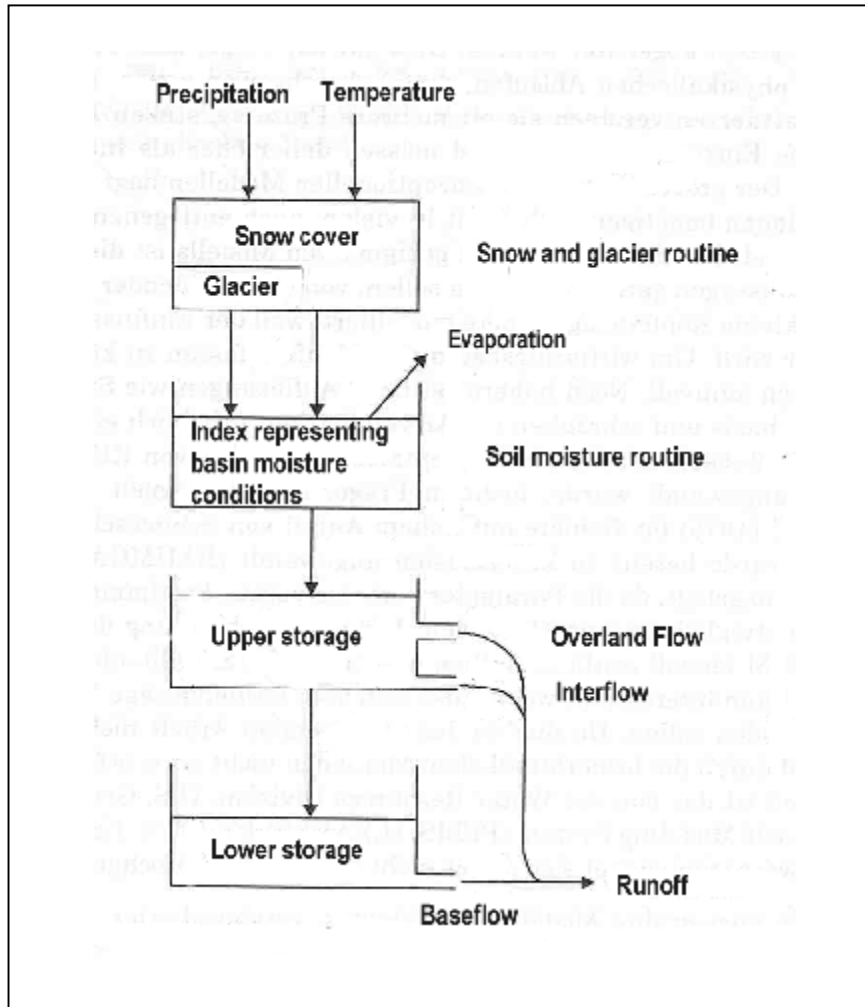
The essential difference between the two models is that the HBV is a linear reservoir model which uses daily temperature and hydrological input and produces daily runoff output. It has therefore a higher prediction power than the OEZ model, which uses monthly hydrometeorological data as its input and produces monthly values of the water balance as its output and is thus climatological in nature.

How the models are used is briefly described below, tables summarising how the models compare / differ are listed in the following section 4.2.

4.1.2 Applying the HBV model

The following summary is adapted from Hagg (2003). *Fig 4.1.2* below is a schematic depiction of the structure of the HBV model (Hagg 2003).

Fig 4.1.2 Structure of the HBV model



Input data:

Topographical data input consists of the total and glaciated area of each elevation belt of the catchment (spanning 200 m of altitude, though this is variable). In order to account for varying solar radiation intensities, the area-elevation data is further differentiated according to its aspect and slope, with three classes: North-facing; South-facing; East-facing, West-facing and horizontal.

Hydrometeorological input consists of daily values for temperature, precipitation, and runoff. The latter is necessary for the calibration of model parameters.

1st module - Snow and glacier routine:

Differentiation between liquid and solid precipitation is done using temperature-gradient and a threshold temperature (both of which are optimisation parameters), above which precipitation falls as rain, and below which it falls as snow. Mixed precipitation is not accounted for.

Calculation of basin precipitation: measured precipitation values are corrected using a rainfall / snowfall correction optimisation factor, in order to compensate for measurement errors, as well as the lack of representativity of the point-measurements for the catchment as a whole. Precipitation increase with altitude is calculated using a precipitation gradient, which is an optimisation parameter.

Snow cover depletion and glacier melt: snow and ice melt is calculated using the temperature-index method. The amount of meltwater is calculated using daily mean air temperature, a threshold temperature above which melt takes place, and the degree-day factor (mm w.e. (water equivalent) melt of snow or ice per positive degree-day):

$$\text{mm meltwater} = \text{degree-day factor (mm w.e. K}^{-1} \text{ d}^{-1}) * (\text{daily mean temperature} - \text{threshold temperature})$$

Because in reality the degree-day factor varies with angle of insolation and snow metamorphosis, the HBV model accordingly varies the degree-day factor over the year using a sine-wave function, with its maximum at summer solstice and its minimum at winter solstice. The minimum and maximum values of the degree-day factor are optimisation factors. Additionally, the degree-day factor is varied depending on aspect (lowered from seasonal reference-value for north-facing slopes, and increased for south-facing, as well as whether snow or ice melt is taking place. The factors raising or lowering the degree-day factor for aspect, and raising it for ice melt (due to the lower albedo of the ice surface) are optimisation parameters.

Refreezing and storage of meltwater retention in snow cover: to account for meltwater infiltrating the firn-pack, refreezing and thus releasing heat energy which warms up the surroundings, the HBV model has a refreezing coefficient (optimisation parameter) to account for this, and it can only take place below the threshold temperature for melt. Meltwater retention in the snow cover is calculated using millimetres water equivalent of the snowcover, multiplied by the retention capacity of the snowcover (the latter being an optimisation parameter).

2nd module - Soil moisture routine:

The sum of rainwater and meltwater from the snow and glacier routine is the input for the soil moisture routine.

This routine contains all water losses due to evaporation. Actual evaporation is calculated by multiplying potential evaporation with an index value representing moisture conditions in the catchment. The value for potential evaporation varies

according to time of year, and again a sine-wave describes the variation from a maximum on the 1st of August to a minimum on the 1st of February.

A coefficient, which is an optimisation parameter, controls the flow of water which did not evaporate into the upper storage.

3rd module - Calculation of runoff:

This module consists of two storage components. The upper storage has two outlets - fast and slow. The former is comparable to overland flow, the latter to interflow. The fast outlet only comes into effect when a threshold value for the upper storage (optimisation parameter) is exceeded. Another optimisation parameter controls the percolation of water into the lower storage component. The lower storage empties linearly through an outlet, analogous to the behaviour of a groundwater body.

Output data:

The HBV model produces the following output data:

- Runoff (mm)
- Basin precipitation (mm)
- Evapotranspiration (mm)
- Storage change, for
 - Glaciers (mm)
 - Snow (mm)
 - Groundwater (mm)

Calibration:

One half of the available data series is used for calibration.

The adjustment of optimisation parameters is done using inverse-modelling, i.e. by comparing values computed by the model (output) to measured values and thereby drawing conclusions as to the values that the parameters need to be given. Model output is compared principally to measured runoff, though glacier mass balance values and snow cover values can be used in addition, if available.

Optimisation parameters are adjusted manually using numerical and optical criteria for goodness of fit, leaving room for subjectivity on the part of the modeller. The numerical criteria used are the accumulated difference between measured and simulated discharge, and the Nash-Sutcliffe efficiency criterion (Hagg et al., 2003).

Validation

Once the model has been calibrated, it is applied to the second half of the data series in order to check the quality of calibration.

Adaptation for future scenarios:

Meteorological data are not adjusted to a climate scenario using a general monthly factor. Instead, in the case of warming, single hot days with additional convective rainfall are added until the predicted monthly means of temperature and precipitation are reached. This is closer to what would happen in reality than a general shift in temperature and precipitation values (Escher-Vetter et al., 1999).

In Hagg (2003), and Hagg et al. (2003), two runoff scenarios per catchment were generated based on two reference years from the calibration period with as different meteorological and mass-balance characteristics as possible. The reasons are twofold: firstly, in order to avoid having to discuss how the peculiarities of a single year might skew the picture of runoff change (Hagg et al., 2003), and secondly to display the breadth of possible reactions of runoff to climate change. The more the meteorological reference years come from the extremes of measured climate variability, the better the picture of the spectrum of runoff scenarios that might result.

The scenarios produced by the HBV model are meteorological in nature, i.e. weather patterns and associated runoff are simulated for the new climate conditions. Scenarios are run for current glacier extent, 50% of current glaciation, and total loss of glaciation. Glacier area was reduced by removing it from the lowest glaciated elevation bands first, working upwards until the new extent was reached.

4.1.3 Applying the OEZ model

The following summary is adapted from Kuhn and Batlogg (1999), and Kuhn (2000, 2003).

Calibration:

The model is calibrated using the full length of the available hydrometeorological data series, which ideally ought to span two to three decades.

The model requires the following topographical information: total, glaciated, and forested area for each elevation belt (spanning 100 m of altitude) of the catchment. The model uses four iterations (steps):

- 1) Annual basin precipitation is determined from the annual values of a first approximation of evaporation, measured runoff, and measured basin storage (effectively glacier mass balance, because the long-term average movement of groundwater is assumed to be zero):

$$\text{Basin precipitation} = \text{Runoff} + \text{Evaporation} + \text{Basin storage}$$

Simulated values for evaporation suffice for catchments where evaporation is much lower than runoff and precipitation, because errors in evaporation are significantly smaller than errors of runoff measurement. Measured mass balance values using the direct glaciological method should ideally be available for the catchment being studied. They may, however, be transferred from nearby catchments, if specific balance profiles for the relevant time-period are available. This allows transferral of storage change values within elevation belts, which are then weighted proportionately to glacier area extent for each elevation belt, net glacier balance calculated, and then adjusted for total catchment area.

Annual basin precipitation determined using the above mentioned water balance equation is then distributed over the months proportional to the rainfall pattern as recorded by one or two meteorological stations.

- 2) Precipitation gradients for each month of the year need to be determined from the precipitation records of representative stations in the area. These are used to determine the increase of precipitation with altitude, which is first expressed as a matrix of relative values, and subsequently converted to a matrix of absolute values such that basin precipitation is conserved. Monthly precipitation values are then recalculated in accordance with the seasonal course of the precipitation gradients.

- 3) Monthly mean air temperatures are taken from two reference stations and adapted to the proper altitude using altitudinal temperature gradients, again determined from the surrounding station network and extrapolated to the upper levels of the basin. Temperature for each month and elevation belt is needed for two applications: the decision whether precipitation is rain or snow, and the production of melt using a “degree-day factor” that determines melt rate. Potential melting on ice-free areas is limited by the amount of snow presently on the ground and proceeds at the potential rate on glaciers.

Evaporation is determined only according to the state of the ground (snow, bare ground, grass and forest), time of year and altitude, ranging from 0.5 mm/day over snow to 2 mm/day from vegetation in summer. Evaporation is subtracted immediately from precipitation.

The calculation of snow cover for each elevation belt includes the snow of the previous month, solid precipitation, potential melt, and evaporation. As a result, evaporation has to be recalculated, as it depends on snow cover, among other things.

Total storage change per month (mo) and elevation belt (h) can now be determined from the water balance equation: $Storage(h, mo) = Precipitation(h, mo) - Runoff(h, mo) - Evaporation(h, mo)$.

Runoff is accounted separately for rain and melt water.

- 4) Calculated runoff is compared to, and brought into agreement with, measured runoff to better than 20 mm, using the following optimisation parameters:

The redistribution factor: This is a factor which allows more snow accumulation on glaciated areas relative to ice-free areas, which is what happens in reality (Kuhn, 2003). Its principal purpose is to improve the model’s internal mass balance. The original OEZ model without redistribution capability used to produce acceptable total storage values, but details of mass balance were unsatisfactory (Kuhn, 2003). It is in keeping with the nature of a conceptual model that its inner workings should reflect reality as well as possible. Improving internal mass balance is not just a glaciological exercise, however, because adjusting the redistribution factor affects the values of the other optimisation parameters, especially the degree-day factor, which in turn affects the model’s future runoff scenarios. Practically, this means that the adjustment of the other optimisation parameters follows the adjustment of the redistribution factor.

The annual sums of measured and simulated runoff are brought to agreement by concurrently tuning:

- the degree-day factor (mm w.e. $K^{-1} d^{-1}$)
- the first part of the equation determining the fraction of solid precipitation r , i.e. $r = 0.6 - 0.055 * \text{temperature} (h, mo)$
- “initial snowcover”, a factor describing the proportion of the ice-free area of the catchment covered by snow in each month.

These optimisation parameters not only affect the simulated annual runoff total, but also have a lesser effect on simulated monthly runoff values (i.e. the shape of the runoff curve).

Simulated and measured monthly runoff values are finally brought into agreement using a function allowing the separation of liquid storage (meltwater retention in snowpack and groundwater) from solid (ice, snow). Winter runoff must come from liquid storage, decrease asymptotically, and has to be stored in summer. Liquid storage change must have an annual sum of 0 mm.

Output data:

The OEZ produces the following output data:

- Runoff (mm)
- Basin precipitation (mm)
- Evaporation (mm)
- Storage change (mm)
- Specific balance and snow accumulation profiles (latter is for ice-free areas as well as glaciated)

Validation:

According to the findings published in Kuhn (2000), the model can be successfully validated by applying the calibrated version to subsets of the calibration period, of the order of one decade, which differ significantly from one another concerning mean temperature (differences in precipitation vary). Validation for single years did not produce reliable results. This is not the typical method of validation, in that the validation data are not independent of the calibration data.

Adaptation for future scenarios, as prescribed in Kuhn and Batlogg (1999):

A climate scenario means that temperature or precipitation are changed by the same amount for all months, which leads to a recalculation of all dependent quantities, resulting in runoff values which correspond to the new situation.

- 1) For temperature scenarios: precipitation $P(h,mo)$ from the fourth iteration is used and kept constant. Together with new values for temperature, new values for effective precipitation and snowcover are determined. Using the new values for snowcover and temperature, evaporation, snowcover (a new approximation), and the mass balance of the basin's glaciers are recalculated. Changing model parameters must be avoided at all costs in order to maintain controlled conditions for comparison. In the equivalent of the fourth iteration, monthly liquid storage needs to be re-adjusted, in order to take account of earlier or later meltwater production.
- 2) For precipitation scenarios: temperature and all model parameters are kept constant. The new precipitation is entered in the equivalent to the third iteration and then fixed. Evaporation and glacier mass balance are approximated anew, liquid storage is modified, and runoff re-calculated.

Because scenarios are based on average values from the calibration period, the runoff predictions are of a climatological nature – i.e. average conditions over several years or decades.

Changes to the prescribed adaptation of the model for future scenarios:

In order to produce runoff scenarios comparable to those generated by the HBV, it was necessary to make the following modifications to the adaptation of the OEZ for future climate scenarios:

- Combined temperature and precipitation scenarios
- Monthly values for temperature and precipitation were adjusted by different amounts in accordance with the GISS predictions for future climate.
- Runoff scenarios were produced for future climate conditions not only with 100% of current glaciation, but also for a reduction to 50% of current extent, and also to 0%. Glacier area was reduced by removing it from the lowest glaciated elevation bands first, working upwards until the new extent was reached.

These changes in the adaptation procedure for future scenarios are, to the best of my knowledge, new territory for the OEZ model. This is an additional challenge to the short data series which the model has to work with.

4.2 Comparison of models

Both models require information about the area-elevation distribution of the catchments for total and glaciated areas; the OEZ uses 100 m elevation belts, the HBV uses 200 m belts for the catchments in this study. The OEZ also requires forested area. The HBV further subdivides area-elevation into aspect classes. The length of the data series available for modelling mean that for both models validation may only be attempted for Abramov (Hagg et al., 2003). The HBV model uses daily values for hydrometeorological input; the OEZ uses monthly values. Daily values are not so widely available for Tien Shan catchments, limiting the application of the HBV. The OEZ requires calculated temperature and precipitation gradients for each month of the year, whereas the HBV uses general values which are determined by optimisation. Mass balance data may be used as an additional check for HBV calibration, but are a must for the OEZ calibration. However, if mass balance data are not used, there is a risk that wrongly calculated basin precipitation can be compensated using wrongly simulated mass balance in order to produce correct runoff. Conversely, errors in ice melt rates can be compensated by erroneous precipitation inputs (Braun and Aellen, 1990). The OEZ has five intended optimisation parameters, the HBV as used by Hagg (2003) uses nineteen. On the one hand it increases the likelihood of the model being able to compensate for errors, but on the other hand it risks doing so wrongly, as mentioned above.

Adapting the HBV to future climate scenarios is done by making changes to the meteorological values for individual days until the new monthly means are replicated. Glacier area is reduced, and runoff scenarios are based on two of the calibration years, permitting a spectrum of results (which vary according to the “meteorological character” of the reference years). The OEZ’s adaptation for future scenarios is based on the mean values used for model calibration providing only one result per scenario. The prediction is climatological and gives an idea of the norm around which future climates can be expected to cluster. The prescribed method of adaptation according to Kuhn and Batlogg (1999) allows for a change in either temperature or precipitation, and does not consider a reduction in glacier area extent. Consequently, predicted runoff may be too high, possibly overestimating flood risk potential. In order to be able to compare OEZ results to the HBV scenarios, the model was adapted differently to the prescribed method by changing both temperature and precipitation, as well as reducing glacier area extent.

4.3 Data Series and data preparation

Table 4.3.1 provides an overview of the hydrometeorological data available for each of the catchments, and how missing data were dealt with. The processes involved are explained in greater detail below.

Table 4.3.1 Available data

	Oigaing	Ala archa	Abramov
Precipitation: full data series available	1962/63 – 1994/95 (except Oct – Dec 1962)	1958/59 – 1973/74 (except Oct 1958, Aug – Dec 1973)	1967/68 – 1993/94
Precipitation: data series used by both models for water balance simulation, & by OEZ for calibration	1962/63 – 1964/65, 1971/72 – 1973/74, 1978/79 – 1979/80	1960/61 – 1964/65, 1971/72, 1973/74	1968/69 – 1987/88
Comments	Gradients from formula (Aizen et al., 2000)	calculated gradients	gradients treated as optimisation parameter
Further details in:	Table C5, appendix C	Table C5, appendix C	Table C5, appendix C
Temperature: full data series available	1962/63 – 1994/95 (except Oct – Nov 1962)	1958/59 – 1973/74 (except Oct 1958, Aug – Dec 1973)	1967/68 – 1997/98
Temperature: data series used by both models for water balance simulation, & by OEZ for calibration	1962/63 – 1964/65, 1971/72 – 1973/74, 1978/79 – 1979/80	1960/61 – 1964/65, 1971/72, 1973/74	1968/69 – 1987/88
Comments	gradients from formula (Aizen et al., 2000)	calculated gradients	gradients treated as optimisation parameter
Further details in:	Table C4, appendix C	Table C4, appendix C	Table C4, appendix C
Runoff: full data series available	1963/64, 1971/72 – 1973/74, 1978/79 – 1979/80	1960/61, 1962/63 – 1963/64, 1974	1968/69 – 1987/88
Comments	The length of runoff measurements are the limiting factor for data series length for modelling		
Runoff: data series used by both models for water balance simulation, & by OEZ for calibration	1963/64, 1971/72 – 1973/74, 1978/79 – 1979/80	1960/61, 1962/63 – 1963/64, 1974	1968/69 – 1987/88
Glacier mass balance:	Not available	Not available	1967/68 – 1997/98 available, 1968/68 – 1987/88 used
Comments	Assumed to be zero for calibration period.	Determined using the hydrological method.	Source: Sanigmi Proceedings (2001)
Area-elevation data	Forest cover data relevant	No forestation	No forestation
Comments	not available		
Data source	Central Asia Data Base	Central Asia Data Base	Abramov glacier data reference book (1996)

See pages 62 to 63 for Appendix C

Only the Abramov data series of 20 years permitted validation of model calibration by both the HBV and OEZ (Hagg, 2003). Only Ala Archa has an appropriate network of meteorological stations permitting temperature and precipitation gradients to be calculated from measured data. For Oigaing, formulae were available as substitutes (Aizen et al., 2000), and for Abramov there was no other choice but to treat them as extra optimisation parameters.

Measured evaporation was not available for any of the catchments. Average snow cover duration information is necessary for the input of evaporation in the first iteration of the OEZ. For adjustment of evaporation in the following iterations, forest cover and calculated snow cover data are needed. Forest cover data are not available for any of the catchments, and snow cover data for the OEZ calibration period are only available for the lowest elevation band of the Ala Archa basin (source: Central Asia Data Base), which is not sufficient for the estimation of average snow cover duration for the catchment as a whole.

Evaporation rates were fixed at a minimum of 0.5 mm/day (corresponding to the year-round value for elevations above 2600 m in the Alps in Kuhn and Batlogg (1999)) for all but the lowest elevation bands for all three catchments. This was done because the necessary data permitting a more accurate picture of basin evaporation was missing, and so the model was set so that the direction of potential error was known (i.e. risk of slight underestimation).

Justification for adapting minimal rates in the case of Ala Archa and Abramov is found in the high elevation of the entire catchments. Here, the presence of forests and associated evapotranspiration can be dismissed. Minimal rates for Oigaing are possibly not so close to reality because the catchment's lowest elevation belts are within the forested zone, which stretches from 1500 m to 2800 m (Aizen et al., 1996). However, with neither average snow cover duration data nor forest cover area data, I felt I was left with no other choice but to adapt the same procedure for Oigaing. However, the simulation of water balance resulting from model calibrations presented in *table 5.1.1 on page 37* shows that the OEZ evaporation values are still higher than those produced by the HBV.

Measured mass balance data for Oigaing and Ala Archa are missing. As a substitute, calculation of mass balance for both Oigaing and Ala Archa was attempted using the hydrological method, where measured precipitation was extrapolated over the catchment using precipitation gradients and area-elevation data. The thus derived basin precipitation can be used to calculate basin storage using the water balance equation:

$$\text{Basin storage} = \text{Basin precipitation} - \text{Evaporation} - \text{Runoff}$$

The error risk of this procedure (i.e. the precipitation records not being representative in a way that permits extrapolation to the rest of the catchment) is precisely what the OEZ model aims to avoid by using the water balance equation to calculate basin precipitation as a residual (see *section 4.1.3*).

This risk was confirmed in Oigaing's case. The result was rejected, because a storage value of +316 mm for catchment average, where glaciers cover approximately 9% of the area, would lead to enormous mass balance gain for the glaciers. Strongly positive mass balances do not match glaciological observations of the period, where for example changes in the length of the Severtsova glacier (Fluctuations of glaciers, vol. 2-4) indicate relative stability (Hagg et al., 2003). My compromise was to enter a mass balance value of 0 mm for the OEZ. Hagg was also surprised by the positive mass balance which resulted from modelling using the HBV (Hagg, personal communication).

Determining mass balance for Ala Archa also had to be attempted using the hydrological method because the glaciologically determined mass balance data available for the neighbouring Golubin glacier were not transferable as prescribed for the OEZ model (see section 4.1.3). Specific balance profiles were not available for any of the seven calibration years.

The result of the hydrological method was deemed acceptable because precipitation gradients could be calculated, and the value of -105 mm (catchment average), or -290 mm for the glaciated area, seemed within the realms of plausibility, in the light of net balance values for the Golubin glacier of -109 mm, -391 mm, -462 mm for the years 1972, 1973 and 1974, respectively. This remains a very crude comparison and justification, firstly because Golubin mass balance values for the other five calibration years are unknown, and secondly because the elevation of median glaciation extent is approximately 300 m above that of Ala Archa. As Kuhn et al. (1985) have observed, differences in glacier topography can have a very large impact, such that two neighbouring glaciers may display very different mass balance regimes under the same climatic forcing.

It is clear that due to shortfalls concerning data series length, temperature and precipitation gradients, forest cover, and mass balance data, applying the OEZ to these catchments cannot be done entirely as prescribed by the model's authors. How well the model is able to work with this type of dataset will be evaluated by looking at the simulated water balance values for current climate conditions, comparing them to measured values as well as to the equivalent output of the HBV model (Hagg et al., 2003). This is followed by an evaluation of the integrity of model scenario output – i.e. how runoff varies as first climate input is adapted for CO₂ x 2, and then glaciation extent is reduced. Finally, the OEZ runoff scenarios for 50% glaciation remaining and complete loss of glaciation are compared to the HBV results obtained by Hagg (2003), and Hagg et al. (2003).

4.4 Plausibility tests of Calibration

The goodness of fit of a model calibration is normally tested by validating it using a different data set to the one with which the model was calibrated. Other tests of the plausibility of calibration can be used, however, and this is advantageous where not all models can be successfully validated due to lack of sufficient data series, as was the case for Oigaing and Ala Archa. Hagg (2003) and Hagg et al. (2003) used both the Nash-Sutcliffe coefficient test and accumulated difference between measured and simulated discharge in mm per year (percentage of the measured value). Kuhn (2003) uses various aspects of the OEZ's internal mass balance distribution, some of which have been used in this study and are discussed below.

4.4.1 Goodness of fit for HBV calibration

Hagg et al. (2003) used the model efficiency criterion by Nash & Sutcliffe (1974) to test the quality of calibration, and the R^2 value achieved for the simulated versus measured runoff are presented in *table 4.4.1* below. Values vary between 0 and 1, where 1 signifies a perfect fit between measured and simulated runoff curves. A value of 0 signals that the mean of the simulated curve fits the measured curve better than the simulated curve itself.

Table 4.4.1 Nash-Sutcliffe coefficient (R^2) values for HBV simulation of measured runoff

	Oigaing	Ala Archa	Abramov
R^2 mean, min., max.	0.89 , 0.77 , 0.96	0.88 , 0.80 , 0.94	0.85 , 0.77 , 0.91

Source: Hagg et al. (2003)

Comparison of conceptual runoff models (Rango, 1992) has shown that R^2 values above 0.8 are above average for runoff modelling of daily time-steps in glaciated catchments. In the light of these findings, the calibration results for all three catchments are, according to the R^2 criterion, absolutely acceptable (Hagg 2003). Comparing R^2 values for different basins with one another needs to be regarded with caution, as this statistical item is strongly affected by runoff variability Hagg et al. (2003).

4.4.2 Goodness of fit for OEZ calibration

As already mentioned in section 4.1.3, the redistribution factor was introduced to the OEZ model in order to improve the internal mass balance distribution (total storage values were already acceptable), such that it might produce glaciologically plausible results (Kuhn 2003). Wind and avalanches remove snow from ridges and steep slopes and redeposit it in cirques and depressions. Redistribution of snow in a glaciated catchment is decisive for a distinction between ice-free and glaciated areas, and in particular for the reproduction of the altitudinal mass balance profile $b(z)$ (Kuhn 2003).

This adaptation, however, also has ramifications for the model's future scenario runoff output by necessitating a change in calibration: Kuhn (2003) demonstrates that moving snow from ice-free areas to glaciated areas (logically) increases glacier mass balance. Therefore, if total storage is to be kept constant, increasing the redistribution factor requires increasing the degree-day factor as well, as more ice melt is needed in summer. It is reasonable to expect that a higher degree-day factor will change runoff predicted under a future climate scenario. A higher degree-day factor will intensify snowmelt, shortening the duration of its contribution to runoff. The intensification of ice melt raises its contribution to total runoff, and the higher the degree of catchment glaciation, the greater the impact.

For this reason, I chose to test two OEZ calibration settings for all three catchments: one with no redistribution factor (i.e. set to a value of "1", sometimes abbreviated to "rdf=1"), and one where the redistribution factor was set to two (doubling the amount of snowfall falling on glaciers relative to ice-free areas, sometimes abbreviated to "rdf=2"). The latter setting was chosen based on Kuhn's observation (1981) that the ratio of net accumulation to simultaneous precipitation as measured in a glacier basin may exceed a factor of two. The resultant degree-day factor values are presented in *table 4.4.2* below. The degree-day factor matrix produced by the HBV model, as well as precipitation gradients and temperature gradients for both models are presented in *tables C1 to C3* in appendix C on page 62.

Table 4.4.2 Degree-day factors (mm w.e. $K^{-1} d^{-1}$) resulting from OEZ calibrations

	Oigaing	Ala Archa	Abramov
Calibration using redistribution factor of 1 (no redistribution)	4.80	2.90	6.60
Calibration using redistribution factor of 2	5.20	4.25	8.85

Checking goodness of fit was done by evaluating three aspects of the internal mass balance distribution: accumulation / ablation profiles of glaciated and ice-free areas, the equilibrium line altitude (ELA) and the accumulation area ratio (AAR). Accumulation / ablation profiles show how much snow gain and ice loss (w.e.) take place in each elevation belt for glaciated areas, and also how much snow (w.e.) is gained by ice-free areas. The ELA is the altitude at which glacier mass balance gain through accumulation is equal to loss by ablation. The AAR is the ratio of the glacier accumulation area to its total area.

Without the redistribution factor, Kuhn (2003) observed that the OEZ model, once calibrated and with an acceptable total storage value, accumulated too much snow in ice-free areas, and displayed unrealistically negative glacier mass balance. Whilst it is true that in years with positive mass balance snow accumulation may exceed melt also in ice-free areas, in the long run this ought not to be the case – glaciers are where they are for a given climatic setting because of topographical effects (Kuhn 2003). The accumulation and ablation curves, therefore, can be used to judge how well a model calibration reflects reality.

*Figs 4.4.3 to 4.4.5 on page 30 show the simulated accumulation / ablation curves for ice-free and glaciated areas, as well as specific mass balance profiles. Values are produced for each 100 m elevation belt. The units are cubic kilometres water equivalent for the accumulation / ablation curves (hence the reason for Oigaing displaying the greatest values), but mm water equivalent for specific mass balance. They demonstrate that, where no redistribution takes place (redistribution factor set to 1), all three catchments show large amounts of accumulation on ice-free areas. Setting the redistribution factor to 2 reduces ice-free snow accumulation significantly, and reduces the negativity of glacier mass balance. In the cases of Oigaing and Ala Archa, snow build-up on ice-free areas is almost eliminated (catchment averages are reduced by 91% from 78 mm to 7 mm, and by 96% from 30 mm to 1 mm, respectively). For Abramov, raising the redistribution factor only approximately halves the accumulation of snow on ice-free areas (from 214 mm to 99 mm), suggesting that the rdf=2 calibration still does not reflect reality adequately. I experimented with a further increase of the redistribution factor, but even when set at the unlikely value of 3, snow accumulation on ice-free areas was still higher than that of Oigaing and Ala Archa with a redistribution factor of 2. Furthermore, I felt that with every increment of the redistribution factor above 2, the plausibility of the degree-day factor and groundwater movement were further compromised (see *discussion on page 33*). I judged that OEZ calibrations with redistribution factors above 2 were not going to improve the OEZ's performance.*

Fig 4.4.3 Oigaing: OEZ Accumulation / ablation curves & specific mass balance for calibration (CO₂ x 1)

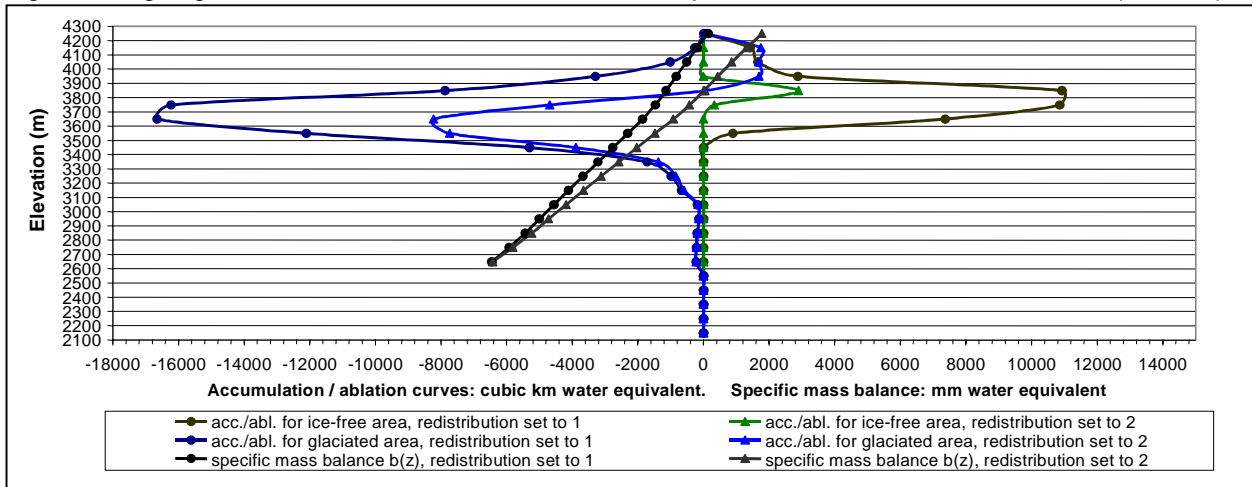


Fig 4.4.4 Ala Archa: OEZ Accumulation / ablation curves & specific mass balance for calibration (CO₂ x 1)

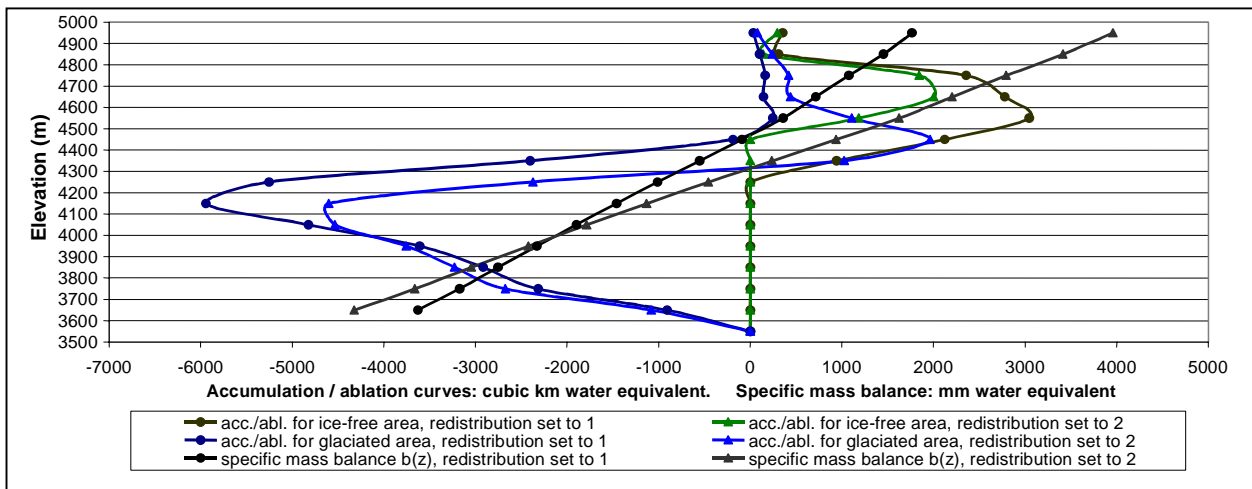
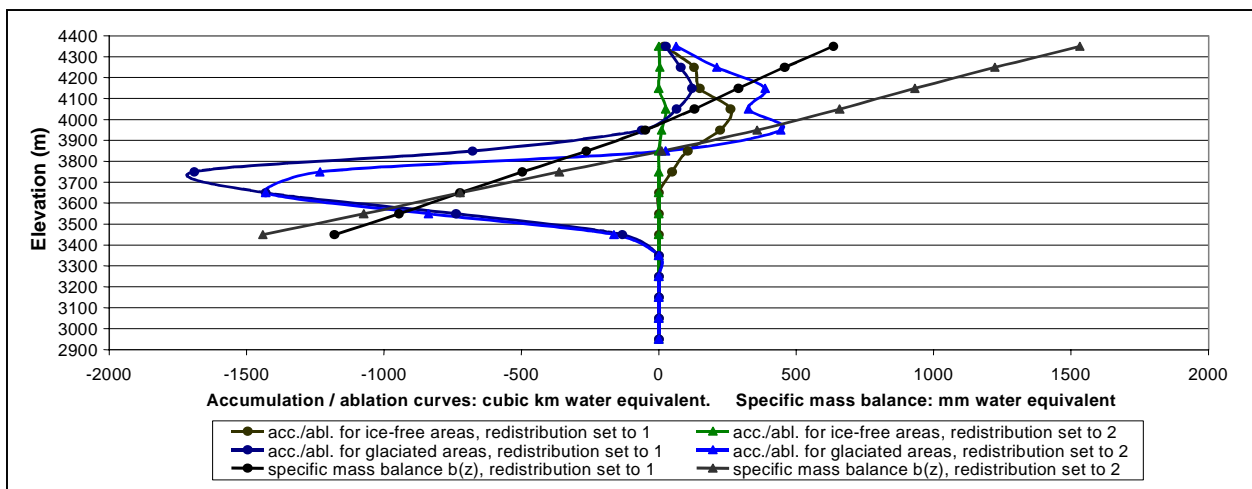


Fig 4.4.5 Abramov: OEZ Accumulation / ablation curves & specific mass balance for calibration (CO₂ x 1)



Raising the redistribution factor to 2 steepens mass balance gradients in all three catchments, lessening the negativity of net balance, lowers the Equilibrium Line Altitude and so increases the accumulation area ratio.

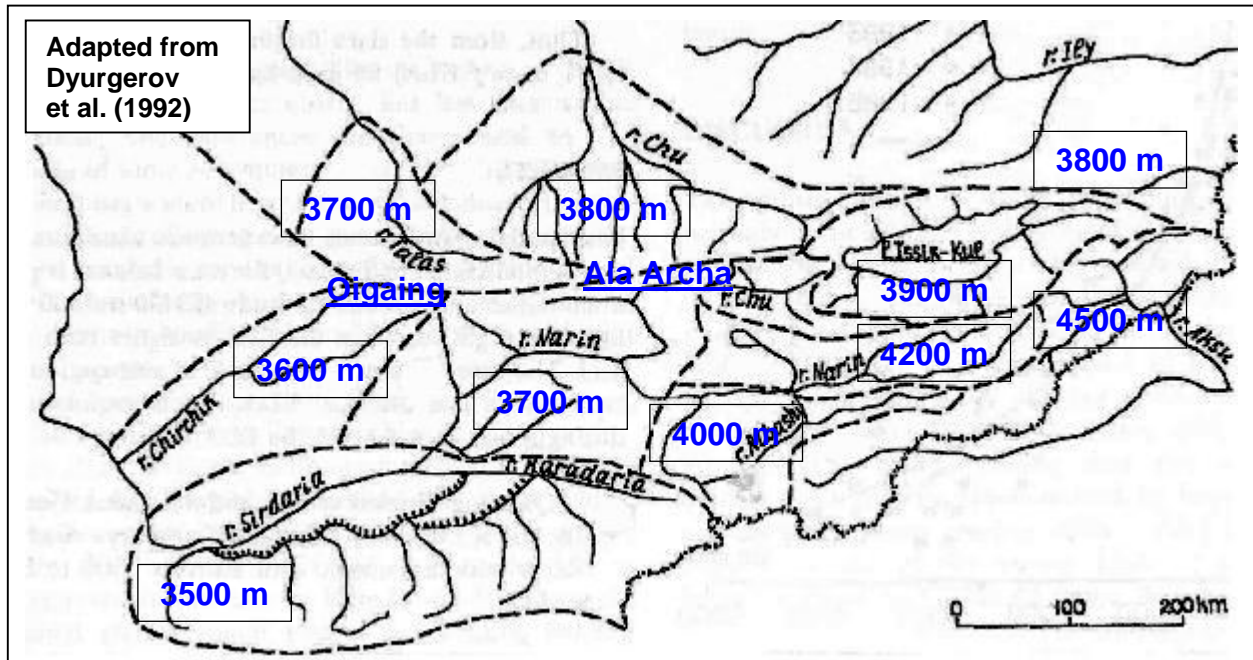
Table 4.4.6 Effect of redistribution factor on ELA and AAR

	Oigaing	Ala Archa	Abramov
ELA for rdf=1	4200 m	4000 m	4500 m
ELA for rdf=2	3800 m	3800 m	4300 m
AAR for rdf=1	0	0.10	0.05
AAR for rdf=2	0.33	0.44	0.33

It is immediately clear from *table 4.4.6* that the AAR values produced by calibrations with the redistribution factor set to 2 are more plausible. Compared to the example in Kuhn (2003) where a catchment with a simulated storage change value of +26 mm produced an AAR of 0.69 (accumulation area constitutes 2/3 of total glacier area, which is typical of glaciers in equilibrium or “steady state”), the rdf=2 AAR values are plausible for glaciers with negative mass balances. That Ala Archa has a higher AAR than Abramov is in keeping with the fact that the calculated basin storage change value of –105 mm for Ala Archa is less negative than the measured value of –284 mm for Abramov. It is interesting to note that the AAR for Oigaing is the same as for Abramov, which is not in keeping with the “guesstimated” basin storage change value of zero (assumption of steady state or equilibrium glacier conditions for the calibration period), which ought to produce an AAR similar to that of the catchment modelled by Kuhn (2003). Calculated ELA for Oigaing and Ala Archa can be compared to the findings of Dyurgerov et al. (1992) presented in *Fig 4.4.6* below where the Tien Shan were divided into three major regions with different mass balance characteristics, based on data from the USSR Glacier Inventory 1969 – 1979:

- The first area, classed as W and NW Tien Shan, covers the locations of both Oigaing and Ala Archa. Here ELAs typically lie between 3500 and 3800 m.
- The second region is the inner Tien Shan, with ELAs ranging from 3800 to 4000 m.
- The third is the highland part of glacierisation of central Tien Shan, with ELAs ranging between 4300 and 4500 m.

Fig 4.4.6 Map of mass balance regions of the Tien Shan as defined by ELA



Oigang's $rdf=1$ ELA lies well above the range for W and NW Tien Shan, and raising the redistribution factor to two brings the ELA down into the range of the major region. Compared to the local regions, however, the $rdf=2$ ELA of 3800 m is significantly higher than the 3500 m ELA for the Chirchik region, and higher also than the 3700 m ELAs for Talas and Narin. This, together with the AAR which is not in keeping with entered mass balance, may well call the assumption of steady-state behaviour for the calibration period into question, and may verify at least the tendency of both the HBV and OEZ models to produce positive mass balances for the Oigang catchment for the calibration period (with lower ELAs compared to those produced by calibration using a mass balance value of 0). This does not, however, increase the likelihood of the hydrologically determined basin storage value of +316 mm. The ELA for Ala Archa fits very well with the ELAs of both the major and local regions, supporting the hydrologically determined basin storage value used for model calibration.

Abramov lies outwith the region covered by Dyurgerov et al. (1992). However, ELA values for most of the modelling years are available and are presented in the Abramov Glacier Data Reference Book (1996). The mean ELA of the modelling period is 4237 m. The $rdf=2$ ELA agrees quite well with this value, whereas the $rdf=1$ ELA is again too high.

It can be concluded that the calibrations with redistributions set to 2 produce the more plausible internal mass balance distributions for all three catchments, though the improvement is not equally good for all three. Oigang's accumulation / ablation curves improve in the manner intended by Kuhn (2003), but the AAR seems too low for the mass balance value of 0 used. ELA values are within the ELA range calculated by Dyurgerov et al. (1992) for W and NW Tien Shan, but in detail are higher than the ELAs

calculated for the three closest regions. The results of Ala Archa's $\text{rdf}=2$ internal mass balance are satisfying on all accounts. Abramov's AAR values for $\text{rdf}=2$ compared to $\text{rdf}=1$ are an improvement, the ELA fits well, but the accumulation / ablation profiles do not show the same improvement displayed by the other two catchments. Assuming that a replication of current conditions promises better simulation of future scenarios, the $\text{rdf}=2$ calibrations have the greater potential, and are therefore the calibrations whose runoff scenarios are compared to the HBV scenarios of Hagg et al. (2003). An example of how runoff scenarios produced by the $\text{rdf}=1$ calibrations differ to those produced by $\text{rdf}=2$ is shown in *fig D1* on page 64 of appendix D.

Doubts as to the quality of both $\text{rdf}=1$ and $\text{rdf}=2$ calibrations for Abramov, despite good AAR and ELA results for $\text{rdf}=2$, were raised by the fact that September runoff could only be reproduced using what I felt were improbable groundwater movements - i.e. summer intake up to and including August, followed by a release of over 100 mm for September alone, compared to a groundwater release of 160 mm required for October to April. The large runoff deficit in September forces the raising of the degree-day factor, in order that compensatory runoff (of the order of 80 mm) be generated during the summer for injection into groundwater storage in order to bring the long-term mean to zero. The resultant degree-day factors for both calibrations are much higher than those for the OEZ calibrations for the other two catchments – twice as high as the equivalent degree-day factors for Ala Archa, whose degree of glaciation is not much lower than Abramov's (*see table ...*). Thus there is a risk that the degree-day factors for Abramov produce melt of too great an intensity, thereby shortening the duration of snowmelt contribution to runoff.

The only alternative method to producing enough runoff through a large release of groundwater would have been to reduce temperature gradient for September to $-0.1^\circ\text{C}/100\text{ m}$, increasing the simulated temperature in the higher elevation belts and so enhancing ice melt. The experiment succeeded in reducing the degree-day factor for the redistribution factor 1 calibration from 6.6 to 5.87 mm w.e. $\text{K}^{-1}\text{ d}^{-1}$, and from 8.85 to 7.82 mm w.e. $\text{K}^{-1}\text{ d}^{-1}$ for a redistribution factor of 2. This temperature gradient setting, however, is meteorologically much less plausible than the $-0.3^\circ\text{C}/100\text{ m}$ gradient used.

4.5 Validation

4.5.1 Validation of HBV calibration for Abramov

Only Abramov had a data series long enough to permit dividing it into a calibration and a validation period (Hagg et al., 2003). Comparison of the r^2 values for the calibration and validation period shows that there is only a small decrease in minimum and therefore also mean values, which indicates that according to the Nash-Sutcliffe coefficient test, the calibration was a success.

Table 4.5.1 Comparison of R^2 values for Abramov calibration and validation

	Plausibility test used	Abramov
Calibration (1968/69 – 1977/78)	R^2 mean, min., max.	0.85 , 0.77 , 0.91
Validation (1979/80 – 1987/88)	R^2 mean, min., max.	0.83 , 0.70 , 0.91

(Source: Hagg, 2003)

4.5.2 Validation of OEZ calibration for Abramov

According to the findings in Kuhn (2000), only Abramov has a data series long enough to permit a validation of the OEZ calibration, because the minimum data period necessary is approximately a decade, which in turn should be a subset of the calibration period (see section 4.1.3). The full two decades of data were used for calibration, and separate validations were carried out for both the first and second decades.

The first and second decades differed from each other temperature-wise by 0.2°C (1st decade mean annual temperature of -4.2°C , 2nd decade = -4.0°C). This cannot be described as significant, and is much smaller than the 1°C difference of the validation datasets in Kuhn (2000). Measured mean annual precipitation was 730 mm for the first decade and 677 mm for the second.

The principal test is the goodness of fit of simulated runoff to measured values. As shown by *Table 4.5.2* below, neither decade validate very well, and the main problem lies with reproducing runoff for June, which is overestimated in the first decade and underestimated in the second. In both cases, the $\text{rdf}=2$ calibration is more accurate than the $\text{rdf}=1$, confirming that the former is better than the latter, but also demonstrating that neither is particularly good. The validation sheds new light on the difficulties experienced during calibration, in that not only September runoff is reproduced shakily, but at least June's as well.

Table 4.5.2: Discrepancies between measured and simulated runoff in mm for calibrations and validations

	Oct	Nov	Dec	Jan	Feb	Mar	Apr	May	Jun	Jul	Aug	Sep	Year
Rdf=1, C	-2	+1	0	+3	0	+2	+2	+1	+4	+2	+6	-19	0
Rdf=2, C	-2	+1	0	+3	0	+2	+2	+2	-4	-3	+6	-7	0
Rdf=1, V1	-1	+1	0	+3	0	+2	+1	+1	+75	-14	-2	-27	40
Rdf=2, V1	-1	+1	0	+3	0	+2	+1	+2	+55	-13	+8	-16	42
Rdf=1, V2	-4	+1	0	+3	0	+2	+2	+1	-63	+19	+13	-11	-36
Rdf=2, V2	-4	+1	0	+3	0	+2	+2	+2	-56	+3	+8	+3	-36

C = mean values from OEZ calibration

V1 = mean values from 1st validation decade 1968/69 – 1977/78

V2 = mean values from 2nd validation decade 1978/79 – 1987/88

Rdf=1: Model runs with redistribution factor set to 1

Rdf=2: Model runs with redistribution factor set to 2

A look at the mean values of precipitation and temperature for the OEZ calibration and validation periods (see *table 4.5.3* below) suggests that it is the difference in June temperature that is the reason for the failure of the OEZ in replicating runoff. The mean monthly temperatures of the first and second validation decades for June differ by 0.9°C, deviating 0.4°C either side of the calibration mean value, and this is enough to cause significant errors in replicating measured runoff. It is possible that problems with the runoff of the other summer months are not exposed due to the fact that the mean monthly temperatures of the validation decades differ only very slightly to those of the calibration period. That differences in precipitation are the cause of failure of replication of June runoff can be discounted because differences for June are comparable to, or smaller than for the other summer months, which are validated successfully.

Table 4.5.3: Mean measured temperature and precipitation values for OEZ calibration compared to means for first and second validation decades, and the differences between them

	Oct	Nov	Dec	Jan	Feb	Mar	Apr	May	Jun	Jul	Aug	Sep
P(mo) (mm), C	68	51	66	52	46	97	90	102	61	48	21	28
P(mo) (mm), V1	69	34	64	53	42	97	77	93	54	53	14	28
ΔP(%) V1 to C	+2	-34	-3	0	-9	-1	-15	-9	-12	10	-31	-1
P(mo) (mm), V2	67	68	68	52	50	98	103	111	68	43	27	29
ΔP(%) V2 to C	-2	+34	+3	0	+9	+1	+15	+9	+12	-10	+31	+1
T(mo) (°C), C	-3.4	-8.6	-12.0	-14.3	-13.7	-9.8	-3.9	-0.9	2.8	6.2	6.4	2.0
T(mo) (°C), V1	-3.5	-8.6	-12.2	-15.2	-14.2	-9.5	-3.9	-0.9	3.3	6.1	6.4	1.9
ΔT(°C) V1 to C	0.0	0.0	-0.2	-0.8	-0.5	0.2	0.0	0.0	0.4	-0.1	0.1	-0.1
T(mo) (°C), V2	-3.5	-8.5	-11.5	-13.5	-13.2	-10.0	-4.0	-0.9	2.4	6.3	6.3	2.1
ΔT(°C) V2 to C	-0.1	0.1	0.5	0.8	0.5	-0.2	-0.0	-0.0	-0.4	0.1	-0.1	0.1
ΔT(°C) V1 to V2	0.1	0.2	0.8	1.7	1.0	0.5	0.0	0.1	0.9	0.2	0.1	0.2

C = mean values from OEZ calibration

V1 = mean values from 1st validation decade 1968/69 – 1977/78

V2 = mean values from 2nd validation decade 1978/79 – 1987/88

P(mo) (mm) = recorded monthly precipitation in mm

ΔP(%) V1 to C = % difference of decade mean to calibration mean

T(mo) (°C) = recorded monthly temperature in degrees Celsius

ΔT(°C) V1 to V2 = difference of decade mean to calibration mean in degrees Celsius

5. Results and Discussion

5.1 Simulation of current conditions

Application of the OEZ model to the study of runoff change was successful for two out of the three catchments, even though not all prescribed data requirements were met. In order to permit comparison to runoff scenarios already carried out for the three Tien Shan catchments using the HBV3 ETH9 model (Hagg, 2003; Hagg et al., 2003), the OEZ model had to be adapted for future climate using a procedure different to that prescribed by Kuhn and Batlogg (1999). This alternative procedure proved itself to be viable.

Two OEZ calibration settings were tested, one where no differentiation was made between snow accumulation in glaciated and ice-free areas, and one with the redistribution factor set to two (i.e. twice as much snow accumulation on glaciated areas compared to ice-free). Tests of the goodness of fit using internal mass balance distribution proved the calibrations with the redistribution factor set to 2 to be best for all three catchments. Difficulties in calibrating the OEZ model for the Abramov catchment using plausible optimisation parameter values, followed by unsatisfactory validation raised doubts as to the quality potential of OEZ runoff scenarios for this catchment from the beginning.

Table 5.1.1 below presents the values of the water balance produced by the calibrated models, contrasting them with available measured values for the same time period (see *figs 5.1.2 to 5.1.4* on page 38). The OEZ values presented are those produced using a redistribution factor of 2. Values produced by calibrations with no redistribution (factor set to 1) differ to those listed above by only a few millimetres, if at all. Evaporation, runoff, and basin precipitation values produced by the OEZ are consistently higher than those of the HBV, irrespective of the data sets upon which calibration is based. The difference in basin precipitation is small for Oigaing and large for Ala Archa and Abramov. Surprisingly, basin precipitation for Ala Archa produced by the HBV model is lower than the mean recorded by the meteorological reference station located in the lowest part of the basin. HBV basin storage is much more negative than that generated by the OEZ for both Ala Archa and Abramov, and in the case of the latter, available mass balance measurements suggest that the HBV value is too negative. The OEZ value fits well due to the fact that mass balance is an input for the model, and not only a check (as is the case for the HBV). The plausibility of the mass balance value for Ala Archa used by the OEZ as an input, which was calculated using the hydrological method, is supported by the model's calculated AAR, ELA and accumulation / ablation profiles. Comparison of HBV basin precipitation and basin storage change to measured values raise the question as to whether basin precipitation calculated by the HBV model for both catchments may be underestimated and compensated by mass balance simulations which are too negative. We see here the risk mentioned by Braun and Aellen (1990), namely that erroneous basin precipitation may be compensated by erroneous mass balance values.

It is to be expected that the OEZ's tendency to produce significantly higher basin precipitation for Ala Archa and Abramov will consequently cause a tendency for the model to produce more runoff than the HBV for future runoff scenarios. This effect may be more or less apparent, depending firstly on the impact of other runoff-generating processes (principally the production of meltwater), and secondly on how different the reference meteorological data sets for the OEZ and HBV runoff scenarios are. The OEZ runoff scenarios are based on adaptation of the model for future climate based on mean temperature and precipitation values for the calibration period, whereas the HBV model has two scenarios for each catchment based on single years from the calibration data series, which differ from one another in hydrometeorological character. Differences in runoff amount are most likely to become apparent in the scenarios with 0% glaciation where meltwater generation is limited to snow.

Table 5.1.1 Annual water balance values produced by OEZ and HBV calibrations

Mean measured annual values from the data series upon which model calibrations are based

	Oigaing		Ala Archa		Abramov	
	HBV	OEZ	HBV	OEZ	HBV	OEZ
Precipitation (mm)	722	722	662	662	730	730
Runoff (mm)	899	899	897	897	1653	1653
Total Storage Change (glacier, mm)					-689	-689
Total Storage Change (basin, mm)					-284	-284

Simulated annual values produced by model calibration

	Oigaing		Ala Archa		Abramov	
	HBV	OEZ	HBV	OEZ	HBV	OEZ
Basin Precipitation (mm)	997	1080	636	964	1146	1551
mm difference to P meas	275	358	-26	302	416	821
% difference to P meas	+38	+50	-4	+46	+57	+112
Runoff (mm)	778	886	845	901	1348	1653
mm difference to R meas	-121	-13	-52	4	-305	0
% difference to R meas	-13	-1	-6	0	-18	0
Evaporation (mm)	148	181	151	171	167	183
Basin Storage Change (mm)	70	13	-360	-108	-369	-285
mm difference to S meas					-85	-1
% difference to S meas					-30	0
HBV glacier (mm)	10		-382		-460	
HBV snow (mm)	55		12		57	
HBV groundwater (mm)	5		10		34	

(Data source for HBV values: Hagg et al., 2003)

Figs 5.1.2 to 5.1.4 compare simulated seasonal variation of runoff under current climate conditions to measured runoff for the same period as the annual water balance values listed in table 5.1.1. They show that the OEZ monthly values are much closer to the measured means. This is not surprising in the light of the fact that the principal OEZ requirement for successful calibration is that simulated monthly and annual runoff deviate from measured runoff by less than 20 mm. However, as discussed in section 4.2.2, the good fit may be deceptive in the case of Abramov. The HBV simulations of current runoff for Oigaing and Ala Archa come close to fulfilling this requirement as far as monthly values are concerned, whereas the HBV simulation of current runoff for Abramov deviates from measured runoff by up to 112 mm for June alone.

Fig 5.1.2 Oigaing current climate: Comparison HBV & OEZ runoff simulations to meas. monthly means

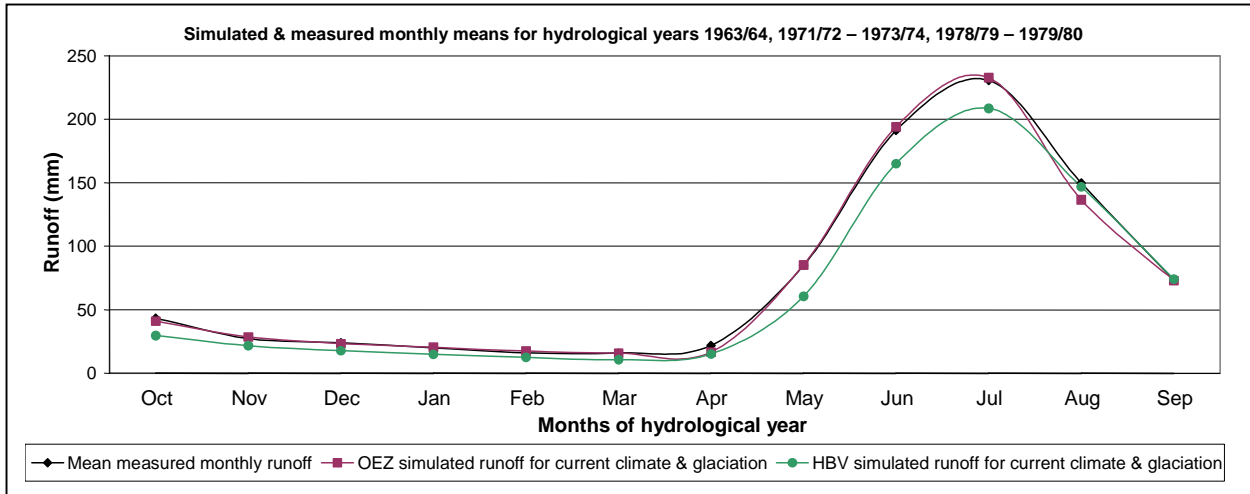


Fig 5.1.3 Ala Archa current climate: Comparison HBV & OEZ runoff simulations to meas. monthly means

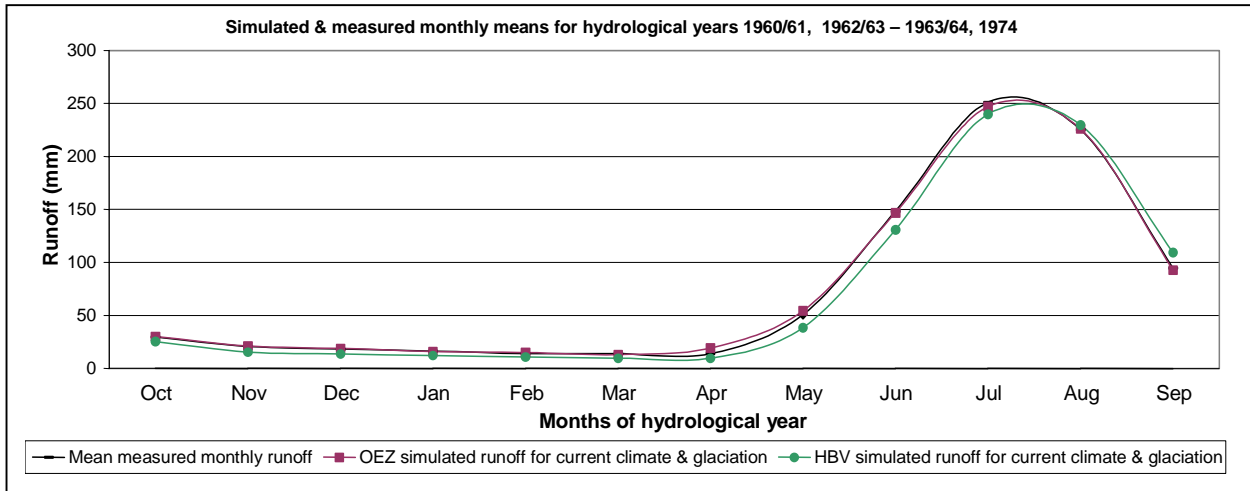
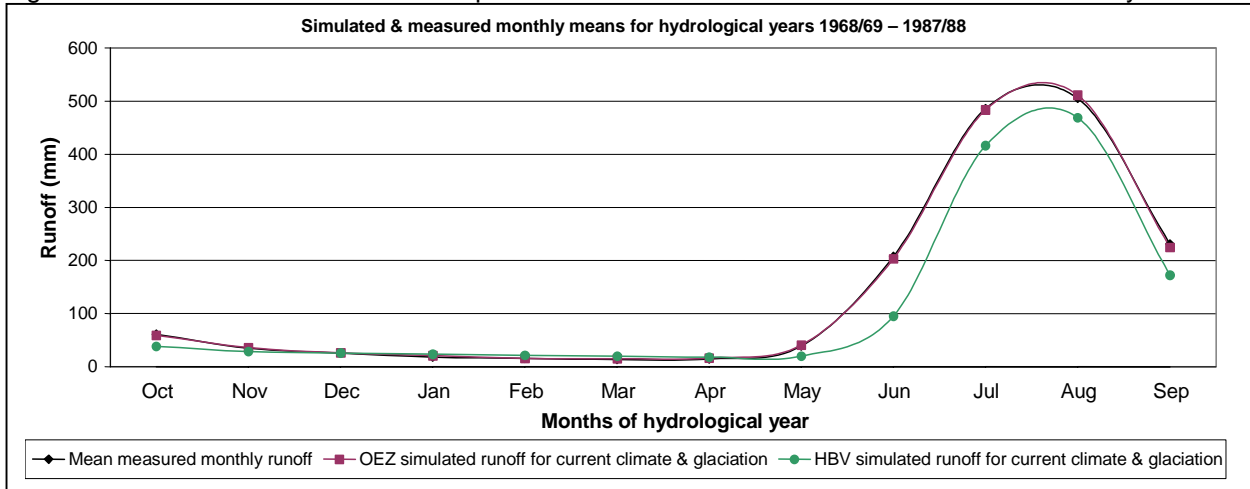


Fig 5.1.4 Abramov current climate: Comparison HBV & OEZ runoff simulations to meas. monthly means



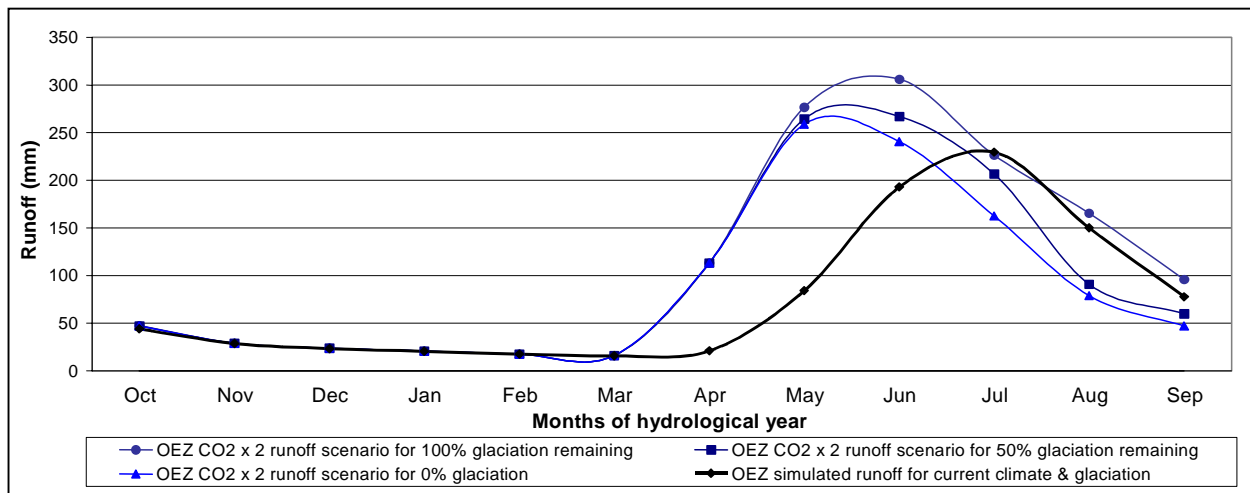
5.2 Simulation of future scenarios

The results of runoff scenarios for climate change caused by the doubling of atmospheric CO₂ are discussed below. The integrity of the OEZ model's behaviour is looked at first, followed by comparison of the OEZ runoff scenarios to the HBV runoff scenarios based on "hot" and "cool" reference years. This is done for climate change as predicted by the GISS GCM, with 50% of current glaciation remaining, and with complete loss of glaciation.

5.2.1 Logical progression of OEZ runoff curve change

As shown by *fig 5.2.1*, the progression of change in the Oigaing runoff curve in response to adaptation for future climate conditions, and subsequent reduction in glaciation extent, is logical and plausible. (See *table E1*, appendix E, page 65 for further details.)

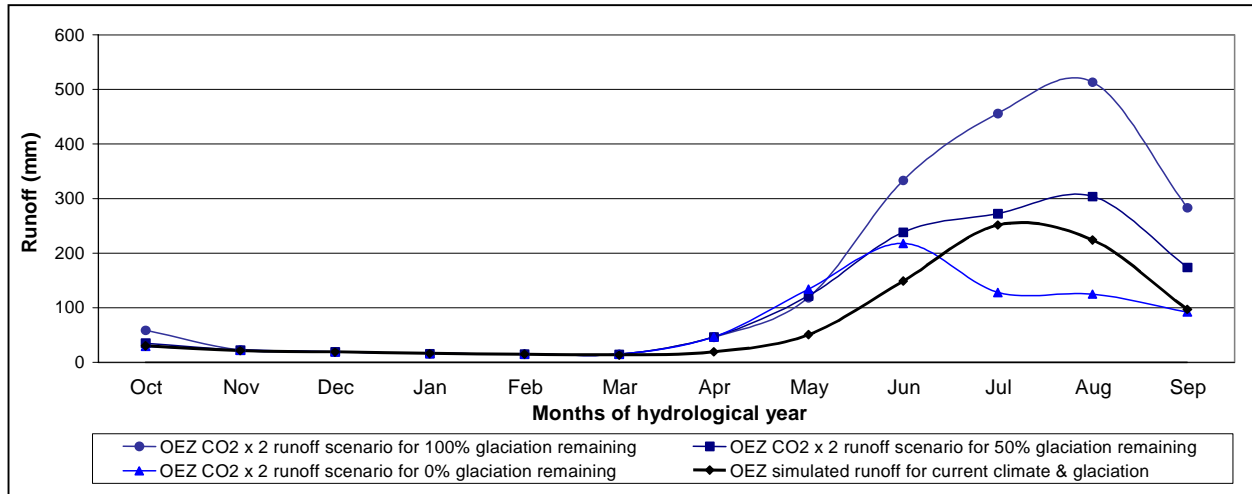
Fig 5.2.1 Oigaing: OEZ progression of runoff curves as glaciated area is reduced



Under future climate conditions, but with 100% of glaciation extent conserved, the runoff curve rises and peaks a month earlier - in June. May and June runoff levels are above the July peak of the runoff curve for current conditions. Runoff levels for July to September show little change. Thus the 100% glaciation curve shows the expected effect of an earlier and more intense spring snowmelt. Reducing glaciation area to 50% has no further effect on runoff for April and May, but lowers June runoff to levels similar to May. Runoff predicted for July to September is reduced to levels below those of the runoff curve for current climate, with the largest effect in August. The effect of more intense snowmelt remains, but the reduction of glaciation extent affects summer runoff negatively. With no glaciation remaining, runoff for June to September is reduced further, showing that even at around 4% glaciation, ice melt generated by the OEZ model makes a significant contribution to summer runoff. Runoff now peaks in May, and runoff deficit relative to current conditions is greatest in July and August.

As *fig 5.2.2* illustrates, the progression of change in the Ala Archa runoff curve in response to adaptation for future climate conditions, and subsequent reduction in glaciation extent, is logical and plausible. (See *table E2*, appendix E, page 65 for further details.)

Fig 5.2.2 Ala Archa: OEZ progression of runoff curves as glaciated area is reduced



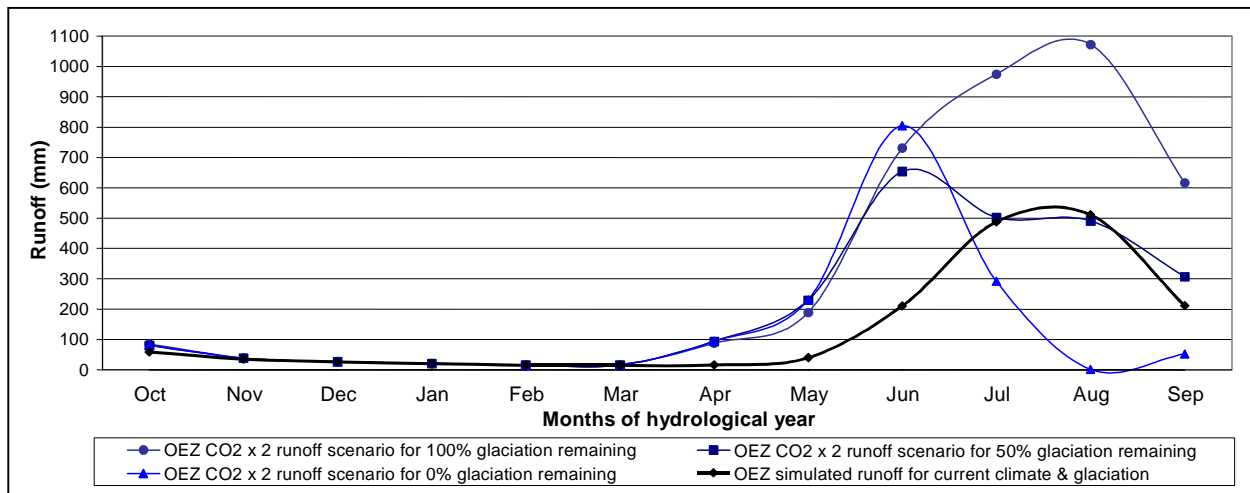
Under future climate conditions, but with 100% of glaciation extent conserved, the runoff curve begins to rise a month earlier. Runoff levels for June, July, August and September are higher than the maximum value for runoff under current climate conditions. Peak runoff moves back from July to August, and is roughly twice as high as that of runoff for current conditions. This is the expected effect of the intensification of snow and ice melt. The much greater glacier area compared to Oigaing explains why the "signature" of ice melt is much clearer here, i.e. moving peak runoff back to August, as opposed to bringing it forward as was the case for the Oigaing 100% glaciation runoff curve. Reducing glaciation area to 50% does not change runoff for April and May, but lowers June runoff to levels comparable with the July peak of the current conditions runoff curve. The flattening of the runoff curve means that July runoff is comparable to that of current climate and glaciation, whereas August runoff is still markedly higher and forms the peak. Thus ice melt is still greatest in intensity, though no longer twice as high as current levels. With no glaciation remaining, the runoff curves follows the same shape until June, after which it drops to levels for July, August and September similar to September runoff under current conditions. This is the logical consequence of losing the benefit of summer ice melt.

The progression of runoff curves for Ala Archa illustrate very clearly the significance of the question of how glacier area changes under climate change, especially for moderately to heavily glaciated mountain catchments. In the case of the 100% and 50% glaciation runs, it is the difference between runoff levels moderately higher than those observed under current conditions, and a severe increase in flood risk. Similarly, the difference between the 50% and 0% glaciation runs is the difference between an increase in water availability and a dramatic reduction in runoff in July and August. Thus

it is clear that the issue of reduction in glaciation extent ought to be considered when applying the OEZ to climate change studies.

As can be seen in *fig 5.2.3*, the progression of change in the Abramov runoff curve in response to adaptation for future climate conditions, and subsequent reduction in glaciation extent, is not convincing. (See *table E3*, appendix E, page 65 for further details.)

Fig 5.2.3 Abramov: OEZ progression of runoff curves as glaciated area is reduced



Under future climate conditions, but with 100% of glaciation extent conserved, the change in the runoff curve is similar to that displayed by Ala Archa. Reducing glaciation area to 50%, however, produces a runoff curve which is surprising on two accounts: firstly, the level of runoff in June is lowered only slightly, and this remains well above the peak of the runoff curve for current climate. Secondly, runoff drops from June to much lower levels for July and August – similar to the July, August values for current runoff. Thus once the extent of glaciation is halved, runoff production is more intense for June than for July and August. It seems improbable that spring snowmelt (which is "disadvantaged" by high albedo) produces runoff of greater intensity than summer ice melt in a catchment with 20% of its area still glaciated. Comparison to the 50% glaciation run for Ala Archa, which is less strongly glaciated, confirms that the OEZ is capable of replicating these dynamics. The cause for the unexpected behaviour for Abramov may be found in the high degree-day factor used, as discussed in section 4.4.2 and presented in *table 4.4.2*, causing more intense snowmelt in the lower elevation bands than is realistic. Once this snow is gone, glacier ice melt in the upper elevation bands of the catchment proceeds at rates similar to those under current climate conditions, suggesting that the degree-day factor used is not inappropriate for high summer conditions. This confirms the suspicion which arose during calibration that a factor for the enhancement of ice melt relative to snow would significantly improve the OEZ's ability to reflect the hydrological processes of the Abramov catchment.

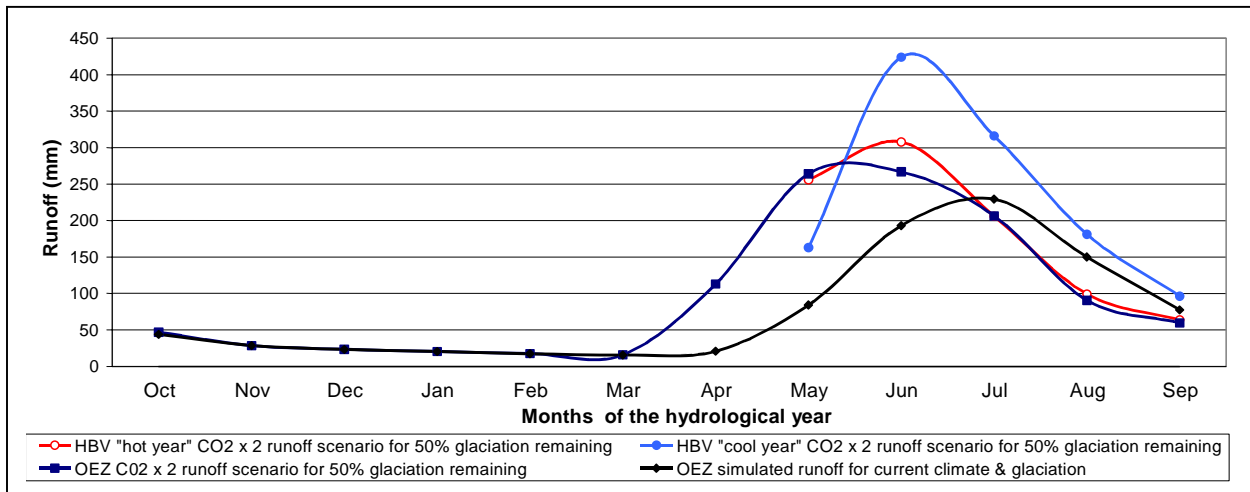
Reducing glaciation extent to 0% provides a further surprise: June runoff increases to a level above that of both the 100% and 50% glaciation runs, which is inexplicable. The sharp drop in runoff after June is to be expected, as the low precipitation levels for July, August, and September leave snowmelt as the sole source of summer runoff. The high degree-day factor almost certainly exaggerates the rise, peak, and fall of the runoff curve. Runoff levels for August are close to zero, though as illustrated in *fig D2* in appendix D (page 64), values for August and September are very sensitive to the re-adjustment of groundwater movement necessary for adapting the OEZ model to future climate (see section 4.1.3).

It can be concluded that the illogical progression of OEZ runoff scenario curves in response to changes in glaciation extent confirms that the model calibration was incapable of replicating measured conditions properly.

5.2.2 Comparison of HBV and OEZ runoff scenarios for 50% glaciation remaining

Fig 5.2.4 shows that OEZ runoff levels for Oigaing are very similar to those predicted by the “HBV hot” scenario for all summer months apart from June, where the HBV peak is higher. The runoff curve for the “HBV cool” scenario rises a month later, but its June peak is 58% higher than that of the OEZ. “HBV cool” scenario runoff values for June to September are not only higher than the “HBV hot” and OEZ scenarios, but also higher than the OEZ simulation of runoff for current climate conditions.

Fig 5.2.4 Oigaing: HBV & OEZ Runoff scenarios for CO₂ x 2, 50% of current glaciation remaining



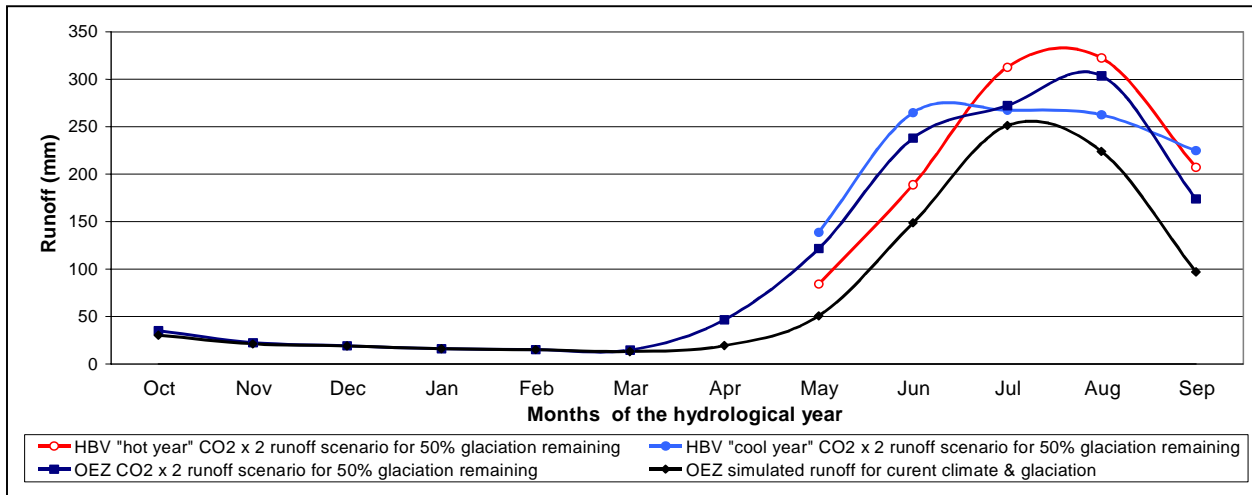
Differences between the three scenarios can be adequately explained by differences in the meteorological data upon which they are based (see *fig F1* and *table F2* in appendix F, page 66). Relative to the means upon which the OEZ scenario is based, the “HBV hot” reference year’s annual precipitation sum is only very slightly lower, and the similarity is also true of winter (April to October) and summer (May to September) subtotals. Mean annual temperature is higher by 1°C. The “HBV cool” reference year’s mean annual temperature is lower than the OEZ mean by 1°C. The “HBV cool” reference year’s annual precipitation is 16% higher than the OEZ mean. Winter

precipitation (October to April) is similar to the mean used by the OEZ, but precipitation from May to September is higher by 55%, and most of this comes from June precipitation, which is 188% higher than the June mean used by the OEZ. Thus there is a very strong indication that runoff deviation from the mean, as demonstrated by the “HBV cool” scenario, is driven by variation in precipitation, and this variation can be large. The remaining glaciation has little buffering effect.

The “HBV cool” scenario signifies the potential for flood risk, which is not captured by the OEZ because scenarios are based on long-term means, and use a monthly time-step. The similarity of the OEZ and “HBV hot” scenario curves and their reference meteorological data, on the other hand, suggest that the “HBV hot” scenario is much more representative of the mean around which future runoff scenarios can be expected to cluster. It is not, therefore, close to representing the lower end of runoff variability. It is of importance for estimations of future water availability that the “HBV hot” and “cool” scenarios do not represent the upper and lower limits of variability. The significance of these results is supported by the fact that the monthly precipitation means upon which the OEZ runoff scenario is based are very similar to those of the full 33-year precipitation data series (see *fig A1* in appendix A, page 55). Thus HBV scenarios based on dry reference years may assist in filling in the picture of potential runoff variability.

As can be seen in *Fig 5.2.5* below, the OEZ runoff scenario for Ala Archa produces a curve which for the most part lies between the “HBV hot” and “cool” scenario curves. Differences between the three runoff scenarios are largely explicable by comparing the meteorological data upon which they are based (see *table F4*, and *fig F3* in appendix F, page 67). Differences for May appear to be temperature driven, whereas for June higher precipitation levels of the reference month adequately explain why the “HBV cool” scenario peaks here at a level above that of both the “HBV hot” and OEZ scenarios. Thus it is evident that with 50% glaciation remaining (covering approximately 18% of the catchment area), some of the runoff variation is induced by fluctuations in summer precipitation. August runoff for the “HBV cool” scenario is below levels of both the OEZ and “HBV hot” scenarios, and coincides with the cool reference year having the lowest mean temperature for August. September runoff levels reflect the precipitation levels of the reference data.

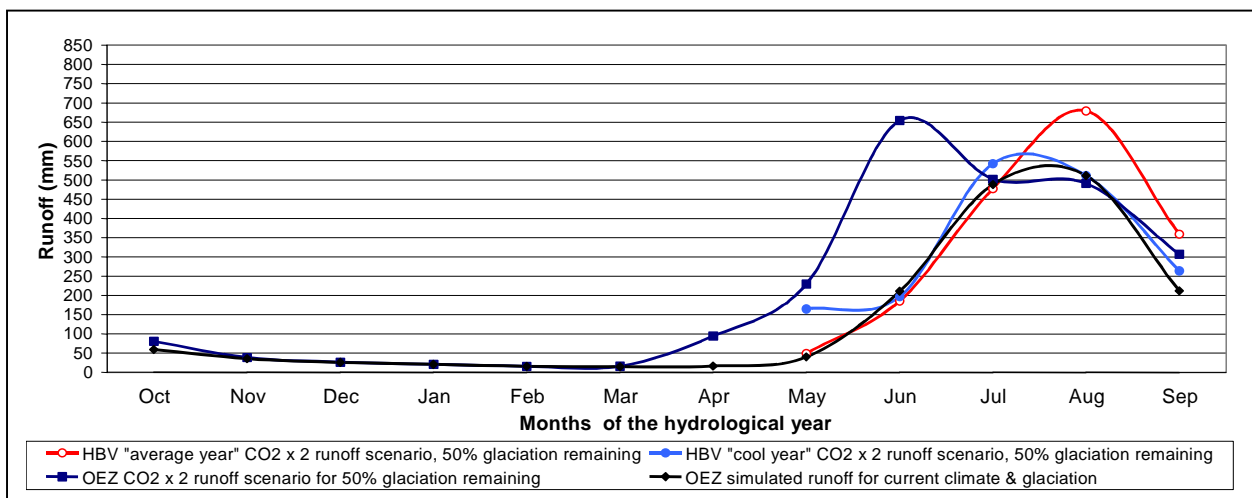
Fig 5.2.5 Ala Archa: HBV & OEZ Runoff scenarios for CO₂ x 2, 50% of current glaciation remaining



Both models, therefore, predict a moderate increase in runoff compared to current levels. Spring snowmelt begins approximately a month earlier and runoff for the months of April to September is increased. Runoff variation is much less dramatic than that predicted for Oigaiing.

Fig 5.2.6 demonstrates clearly that predictions for spring runoff for the Abramov catchment with a 50% glaciation reduction differ dramatically. OEZ runoff levels for July to September are similar to those of the “HBV cool” scenario.

Fig 5.2.6 Abramov: HBV & OEZ Runoff scenarios for CO₂ x 2, 50% of current glaciation remaining



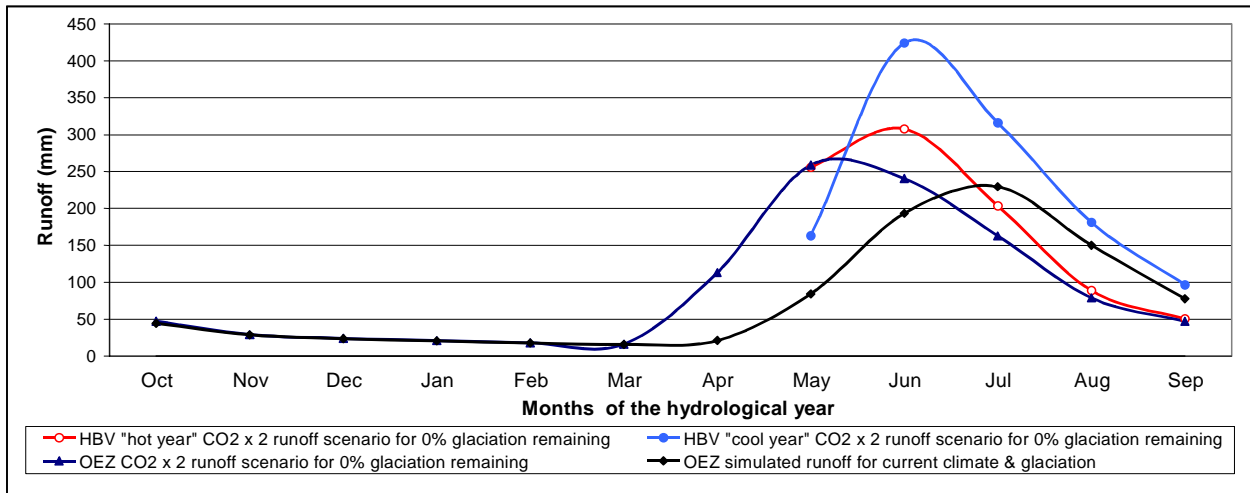
Explanations for differences in the HBV and the OEZ runoff scenarios are hard to find. In the light of the discussion concerning logical progression of runoff curve change, and in comparison to the runoff curve for current conditions, it is the OEZ runoff scenario which seems doubtful, whereas the HBV scenarios appear plausible. Differences

between the “HBV average” and “cool, wet” scenarios can be adequately explained by differences in their reference meteorological data. The only slight surprise concerning the HBV scenarios is that spring snowmelt does not set in any earlier, despite the predicted increase in mean monthly temperature (see *fig F5* and *table F6* in appendix F, page 68).

5.2.3 Comparison of HBV and OEZ runoff scenarios for 0% glaciation remaining

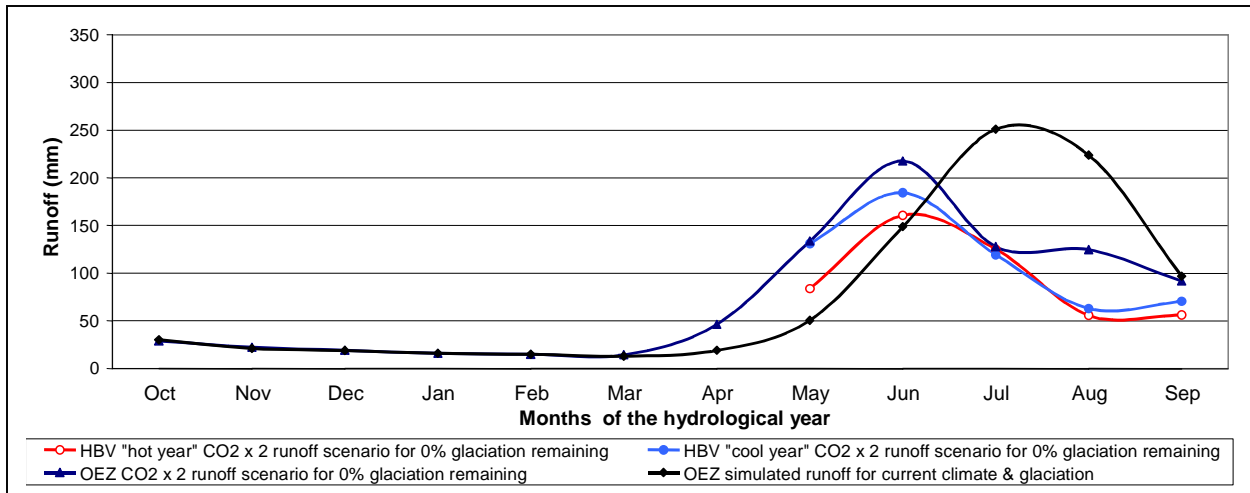
Comparison of the results of *fig 5.2.7* below with *fig 5.2.4* show that the “HBV hot” and cool runoff scenarios for Oigaing are virtually identical to those for the 50% glaciation runs. (see figures F1 and G1, and tables F2 and G2 in appendices F and G, on pages 66 and 69) The further reduction in OEZ runoff caused by complete loss of glaciation, therefore, opens a gap between the OEZ runoff scenario and the “HBV hot” scenario. The HBV scenarios for Oigaing imply that whether glaciation extent is reduced by 50%, or whether glaciation is completely lost, is of no relevance for future runoff. The progression of the OEZ runoff curve as glaciation is reduced from 50% to 0% is therefore more plausible than that of the HBV scenarios. The fact that reducing glaciation caused no change in HBV runoff came as a surprise, a greater difference between 50% and 0% glaciation runs had been expected (Hagg, personal communication).

Fig 5.2.7 Oigaing: HBV & OEZ Runoff scenarios for CO2 x 2, 0% glaciation



As can be seen in *fig 5.2.8* below, all three scenarios for Ala Archa peak in June (of which the OEZ's is the highest), and display a marked drop to very similar runoff levels for July, after which the runoff for both HBV scenarios continues to fall to levels well below the curve for the OEZ scenario.

Fig 5.2.8 Ala Archa: HBV & OEZ Runoff scenarios for CO₂ x 2, 0% glaciation

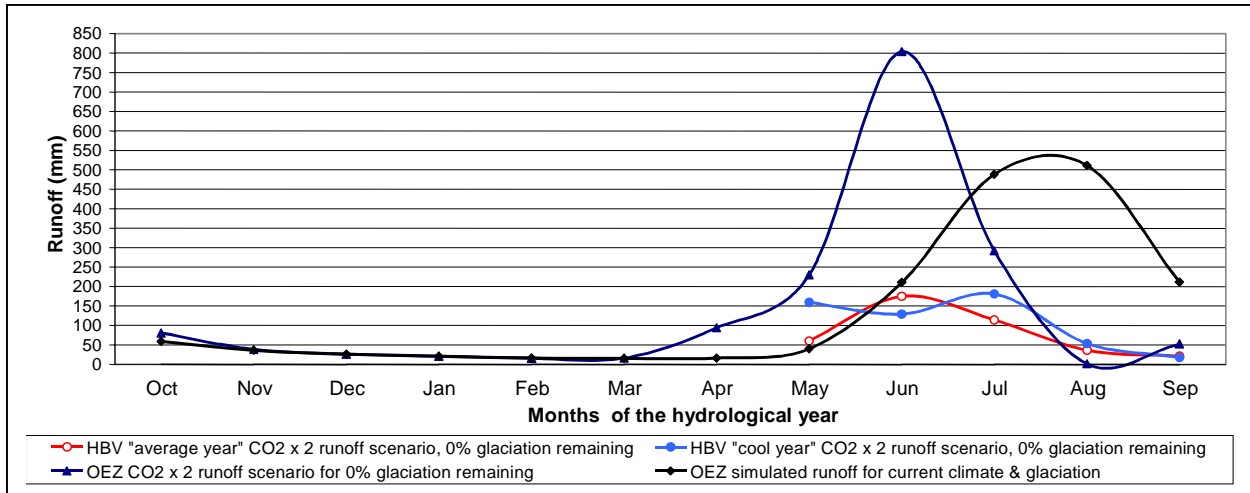


For August, for example, the OEZ predicts a reduction in runoff of around 50% compared to that simulated for current climate and glaciation conditions, whereas both HBV scenarios predict a reduction of runoff by approximately 75%. Consequently, OEZ runoff predicted for May to September is significantly higher than that predicted by both HBV scenarios. These differences cannot be explained through comparison of reference meteorological data. Rather, it is most likely that the predicted influence of the differences in calculated basin precipitation now manifests itself. *Fig G3 and table G4* in appendix G page 70 illustrate that the shape of the OEZ runoff curve is similar to that of OEZ simulation of basin precipitation for CO₂ x 2. The OEZ and HBV scenarios thus frame a range within which future runoff can be expected. Uncertainty is greatest for the second half of summer.

Fig 5.2.9 below demonstrates that, as was the case for 50% glaciation runs, so for the Abramov 0% glaciation runs there are also no good explanations for differences in the runoff curves produced by the OEZ and HBV models, and again the OEZ runoff scenario can be regarded as highly unreliable.

The runoff curve predicted by the OEZ when compared to the runoff curve for current conditions rises, peaks and falls very steeply, indicative of a degree-day factor which is too high. In addition to runoff curve shapes, however, *fig 5.2.9* (see also *table G6* and *fig G5* in appendix G, page 71) demonstrates that the amounts of runoff predicted differ enormously. Referring to *table 5.1.1* on page 37, we see that this is the expected effect of the difference in the simulation of basin precipitation.

Fig 5.2.9 Abramov: HBV & OEZ Runoff scenarios for CO₂ x 2, 0% glaciation



Due to the HBV basin storage produced by calibration being significantly more negative than the glaciologically derived values, it is plausible that basin precipitation is too low and therefore so too is HBV runoff for the 0% glaciation run. Differences between the amounts of runoff predicted by the two models are further enhanced by the influence of groundwater movements for the HBV scenarios, where some runoff is lost to groundwater intake (195 mm in the case of the HBV "cool, wet" scenario, Hagg, personal communication).

Applying the OEZ model to the Abramov 0% glaciation run thus calls the HBV results into question, but without offering a more plausible runoff scenario. Consequently, predictions concerning runoff scenarios for Abramov with complete loss of glaciation are plagued by a high degree of uncertainty and certainly warrants further attempts. For the HBV model, this means primarily closing the gap between measured and simulated mass balance for the water balance produced by model calibration, in order to reduce potential error in basin precipitation calculation. It may also mean selecting reference years with less groundwater movement. For the OEZ this means further attempts at calibrations which produce a lower degree-day factor, possibly by reducing the September temperature gradient in order to enhance ice melt intensity (i.e. the task that is done by the ice melt enhancement optimisation parameter in the HBV model). Clearly, however, temperature gradient manipulation cannot be regarded as a true surrogate for this function.

5.2.4 Summary

The application of the OEZ model to the Oigaing catchment was successful. Differences to predictions made by the “HBV hot” and cool scenarios can be explained by the meteorological data upon which the scenarios are based. Results are similar for both glaciation reduction settings, though the OEZ’s predictions for June and July lower slightly when glaciation is reduced from 50% to 0%. Runoff variability is large for both glaciation runs, and is pluvially driven. Both models predict increased runoff levels for April, May and June, followed by lower runoff levels for July and especially August. Whereas the “HBV cool” scenario run gives an idea of the upper range of runoff variability and associated flood risk, the “HBV hot” scenario is similar to the OEZ runoff scenario and so is more representative of the mean around which future scenarios can be expected to cluster. In order to shed light on the lower limit of runoff variability for Oigaing, HBV runoff scenarios based on particularly dry reference years would certainly be worthwhile. Nevertheless, it must not be forgotten that there is a risk that the underlying assumption of steady state for catchment glaciers during the calibration period may be wrong, affecting the reliability of the runoff scenarios. If mass balance were to be positive, and basin precipitation thus higher than calculated, flood risk might be even higher than depicted by the “HBV cool” scenario, but at the same time the decrease of water availability less severe than predicted.

The application of the OEZ model to the Ala Archa was successful. For the 50% glaciation runs, differences to predictions made by the “HBV hot” and cool scenarios can be adequately explained by the meteorological data upon which the scenarios are based. Runoff variability appears to be driven by both temperature and precipitation. Fluctuations, however, are much less than those displayed by the 50% glaciation run for Oigaing, thus displaying the buffering effect of glaciation on runoff variability. Runoff levels for April to September are predicted by both models to be higher compared to today. The comparability to the HBV scenarios, together with the plausibility of the water balance produced as a result of model calibration, confirm the mass balance value used by the OEZ as being plausible. This is in addition to the good internal mass balance distribution results for accumulation / ablation profiles, ELA and AAR. Reasons for the success of the hydrologically determined mass balance value in the case of Ala Archa, whereas it failed for Oigaing, may be found in the fact that precipitation gradients could be calculated for Ala Archa, and that the recorded precipitation values are more representative for the catchment as a whole. This is in keeping with the fact that the Ala Archa catchment is much smaller than Oigaing, and the meteorological station thus much closer to the glaciers themselves.

With 0% glaciation remaining, predicted runoff for Ala Archa for April to June is expected to be higher than present-day levels according to both models, and they also both predict much lower runoff levels for July and August. Nevertheless, differences in runoff prediction between the OEZ and HBV scenarios are significant, and cannot be explained by differences in the reference meteorological data upon which they are based. Discrepancies seem to be caused by the differences in basin precipitation calculation, as expected. Because mass balance data are not available for the

calibration period, it is not possible to narrow down leeway in basin precipitation calculations. Thus the OEZ and HBV scenarios frame a range within which the “true” runoff scenarios are likely to fall. It is likely that the HBV scenarios form the lower end of this range due to basin precipitation as presented in *table 5.1.1* being lower than recorded precipitation for the same period.

Suspensions that the OEZ calibration for Abramov was not going to produce plausible scenario results were confirmed. HBV results for 50% glaciation seemed plausible, and differences between the “average” and “cool, wet” runs could be adequately explained by differences in reference meteorological data. The “cool, wet” scenario produced runoff similar to that observed under current climate and glaciation conditions, and the “average” scenario predicts a marked increase of runoff for August and September, which are also the two driest months. This is in stark contrast to the OEZ scenario where the greatest increase in runoff is predicted for June.

As predicted, the large differences in basin precipitation for model calibration also produced large differences in runoff for the Abramov 0% glaciation runs. It is likely that the runoff curve predicted by the OEZ rises, peaks and falls too steeply due to a degree-day factor which is too high. A June snowmelt peak approximately 50% higher than the current August ice melt peak does not seem at all realistic. This time, however, HBV scenarios also seem to stand on shaky ground in the light of the water balance values produced by model calibration (see *table 5.1.1*), and due to the influence of groundwater movement. The very low runoff levels predicted by both HBV scenarios appear to be caused at least in part by the model’s low basin precipitation, as well as by loss of water to groundwater intake. Basing HBV runoff scenarios on the means from two to three years, instead of single years, would help minimise the impact of groundwater movement (Hagg, personal communication).

6. Conclusion

Agreement between HBV and OEZ scenario results was best for the Oigaing and Ala Archa 50% glaciation runs. The effect of differences in model simulations of basin precipitation dominated the 0% glaciation runoff scenarios for Ala Archa and Abramov. This confirms the necessity of mass balance in order to constrict error. In addition to basin precipitation simulation, runoff scenarios are also very sensitive to the degree of glaciation change. The subjective alteration of glaciation extent can mean the difference between a prediction of higher runoff levels (compared to those under current climate and glaciation conditions) and a drastic reduction in runoff availability.

Adding the OEZ model to the study of the impact of climate change on runoff from glacierised Tien Shan catchments can be regarded as a success in two out of the three catchments. The alternative procedure used for adapting the OEZ for future climate is viable. The OEZ runoff scenarios were a valuable addition, adding insight to HBV predictions for all three catchments. The HBV and OEZ results compliment one another. The plausibility of OEZ mass balance simulation may be checked using both internal quality controls, as well as against externally derived values. This adds insight concerning confidence in both OEZ and HBV simulation of the water balance resulting from calibration, as well as the runoff scenarios based on these calibrations. The OEZ provides information about the mean around which future runoff can be expected to cluster. The HBV model provides information about runoff variability (amplitude of variation around the new mean) and associated flood and drought risk, which the OEZ cannot.

This study has shown that whilst the addition of the OEZ scenarios to the results of Hagg (2003) and Hagg et al. (2003) were successful and useful, there is potential for further refinement of analysis of the effects of climate change on glacierised catchments. HBV scenarios based on dry reference years would help test the full inter-annual variability of runoff under future climate conditions, in particular for catchments with pluvially dominated hydrology. HBV runoff scenarios based on single reference years risk being influenced by groundwater movement. Release from or intake into groundwater storage may significantly modify runoff predictions. A solution may be to additionally base runoff scenarios on the means of two to three reference years, rather than only single years, in order to minimise and analyse the influence of groundwater movement.

Where mass balance measurements are not available for constricting of error in water balance calculation, the OEZ's internal mass balance distribution may be used to test the sensitivity to, and the plausibility of, various mass balance settings (i.e. the basin storage value required as model input). This may add insight into the quality of runoff scenarios, especially where simulated mass balance can be checked against externally derived values such as ELA. Additionally, if mass balance simulation for current conditions can be checked and is proved accurate, it is worthwhile exploring whether the OEZ mass balance simulation produced by future climate may be reliably used to estimate future glaciation extent. Should this procedure succeed, it will enhance the

quality of runoff prediction. The OEZ model as used in this study is suitable for application to other Tien Shan catchments.

Further work which may involve a change in model structure includes incorporating an optimisation parameter into the OEZ model to allow differentiation between snow and ice melt. I also recommend officially incorporating combined temperature and precipitation adjustment into model procedure for adaptation for future climate, as well as a reduction of glaciation extent. Applying other runoff models to the study of the effects of climate change will add to the insight gained through the results of the HBV and OEZ models.

The findings of this study illustrate the seriousness of the impact that climate change may have on runoff from the Tien Shan and the urgency of the need to reduce CO₂ emissions to the atmosphere. The implication of the findings of especially the 0% glaciation runs for future water resource management in the region is the growing importance of being able to store runoff from spring snowmelt adequately, in order to compensate for loss of runoff during high and late summer.

References

Abramov glacier data reference book (1996), Central Asian regional research hydrometeorological institute, Tashkent

Aizen, V. B. and Aizen, E. M. (1994) Features of regime and mass exchange on some glaciers on central Asia periphery, Bulletin of Glacier research 21, p. 9 – 14, Tokyo

Aizen, V.B., Aizen., E. M. and Melack, J. M. (1996) Precipitation, melt and runoff in the northern Tien Shan , Journal of hydrology 186, p. 229 – 251, Amsterdam

Aizen, V. B., Aizen, E.M., Melack, J.M., Dozier, J (1997) Climate and Hydrologic changes in the Tien Shan, Central Asia, Journal of Climate, vol. 10 no. 6, p. 1393 – 1404

Aizen, V., Aizen, E., Glazirin, G., Loaiciga, H.A. (2000) Simulation of daily runoff in Central Asian alpine watersheds, Journal of Hydrology 238, p. 15-34

Bergström, S. and Forsman, A. (1973). Development of a conceptual deterministic rainfall-runoff model, Nordic Hydrology 4, p. 147-170.

Bergström, S. (1991) Principles and confidence in hydrological modelling, Nordic hydrology, vol. 22, p. 123 – 136

Bergström, S. (1992) The HBV Model – it's structure and applications, SMHI Reports Hydrology, No. 4, April 1992, Swedish meteorological and hydrological institute, Norrköping

Braun, L. & Aellen, M. (1990) Modelling discharge of glacierized basin assisted by direct measurements of glacier mass balance. In: Hydrology of Mountainous Regions: II Artificial Reservoirs; Water and slopes, ed. R. O. Sinniger Monbaron, IAHS publ. no. 193, p. 99 – 106.

Braun, L.N. and Renner, C.B. (1992) Application of a conceptual runoff model in different physiographic regions of Switzerland, Hydrological Sciences-Journal 37, 3, Zürich

CADB: Central Asia Data Base (online), University of Idaho, Idaho, USA

Chaohai, L. and Tianding, H. (1992) Relation between recent glacier variations and climate in the Tien Shan mountains, central Asia, Annals of Glaciology, vol 16., p. 11 – 16, Cambridge

Dyurgerov, M.B. et al (1992) Can the mass balance of the entire glacier area of the Tien Shan be estimated?, Annals of Glaciology, Vol. 16, International Glaciological society, p. 173 - 179

Escher-Vetter, H., Weber, M. and Braun, L. N. (1999) Auswirkungen von Klimaänderungen auf den Wasserhaushalt alpiner, teilweise vergletschertes Gebiete. Schlussbericht BayFORKLIM, Kommission f. Glaziologie, Bayerische Akademie der Wissenschaften. CD-ROM, ISBN 3 7696 3500, München

Fluctuations of glaciers, vol. II (1965 – 1970). Kasser, P. IAHS (ICSI)-UNESCO, 1973, Zürich

Fluctuations of glaciers, vol. III (1970 – 1975). Müller, F. IAHS (ICSI)-UNESCO, 1977, Zürich

Fluctuations of glaciers, vol. II (1975 – 1980). Haeberli, W. IAHS (ICSI)-UNESCO, 1985, Zürich

Hagg, Wilfried (2003) Auswirkungen von Gletscherschwund auf die Wasserspende hochalpiner Gebiete, Vergleich Alpen-Zentralalpen, Münchener Geographische Abhandlungen Reihe A, Münchener Universitätschriften Fakultät für Geowissenschaften, GEOBUCH-Verlag, München

Hagg, W., Braun, L. N., Weber, M., Becht, M (2003) Runoff modelling in glacierized Central Asian catchments for present-day and future climate, unpublished

Hottelet Ch., Braun L. N., Leibundgut Ch. & Rieg A. (1993) Simulation of snowpack and discharge in an alpine karst basin In: IAHS Publ. No. 218 "Snow and Ice", p. 249-260. Wallingford

KazNIIMOSK (1999) Climate change and a defence strategy against mudflows and snow avalanches. National report on the impact and adaption assessment for the mountain region of South and Southeast Kazakhstan and the Kazakh part of the Caspian Sea coastal sector, Netherlands climate change studies assistance programme, Kazakhstan climate change study Vol. 1, Almaty

KfG (1999) Klimaerwärmung – Gletscher. Wie verändern sich die Gebirgsabflüsse? Resultate aus Beobachtung und Modellierung. Kommission für Glaziologie der Bayerischen Akademie der Wissenschaften, CD-ROM ISBN 3 7696 3500 0, München

Klötzli, S. (1996) Umweltzerstörung und –Politik in Zentralasien, eine ökoregionale Systemuntersuchung, Peter Lang Europäische Hochschulschriften Reihe IV Geographie, Band 17, Bern

Konz, M. (2003) HBV3-ETH9 Handbook, Kommission für Glaziologie der Bayerischen Akademie der Wissenschaften, unpublished

Kuhn, M. (1981) Climate and glaciers. IAHS publication 131, p. 3 - 20

Kuhn, M., Nickus, U., Pellet, F. (1982) Die Niederschlagsverhältnisse im inneren Ötztal, 17. Intern. Tagung für Alpine Meteorologie, p. 235 – 237, Deutscher Wetterdienst, Offenbach

Kuhn, M. et al (1985) Fluctuations of climate and mass balance: Different responses of two adjacent glaciers, Zeitschrift für Gletscherkunde und Glazialgeologie Band 21, p. 409 – 416, Universitätsverlag Wagner, Innsbruck

Kuhn, M. and Pellet, F. (1989) Basin precipitation as residual in alpine water balances, Precipitation measurements (ed. by B. Sevruk), p. 275 – 277, WMO / IHAS / ETH workshop on precipitation measurements, St. Moritz, Switzerland, Dec. 1989

Kuhn, M., N. Batlogg, 1998: Glacier runoff in Alpine headwater in a changing climate. Hydrology, Water Resources and Ecology in Headwaters. (Proceedings of the Headwater '98 Conference held at Meran/Merano, Italy, April 1998). IAHS Publ. no. 248, p. 79-88.

Kuhn, M. and Batlogg, N. (1999) Modellierung der Auswirkung von Klimaänderung auf verschiedene Einzugsgebiete in Österreich, Band 46 Schriftenreihe der Forschung im Verbund, Österreichische Elektrizitätswirtschafts-Aktiengesellschaft (Verbundgesellschaft), Wien

Kuhn, M. (2000) Verification of a hydrometeorological model of Glacierised basins, Annals of Glaciology 31, p. 15-18

Kuhn, M. (2003) Redistribution of snow and glacier mass balance from a hydrometeorological model, Journal of Hydrology 282, p. 95-103

Rango (1992) Worldwide testing of the snowmelt runoff model with applications for predicting the effects of climate change, Nordic Hydrology 23, p. 155 – 172, Copenhagen

Viviroli, D. (2001) Zur hydrologischen Bedeutung der Gebirge, Diplomarbeit der Philosophisch-naturwissenschaftlichen Fakultät der Universität Bern, p. 104, unpublished

Appendix A: Full temperature & precipitation data series

Fig A1 Oigaing reference meteorological station: full precipitation series (data source: CADB)

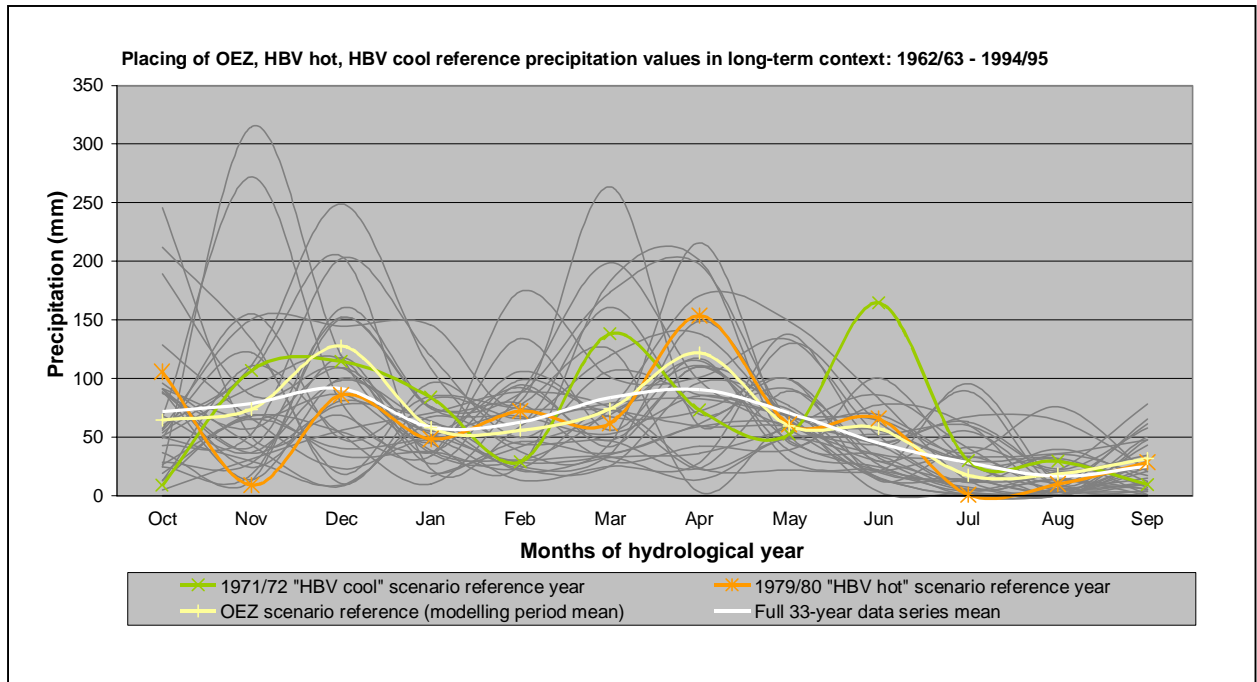


Fig A2 Oigaing reference meteorological station: full temperature series (data source: CADB)

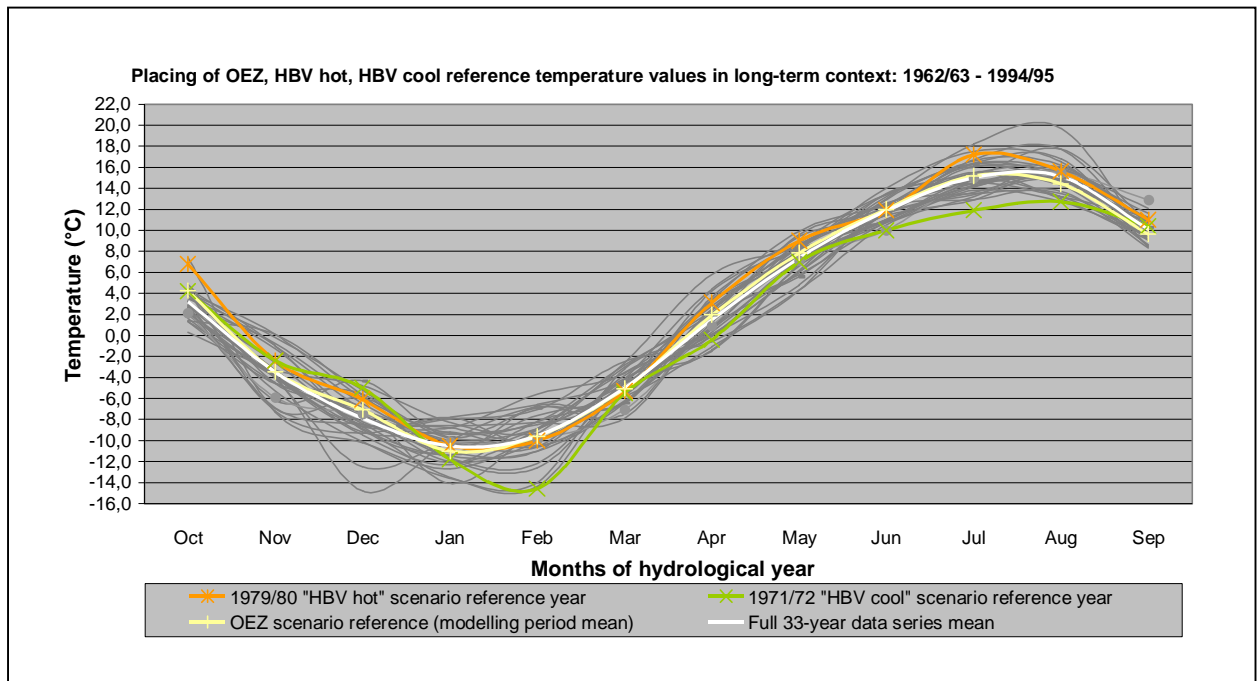


Fig A3 Ala Archa reference meteorological station: full precipitation series (data source: CADB)

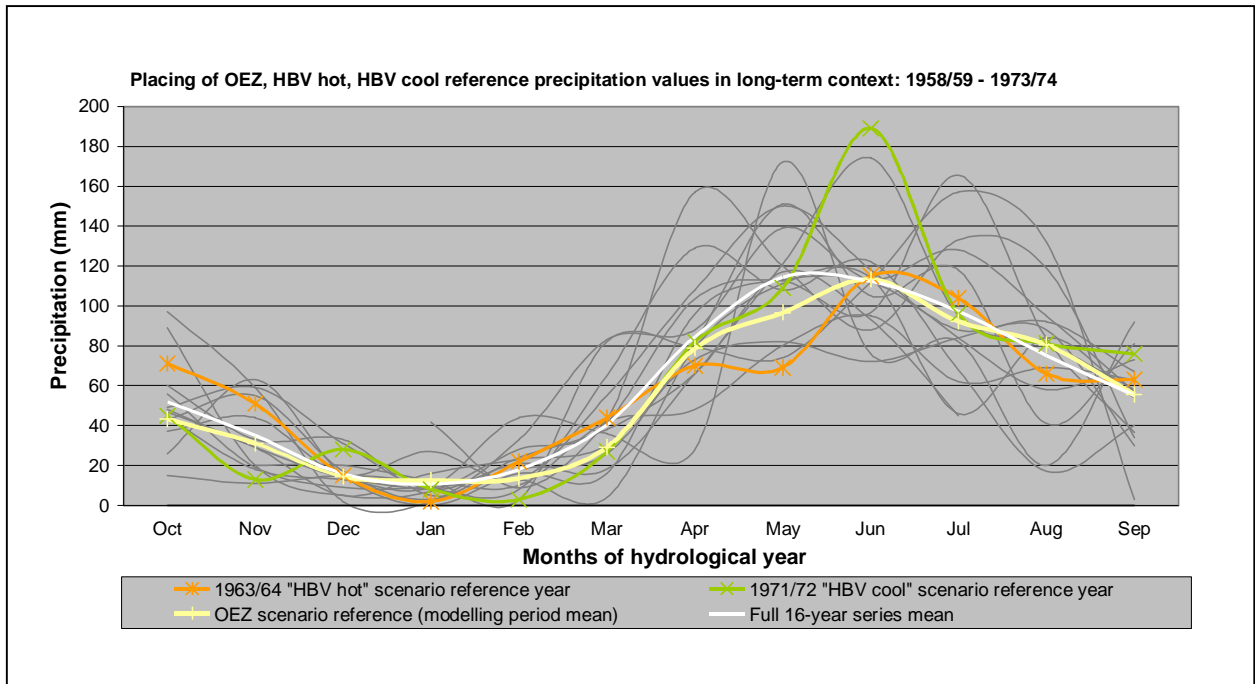


Fig A4 Ala Archa reference meteorological station: full temperature series (data source: CADB)

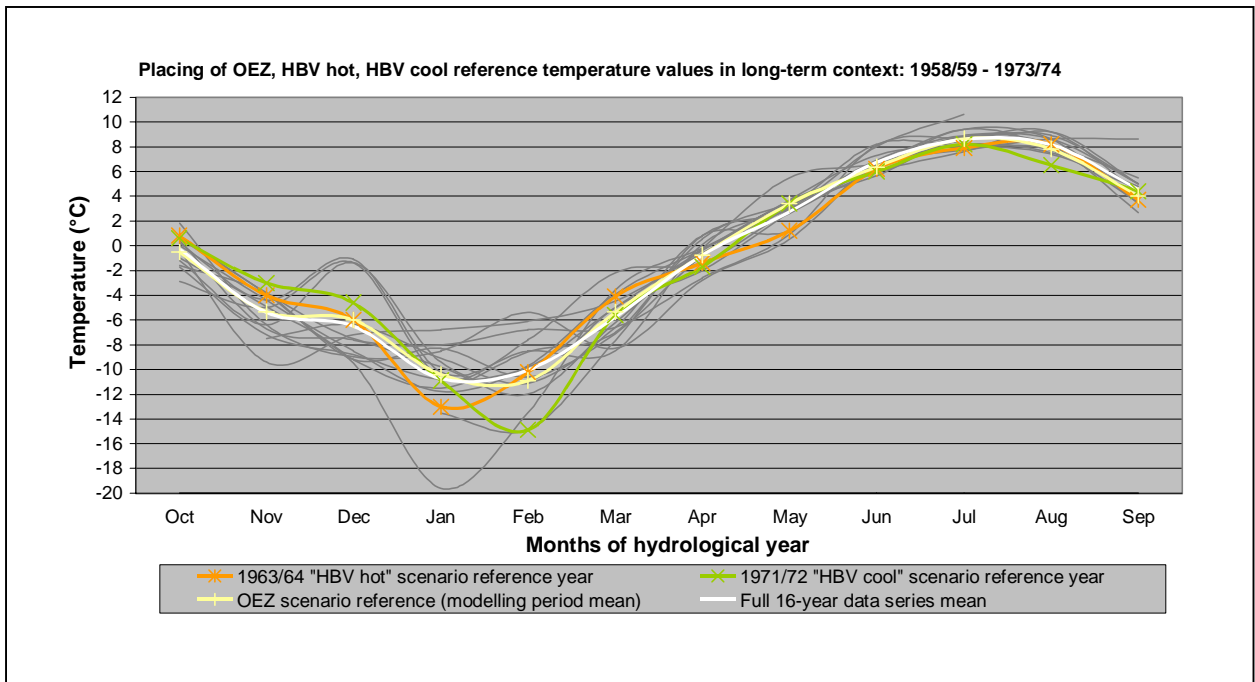


Fig A5 Abramov reference meteorological station: full precipitation series (data source: Abramov Glacier Data Reference Book)

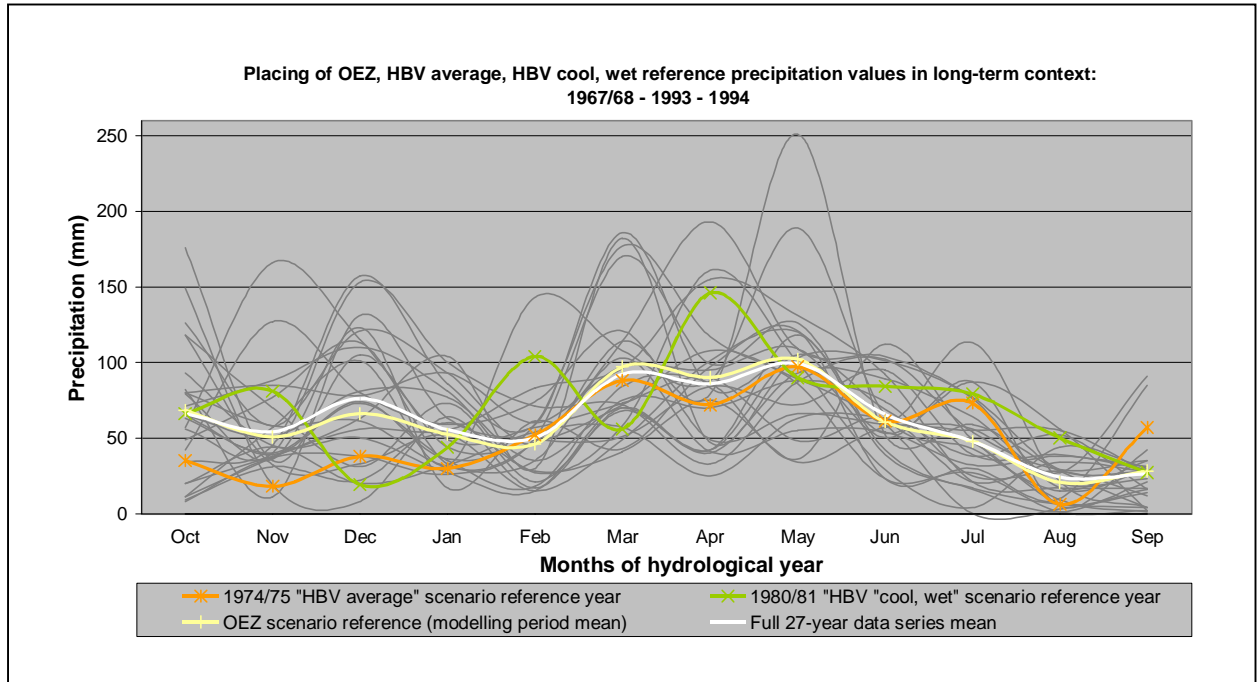
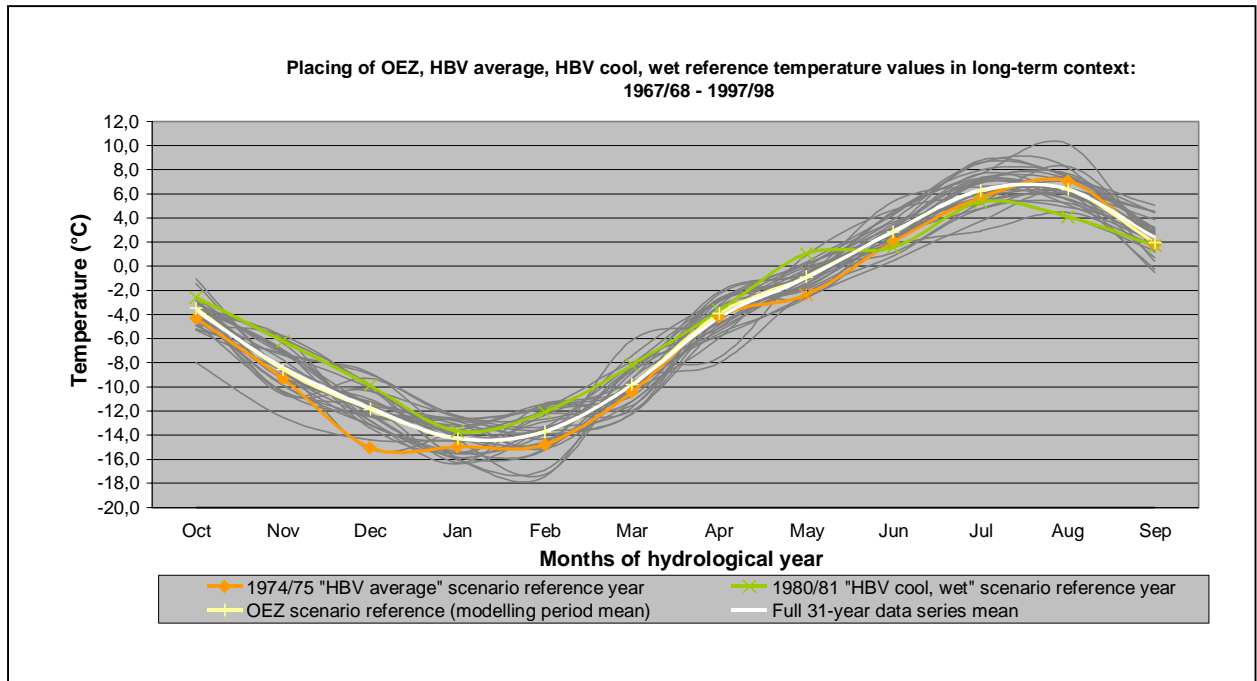


Fig A6 Abramov reference meteorological station: full temperature series (data source: Abramov Glacier Data Reference Book)



Appendix B: OEZ HBV comparison tables

The information in **tables 4.2.1 – 4.2.3** is taken from the following sources: Kuhn, M. and Batlogg, N. (1999), Kuhn, M. (2000), Kuhn, M. (2003), Hagg (2003), Konz (2003).

Table B1: Input data

<u>Feature</u>	<u>HBV</u>	<u>OEZ</u>
Topographical Input		
<u>Area-elevation distribution:</u>		
<i>Using</i>	<ul style="list-style-type: none"> • 200m elevation bands (variable) 	<ul style="list-style-type: none"> • 100m elevation bands
<i>further differentiated by</i>	<ul style="list-style-type: none"> • Glaciated and non-glaciated areas • Aspect (Classes: North; South; East, West and Horizontal) 	<ul style="list-style-type: none"> • Glaciated, non-glaciated, and forested areas
<i>Comments / limitations:</i>		<ul style="list-style-type: none"> ➤ Forest cover data not available, affecting modelling of Oigaing basin, which extends down to between 2000 and 2100 m
Hydrometeorological Input		
<u>Length of data series:</u>		
<i>(intended) minimum requirements</i>	<ul style="list-style-type: none"> • 8 years: 4 for calibration, 4 for validation 	<ul style="list-style-type: none"> • 2 – 3 decades (long-term averages), approx. 10 years of this series then used for validation
<i>Comments / limitations:</i>	<ul style="list-style-type: none"> ➤ Only Abramov has dataserie of required length for both calibration and validation. 	<ul style="list-style-type: none"> ➤ Only Abramov has dataserie of required length for both calibration and validation.
<u>Required data:</u>		
	<ul style="list-style-type: none"> • Mean daily temperature • Sum of daily precipitation • Mean daily measured runoffs 	<ul style="list-style-type: none"> • Mean monthly temperature • Sum of monthly precipitation • Calculated monthly temperature gradients
	<p><i>Not required, but advantageous, if available:</i></p> <ul style="list-style-type: none"> • Water equivalent of snow cover or snow depth of representative points of the catchment • Glacier mass balance 	<ul style="list-style-type: none"> • Calculated monthly precipitation gradients • Mean monthly runoff • Mean annual glacier net mass balance • Average duration of snowcover, for calculation of initial evaporation

Table B1 *continued*: Input data

<u>Feature</u>	<u>HBV</u>	<u>OEZ</u>
Hydrometeorological Input <i>continued</i>		
<u>Required data</u> <i>continued</i> :		
<i>Comments / limitations:</i>	<ul style="list-style-type: none"> ➤ Daily values not so widely available for Tien Shan catchments. ➤ If mass balance data are not used, there is a risk that wrongly calculated basin precipitation can be compensated using wrongly simulated mass balance, in order to produce correct runoff. Conversely, errors in ice melt rates can be compensated by erroneous precipitation inputs (Braun and Aellen, 1990). (<i>See also comment on optimisation parameters in table 4.2.2</i>). 	<ul style="list-style-type: none"> ➤ Calculation of temperature and precipitation gradients: requires more than one meteorological station per region, which is rarely the case, and in this study only possible for Ala Archa. Surrogate formulas were available for Oigaing (Zyx13), and the gradients attained, as well as their variation throughout the year seemed plausible for the catchment's climatic setting and recorded precipitation patterns for the calibration period. ➤ Annual net balance for glaciers: only available for Abramov. Reliable transferral of measured values from nearby catchments was not possible for Oigaing and Ala Archa, where surrogate values were derived using the hydrological mass balance determination method (see section 4.3). ➤ Average snowcover duration data are only available for the Ala Archa station itself (2945 m.a.s.l.). This is insufficient for a reliable estimation of average snowcover duration for the catchment as a whole. However, given it's elevation, it is reasonable to set evaporation in the 1st iteration at the 0.5mm/day minimum. This is also true for Abramov, but not so for Oigaing, because it stretches into lower elevation belts. However, 1st iteration evaporation nonetheless set at minimum, due to lack of data to do otherwise.

Table B2: Optimisation parameters

<u>Feature</u>	<u>HBV</u>	<u>OEZ</u>
Optimisation parameters	<ul style="list-style-type: none"> • Temperature gradient • Precipitation gradient • Coefficient – Snow correction • Coefficient – Rain correction • Factor – for aspect-dependent calculation of melt • Factor – for increased melt of ice compared to snow • Degree-day factor – min • Degree-day factor – max • Threshold value for snow/rain transition and snowmelt calculation • Retention of meltwater in snowpack • Coefficient – refreezing • Max soil moisture storage (field capacity) • Upper limit of potential evapotranspiration • Max evapotranspiration • Coefficient – outflow from soil • Limit for fast drainage, upper zone • Storage discharge constant – upper zone • Percolation capacity into lower zone • Storage discharge constant – lower zone 	<p><i>Intended</i></p> <ul style="list-style-type: none"> • Initial snowcover • Degree-day factor • Snow/rain threshold • Redistribution factor • Liquid storage <p><i>“Extra”</i></p> <ul style="list-style-type: none"> • Temperature gradient • Precipitation gradient
<i>Comments / limitations:</i>	<ul style="list-style-type: none"> ➤ These parameters have been listed in “routing order”, i.e. working from top to bottom of the model as depicted in Fig ➤ When a model has so many optimisation parameters, there is a risk that this can become a weakness by wrongly compensating for errors in the three main processes, namely: regionalisation of precipitation, snowcover build-up and melt, glacier melt. 	<ul style="list-style-type: none"> ➤ Temperature and precipitation gradients had to be treated as optimisation parameters in the case of Abramov, where they could be neither calculated (which was possible for Ala Archa), nor derived from formulae (as in Oigaing’s case).

Table B3: Future scenario adaption and prediction power

<u>Feature</u>	<u>HBV</u>	<u>OEZ</u>
<u>Adaption for scenarios:</u>	<ul style="list-style-type: none"> • Based on any one (or more) of the calibration years – permits a spectrum of results per runoff scenario, which vary according to the “meteorological character” of the reference years • Changes in meteorological values made for individual days until new monthly mean is replicated. • Glaciated area reduced 	<ul style="list-style-type: none"> • Based on the mean values used for model calibration – only one result per scenario. • Monthly values of temperature or precipitation changed by the same amount • Liquid storage readjusted to account for earlier or later melt.
<u>Comments / limitations:</u>	<ul style="list-style-type: none"> ➢ A spectrum of results per scenario provides a picture of the breadth of variability which can be expected as a result of climate change. ➢ No general shift of meteorological values, and therefore more realistic. e.g. increase in the number of hot days with additional convective rainfall. 	<ul style="list-style-type: none"> ➢ May give an idea of the norm around which future runoff can be expected to cluster ➢ General shift – less realistic / oversimplification ➢ Not reducing the glaciated area may mean predicted runoff is too high, because more meltwater is simulated that will realistically be available. ➢ (Readjustment of liquid storage provides a lot of room for manipulation)
<u>Changes to prescribed procedure of OEZ adaption to allow comparison of results to HBV:</u>		<ul style="list-style-type: none"> • Future scenarios for changes in both temperature <i>and</i> precipitation • New monthly values for temperature and precipitation adjusted by different amounts – monthly differentiation, which is more realistic than all months changing by the same amount. • Reduction of glaciated area
<u>Comments / limitations:</u>		<ul style="list-style-type: none"> ➢ These changes in the adaption procedure for future scenarios are, to the best of my knowledge, new territory for the OEZ model. This is an additional challenge to the short data series which the model has to work with.
<u>Prediction power:</u>	<ul style="list-style-type: none"> • Meteorological – i.e. simulation of weather patterns caused by climate change, and resultant runoff. • Indication of spectrum of future climate and runoff variability. 	<ul style="list-style-type: none"> • Climatological – i.e. average conditions over decades. • Indication of norm around which future runoff can be expected to cluster

Appendix C: Selected optimisation parameters

For aspect classes used for the calculation of the average June and August snowmelt see *tables 2.2.1 – 2.2.3* on page 7.

Table C1: Degree-day factors (mm w.e. $K^{-1} d^{-1}$) for Oigaing: HBV3 ETH9 matrix.

North	East West Horizontal	South
HBV3 ETH9 Summer Solstice		
Max. Ice: 2.7	Max Ice: 2.7	Max Ice: 2.7
Max Snow: 2.7	Max Snow: 2.7	Max Snow: 2.7
Min Ice: 1.5	Min Ice: 1.5	Min Ice: 1.5
Min Snow: 1.5	Min Snow: 1.5	Min Snow: 1.5
HBV3 ETH9 Winter solstice		

Degree-day factor total catchment mean for June snowmelt ca. $2.7 \text{ mm w.e. } K^{-1} d^{-1}$
 Degree-day factor mean for August icemelt (glacier area): $< 2.7 \text{ mm w.e. } K^{-1} d^{-1}$

Table C2: Degree-day factors (mm w.e. $K^{-1} d^{-1}$) for Ala Archa: HBV3 ETH9 matrix.

North	East West Horizontal	South
HBV3 ETH9 Summer Solstice		
Max. Ice: 3.4	Max Ice: 5.1	Max Ice: 7.65
Max Snow: 2.0	Max Snow: 3.0	Max Snow: 4.5
Min Ice: 1.14	Min Ice: 1.7	Min Ice: 2.55
Min Snow: 0.67	Min Snow: 1.0	Min Snow: 1.5
HBV3 ETH9 Winter solstice		

Degree-day factor total catchment mean for June snowmelt ca. $2.93 \text{ mm w.e. } K^{-1} d^{-1}$
 Degree-day factor mean for August icemelt (glacier area): $< 4.33 \text{ mm w.e. } K^{-1} d^{-1}$

Table C3: Degree-day factors (mm w.e. $K^{-1} d^{-1}$) for Abramov: HBV3 ETH9 matrix.

North	East West Horizontal	South
HBV3 ETH9 Summer Solstice		
Max. Ice: 5.72	Max Ice: 8.58	Max Ice: 12.87
Max Snow: 3.47	Max Snow: 5.2	Max Snow: 7.8
Min Ice: 2.19	Min Ice: 3.3	Min Ice: 4.95
Min Snow: 1.33	Min Snow: 2.0	Min Snow: 3.0
HBV3 ETH9 Winter solstice		

Degree-day factor total catchment mean for June snowmelt ca. $5.16 \text{ mm w.e. } K^{-1} d^{-1}$
 Degree-day factor mean for August icemelt (glacier area): $< 7.4 \text{ mm w.e. } K^{-1} d^{-1}$

Table C4: OEZ and HBV3 ETH9 Temperature gradients (°C/100m)

OEZ													HBV	
	Oct	Nov	Dec	Jan	Feb	Mar	Apr	May	Jun	Jul	Aug	Sep	Mean	Mean
O	-0.6	-0.7	-0.7	-0.7	-0.7	-0.6	-0.6	-0.5	-0.5	-0.5	-0.5	-0.6	-0.61	-0.65
AA	-0.4	-0.6	0.0	-0.3	-0.3	-0.4	-0.6	-0.6	-0.6	-0.5	-0.5	-0.4	-0.43	-0.65
Abr	-0.3	-0.3	-0.3	-0.3	-0.3	-0.5	-0.6	-0.6	-0.4	-0.6	-0.4	-0.3	-0.40	-0.65

O = Oigiang (OEZ gradients derived using formulae from Aizen et al. (2000))

AA = Ala Archa (OEZ gradients calculated using temperature data from CADB)

Abr = Abramov (OEZ gradients treated as optimisation parameters)

Table C5: OEZ and HBV3 ETH9 Precipitation gradients (%/100m)

OEZ													HBV	
	Oct	Nov	Dec	Jan	Feb	Mar	Apr	May	Jun	Jul	Aug	Sep	Mean	Mean
O	6.7	5.4	5.1	4.1	4.5	4.7	5.3	6.5	8.4	8.9	6.7	5.7	6.0	4.0
AA	0.1	0.4	2.2	3.2	2.2	2.5	1.3	2.9	8.1	8.0	10.1	8.3	2.4	5.0
Abr	5.0	5.0	5.0	5.0	5.0	10.0	8.0	10.0	8.0	5.0	5.0	5.0	6.3	5.0

O = Oigiang (OEZ gradients derived using formulae from Aizen et al. (2000))

AA = Ala Archa (OEZ gradients calculated using precipitation data from CADB)

Abr = Abramov (OEZ gradients treated as optimisation parameters)

Appendix D: Sensitivity of runoff scenarios to the redistribution factor and to groundwater readjustment

Fig D1 demonstrates the difference in the outcome of OEZ runoff scenarios depending on whether the redistribution factor is set to 1 (no differentiation of snow accumulation), or 2 (twice as much accumulation on glaciers relative to snow).

Fig D1: Effect of redistribution factor on runoff Scenarios

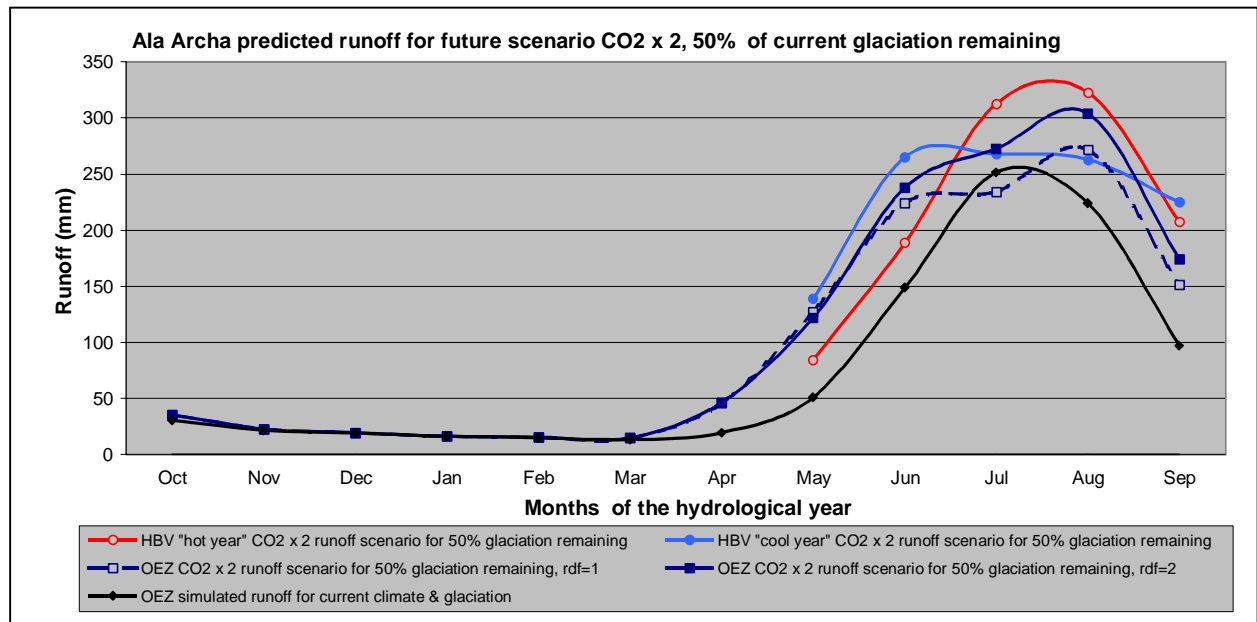
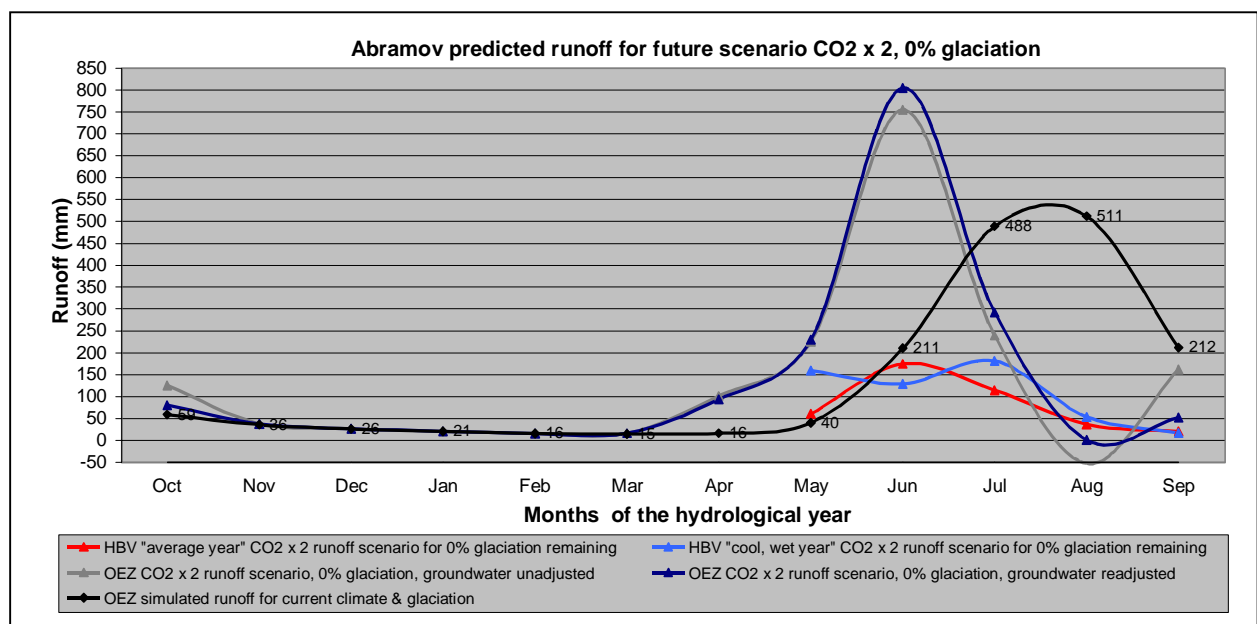


Fig D2 demonstrates the sensitivity of summer runoff (especially late summer) to the readjustment of groundwater movement which adaptation of the OEZ for future climate necessitates. This illustrates how much room for subjectivity adapting the model for future climate leaves the modeller.

Fig D2: Sensitivity of OEZ scenario for Abramov with complete loss of glaciation to groundwater readjustment



Appendix E: Logical progression of OEZ runoff change

Table E1 Oigaing: OEZ Simulated monthly runoff (mm) for CO₂ x 2 climate change, with 100%, 50% and 0% of current glaciation extent remaining

	Oct	Nov	Dec	Jan	Feb	Mar	Apr	May	Jun	July	Aug	Sep	W	S	Y
CCG	41	29	23	21	18	16	17	85	194	233	137	73	164	722	886
100%	47	29	24	21	18	16	113	277	306	226	165	96	267	1070	1338
50%	47	29	24	21	18	16	113	264	267	206	91	60	267	889	1156
0%	47	29	24	21	18	16	113	259	241	163	79	47	267	788	1055

CCG = Runoff for current climate and glaciation

W = Winter runoff (October to April)

S = Summer runoff (May to September)

Y = Annual runoff

Table E2 Ala Archa: OEZ Simulated monthly runoff (mm) for CO₂ x 2 climate change, with 100%, 50% and 0% of current glaciation extent remaining

	Oct	Nov	Dec	Jan	Feb	Mar	Apr	May	Jun	July	Aug	Sep	W	S	Y
CCG	30	21	19	16	15	13	19	54	147	247	226	93	134	767	901
100%	59	22	19	16	15	15	46	119	333	456	513	283	192	1704	1896
50%	35	22	19	16	15	15	46	122	238	272	304	174	169	1109	1278
0%	29	22	19	16	15	15	46	134	218	128	125	92	163	696	859

CCG = Runoff for current climate and glaciation

W = Winter runoff (October to April)

S = Summer runoff (May to September)

Y = Annual runoff

Table E3 Abramov: OEZ Simulated monthly runoff (mm) for CO₂ x 2 climate change, with 100%, 50% and 0% of current glaciation extent remaining

	Oct	Nov	Dec	Jan	Feb	Mar	Apr	May	Jun	July	Aug	Sep	W	S	Y
CCG	59	36	26	21	16	15	16	41	203	484	511	224	189	1463	1653
100%	85	38	27	21	16	16	88	189	731	975	1072	617	291	3585	3876
50%	81	38	27	21	16	16	94	230	654	502	491	307	294	2185	2479
0%	81	38	27	21	16	16	94	230	805	292	1	52	294	1381	1675

CCG = Runoff for current climate and glaciation

W = Winter runoff (October to April)

S = Summer runoff (May to September)

Y = Annual runoff

Appendix F: Comparison of runoff scenarios, 50% glaciation

Fig F1 Oigaing: Meteorological context of HBV & OEZ runoff curves

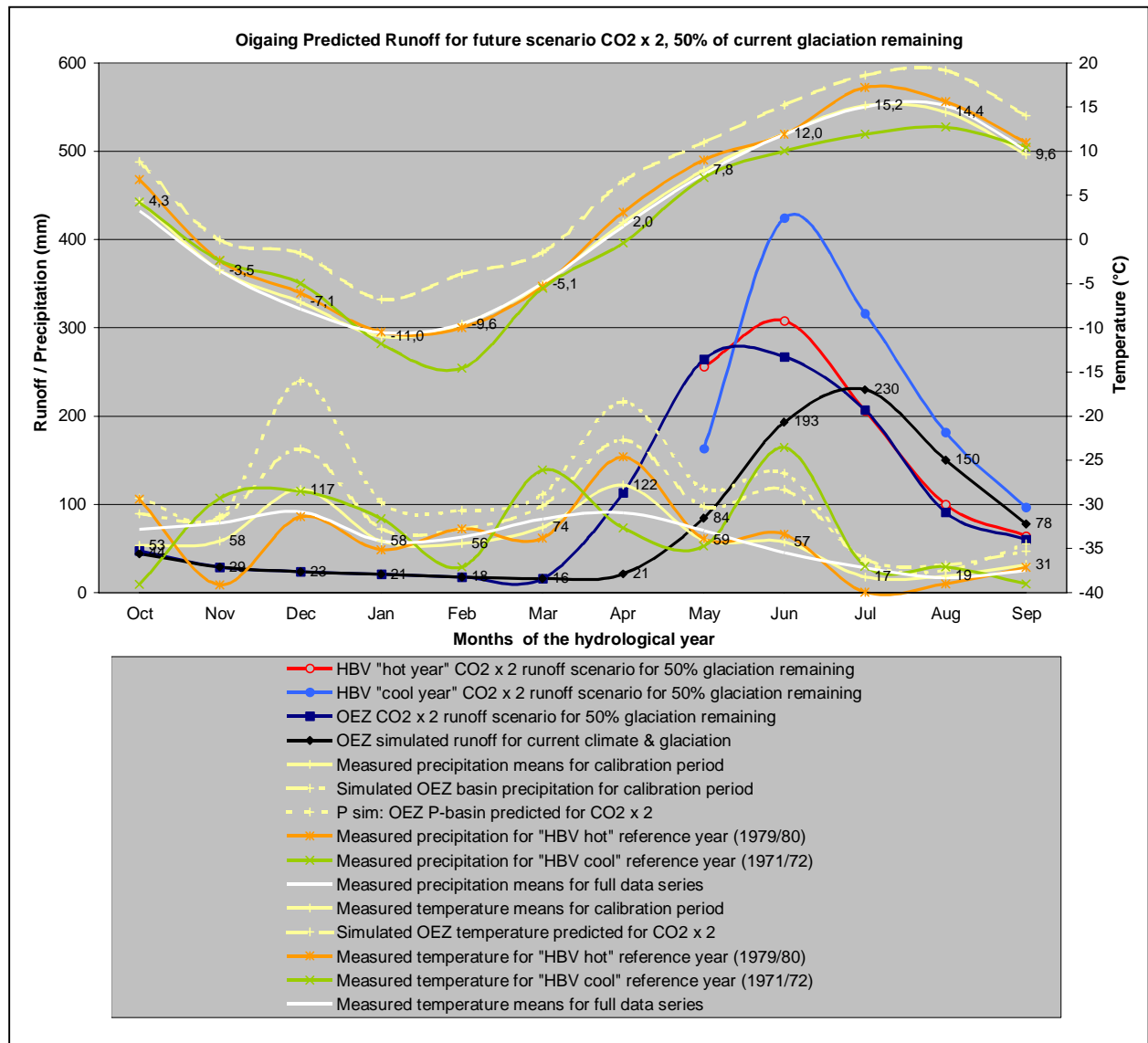


Table F2 Oigaing: Data displayed by Fig F1

	Oct	Nov	Dec	Jan	Feb	Mar	Apr	May	Jun	Jul	Aug	Sep	Oct - Apr	May - Sep	Jul - Aug	Year
OEZ simulated current runoff	41	29	23	21	18	16	17	85	194	233	137	73	164	722	369	886
OEZ CO2 x 2 runoff scenario	47	29	24	21	18	16	113	264	267	206	91	60	267	889	297	1156
HBV "hot year" CO2 x 2 runoff scenario								256	308	206	100	64		933	305	
HBV "cool year" CO2 x 2 runoff scenario								163	424	316	181	96		1181	498	
P meas: mean total data series	72	79	91	58	63	84	90	70	45	28	17	25	537	185	44	721
P meas: calibration period mean	53	58	117	58	56	74	122	59	57	17	19	31	538	184	36	722
P sim: OEZ P-basin for calibration period	89	84	163	72	72	98	173	97	116	38	31	47	751	329	69	1080
P sim: OEZ P-basin predicted for CO2 x 2	107	86	239	103	93	111	216	118	135	36	25	55	955	368	61	1323
P meas: HBV hot ref year (1979/80)	106	9	86	48	72	62	154	61	66	1	10	29	536	166	10	702
P meas: HBV cool ref year (1971/72)	9	107	114	84	29	138	73	52	164	30	29	10	554	285	59	840
T meas: mean total data series	3,3	-3,5	-7,9	-10,5	-9,6	-4,9	1,5	7,4	11,9	15,0	15,1	10,1	-4,5	11,9	15,1	2,3
T meas: calibration period mean	4,3	-3,5	-7,1	-11,0	-9,6	-5,1	2,0	7,8	12,0	15,2	14,4	9,6	-4,3	11,8	14,8	2,4
T sim: HBV predicted for CO2 x 2	8,8	-0,1	-1,6	-6,8	-3,9	-1,5	6,6	10,9	15,2	18,6	19,1	14,0	0,2	15,6	18,8	6,6
T meas: HBV hot ref year (1979/80)	6,8	-2,4	-6,1	-10,5	-10,0	-5,3	3,1	9,0	11,9	17,2	15,6	11,0	-3,5	12,9	16,4	3,4
T meas: HBV cool ref year (1971/72)	4,2	-2,4	-5,0	-11,8	-14,6	-5,5	-0,4	7,0	10,0	11,9	12,7	10,4	-5,1	10,4	12,3	1,4

P = Precipitation
T = Temperature
Meas = Measured
Sim = Simulated

Fig F3 Ala Archa: Meteorological context of HBV & OEZ runoff curves

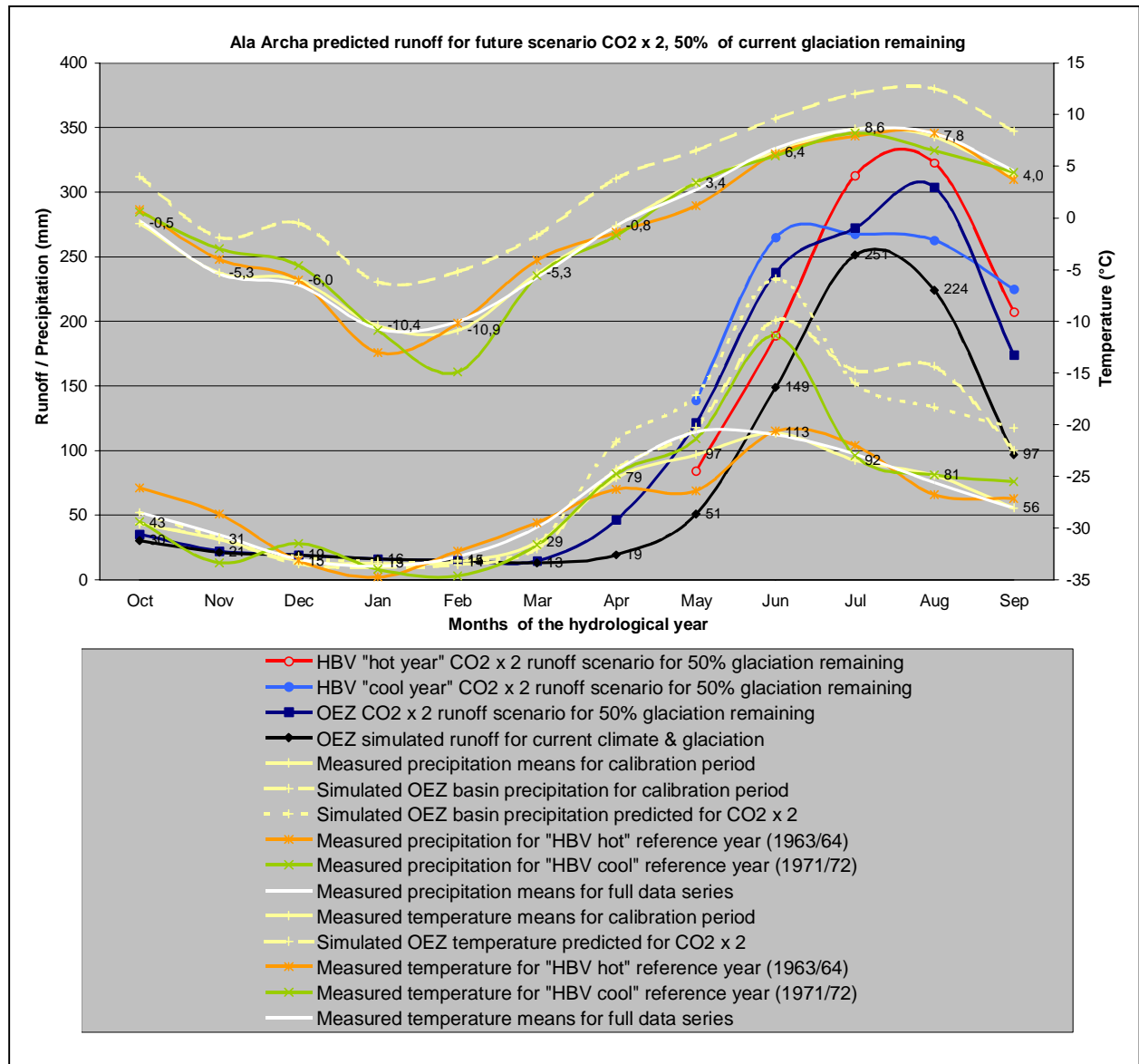


Table F4 Ala Archa: Data displayed by Fig F3

	Oct	Nov	Dec	Jan	Feb	Mar	Apr	May	Jun	Jul	Aug	Sep	Oct - Apr	May - Sep	Jul - Aug	Year
OEZ simulated current runoff	30	21	19	16	15	13	19	54	147	247	226	93	134	767	473	901
OEZ CO2 x 2 runoff scenario	35	22	19	16	15	15	46	122	238	272	304	174	169	1109	576	1278
HBV "hot year" CO2 x 2 runoff scenario								84	189	313	323	207		1116	635	
HBV "cool year" CO2 x 2 runoff scenario								139	265	268	263	225		1159	530	
P meas: mean total data series	52	35	16	11	18	41	85	114	112	97	75	55	256	454	172	710
P meas: calibration period mean	43	31	15	13	14	29	79	97	113	92	81	56	223	438	173	662
P sim: OEZ P-basin for calibration period	43	32	12	10	11	24	85	118	201	162	165	100	218	746	327	964
P sim: OEZ P-basin predicted for CO2 x 2	52	32	18	14	15	27	107	143	233	152	134	117	265	779	286	1044
P meas: HBV hot ref year (1963/64)	71	51	15	2	22	44	70	69	115	104	66	63	275	417	170	692
P meas: HBV cool ref year (1971/72)	45	13	28	8	3	27	82	109	189	96	81	76	206	551	177	757
T meas: mean total data series	-0,3	-5,4	-6,5	-10,7	-10,0	-5,7	-0,8	2,7	6,7	8,6	8,2	4,6	-5,6	6,2	8,4	-0,7
T meas: calibration period mean	-0,5	-5,3	-6,0	-10,4	-10,9	-5,3	-0,8	3,4	6,4	8,6	7,8	4,0	-5,6	6,0	8,2	-0,8
T sim: OEZ predicted for CO2 x 2	4,0	-1,9	-0,5	-6,2	-5,2	-1,7	3,8	6,5	9,6	12,0	12,5	8,4	-1,1	9,8	12,3	3,4
T meas: HBV hot ref year (1963/64)	0,8	-4,0	-6,0	-13,0	-10,2	-4,1	-1,4	1,2	6,2	7,9	8,2	3,7	-5,4	5,4	8,1	-0,9
T meas: HBV cool ref year (1971/72)	0,6	-3,0	-4,6	-10,9	-14,9	-5,6	-1,7	3,4	6,0	8,2	6,5	4,4	-5,7	5,7	7,4	-1,0

P = Precipitation
T = Temperature
Meas = Measured
Sim = Simulated

Fig F5 Abramov: Meteorological context of HBV & OEZ runoff curves

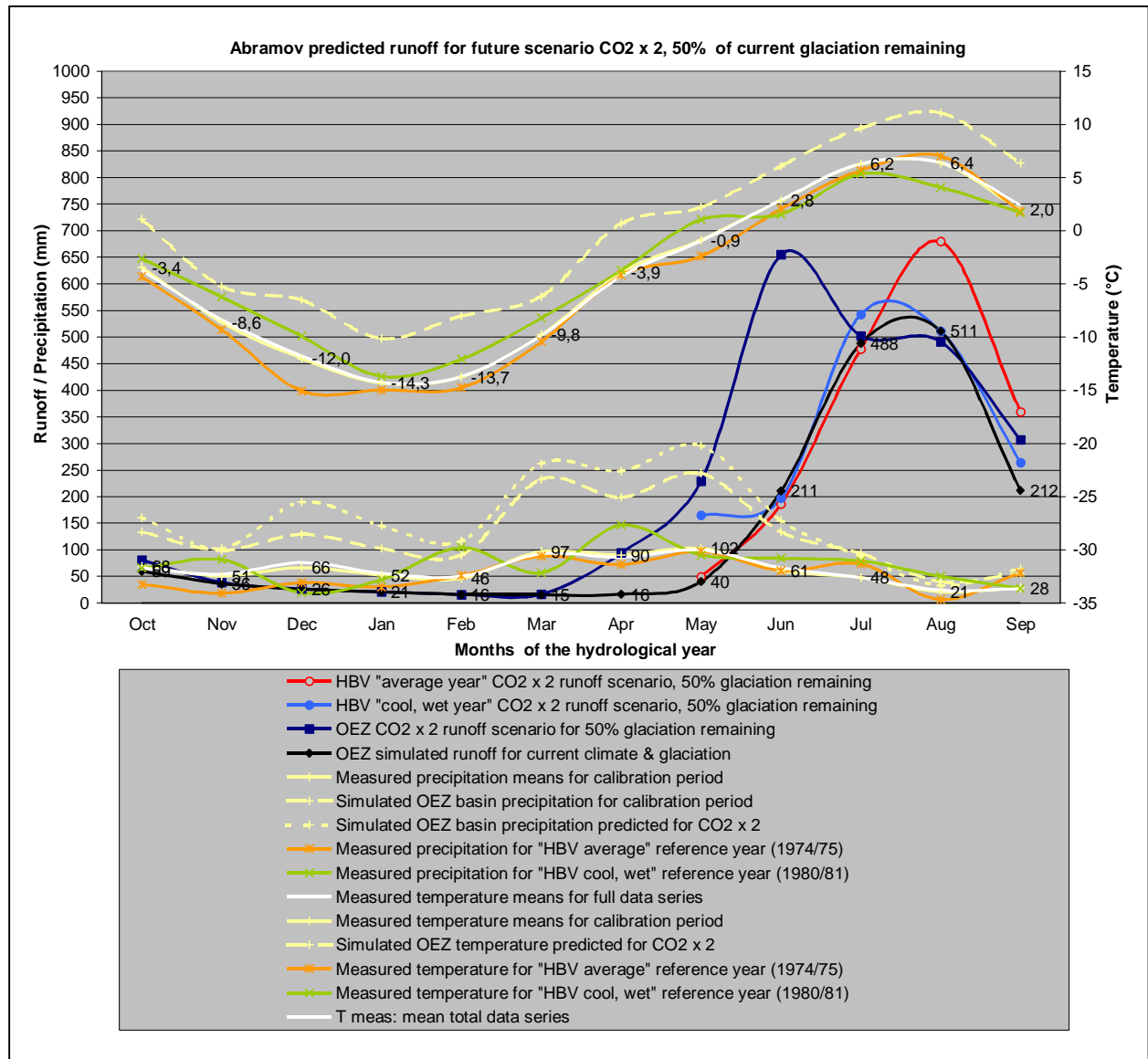


Table F6 Abramov: Data displayed by Fig F5

	Oct	Nov	Dec	Jan	Feb	Mar	Apr	May	Jun	Jul	Aug	Sep	Oct - Apr	May - Sep	Jul - Aug	Year
OEZ simulated current runoff	59	36	26	21	16	15	16	41	203	484	511	224	189	1463	995	1653
OEZ CO ₂ x 2 runoff scenario	81	38	27	21	16	16	94	230	654	502	491	307	294	2185	994	2479
HBV "hot year" CO ₂ x 2 runoff scenario								50	186	478	680	360		1752	1157	
HBV "cool year" CO ₂ x 2 runoff scenario								165	197	543	512	264		1680	1054	
P meas: mean total data series	66	54	76	55	50	92	86	100	66	48	24	26	480	263	72	744
P meas: calibration period mean	68	51	66	52	46	97	90	102	61	48	21	28	471	260	69	730
P sim: OEZ P-basin for calibration period	133	99	129	102	90	232	198	244	134	93	40	55	984	567	134	1551
P sim: OEZ P-basin predicted for CO ₂ x 2	160	102	190	145	116	262	248	296	155	88	33	64	1223	636	121	1859
P meas: HBV hot ref year (1974/75)	35	18	38	30	52	88	72	97	61	73	6	57	333	294	79	627
P meas: HBV cool ref year (1980/81)	66	81	19	44	104	56	146	90	84	79	50	27	516	330	129	846
T meas: mean total data series	-3,7	-8,4	-11,8	-14,3	-13,7	-9,8	-4,3	-1,0	2,9	6,3	6,4	2,4	-9,4	3,4	6,3	-4,1
T meas: calibration period mean	-3,4	-8,6	-12,0	-14,3	-13,7	-9,8	-3,9	-0,9	2,8	6,2	6,4	2,0	-9,4	3,3	6,3	-4,1
T sim: OEZ predicted for CO ₂ x 2	1,1	-5,2	-6,5	-10,1	-8,0	-6,2	0,7	2,2	6,0	9,6	11,1	6,4	-4,9	7,1	10,4	0,1
T meas: HBV hot ref year (1974/75)	-4,3	-9,3	-15,1	-15,0	-14,8	-10,4	-4,2	-2,4	2,1	5,7	7,0	1,8	-10,4	2,8	6,4	-4,9
T meas: HBV cool ref year (1980/81)	-2,6	-6,2	-9,9	-13,7	-12,1	-8,2	-3,7	1,0	1,5	5,3	4,1	1,7	-8,1	2,7	4,7	-3,6

P = Precipitation
T = Temperature
Meas = Measured
Sim = Simulated

Appendix G: Comparison of runoff scenarios, 0% glaciation

Fig G1 Oigaiing: Meteorological context of HBV & OEZ runoff curves

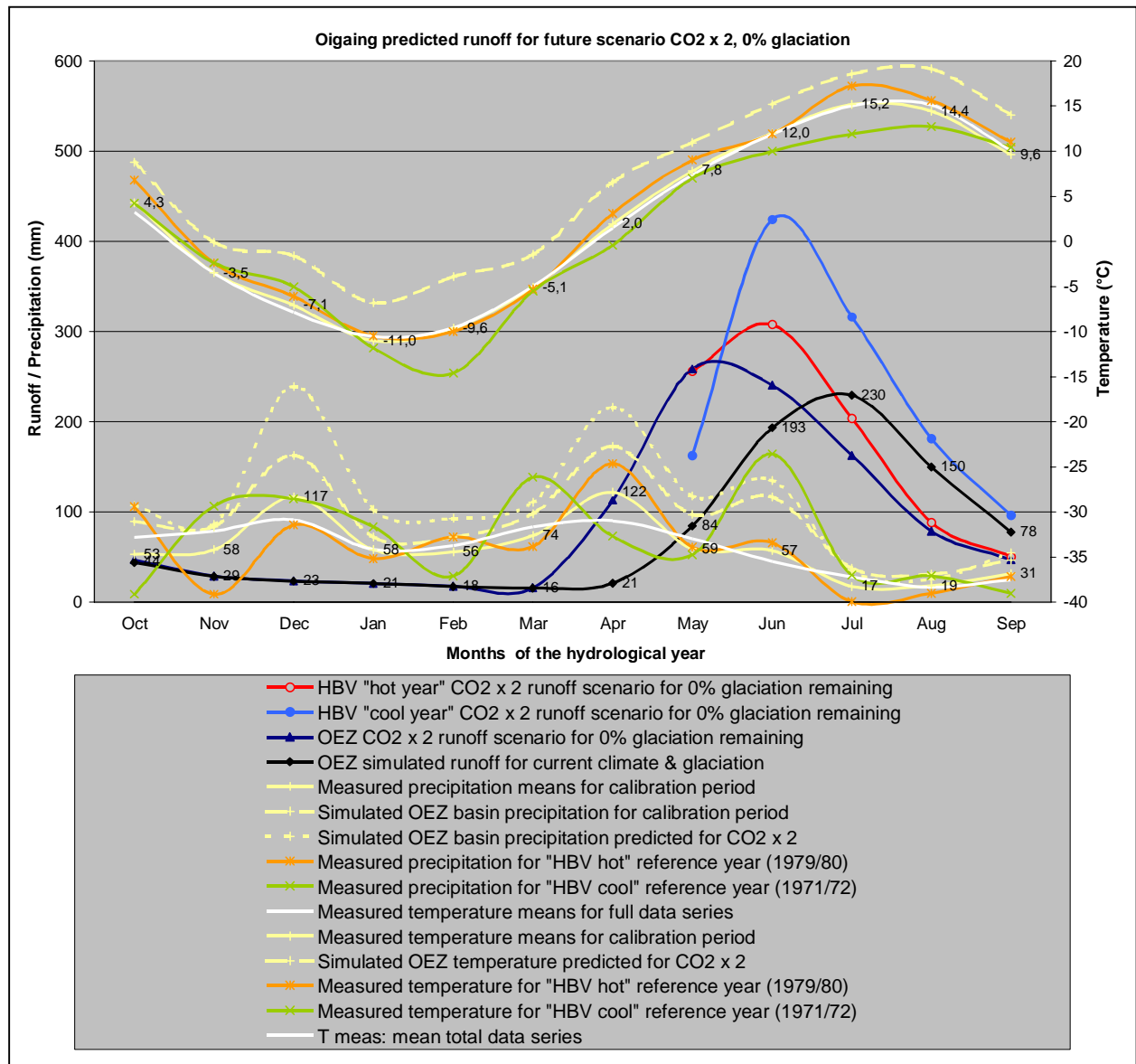


Table G2 Oigaiing: Data displayed by Fig G1

	Oct	Nov	Dec	Jan	Feb	Mar	Apr	May	Jun	Jul	Aug	Sep	Oct - Apr	May - Sep	Jul - Aug	Year
OEZ simulated current runoff	41	29	23	21	18	16	17	85	194	233	137	73	164	722	369	886
OEZ CO ₂ x 2 runoff scenario	47	29	24	21	18	16	113	259	241	163	79	47	267	788	242	1055
HBV "hot year" CO ₂ x 2 runoff scenario								256	308	204	89	50		907	292	
HBV "cool year" CO ₂ x 2 runoff scenario								163	424	316	181	96		1181	498	
P meas: mean total data series	72	79	91	58	63	84	90	70	45	28	17	25	537	185	44	721
P meas: calibration period mean	53	58	117	58	56	74	122	59	57	17	19	31	538	184	36	722
P sim: OEZ P-basin for calibration period	89	84	163	72	72	98	173	97	116	38	31	47	751	329	69	1080
P sim: OEZ P-basin predicted for CO ₂ x 2	107	86	239	103	93	111	216	118	135	36	25	55	955	368	61	1323
P meas: HBV hot ref year (1979/80)	106	9	86	48	72	62	154	61	66	1	10	29	536	166	10	702
P meas: HBV cool ref year (1971/72)	9	107	114	84	29	138	73	52	164	30	29	10	554	285	59	840
T meas: mean total data series	3,3	-3,5	-7,9	-10,5	-9,6	-4,9	1,5	7,4	11,9	15,0	15,1	10,1	-4,5	11,9	15,1	2,3
T meas: calibration period mean	4,3	-3,5	-7,1	-11,0	-9,6	-5,1	2,0	7,8	12,0	15,2	14,4	9,6	-4,3	11,8	14,8	2,4
T sim: OEZ predicted for CO ₂ x 2	8,8	-0,1	-1,6	-6,8	-3,9	-1,5	6,6	10,9	15,2	18,6	19,1	14,0	0,2	15,6	18,8	6,6
T meas: HBV hot ref year (1979/80)	6,8	-2,4	-6,1	-10,5	-10,0	-5,3	3,1	9,0	11,9	17,2	15,6	11,0	-3,5	12,9	16,4	3,4
T meas: HBV cool ref year (1971/72)	4,2	-2,4	-5,0	-11,8	-14,6	-5,5	-0,4	7,0	10,0	11,9	12,7	10,4	-5,1	10,4	12,3	1,4

P = Precipitation
 T = Temperature
 Meas = Measured
 Sim = Simulated

Fig G3 Ala Archa: Meteorological context of HBV & OEZ runoff curves

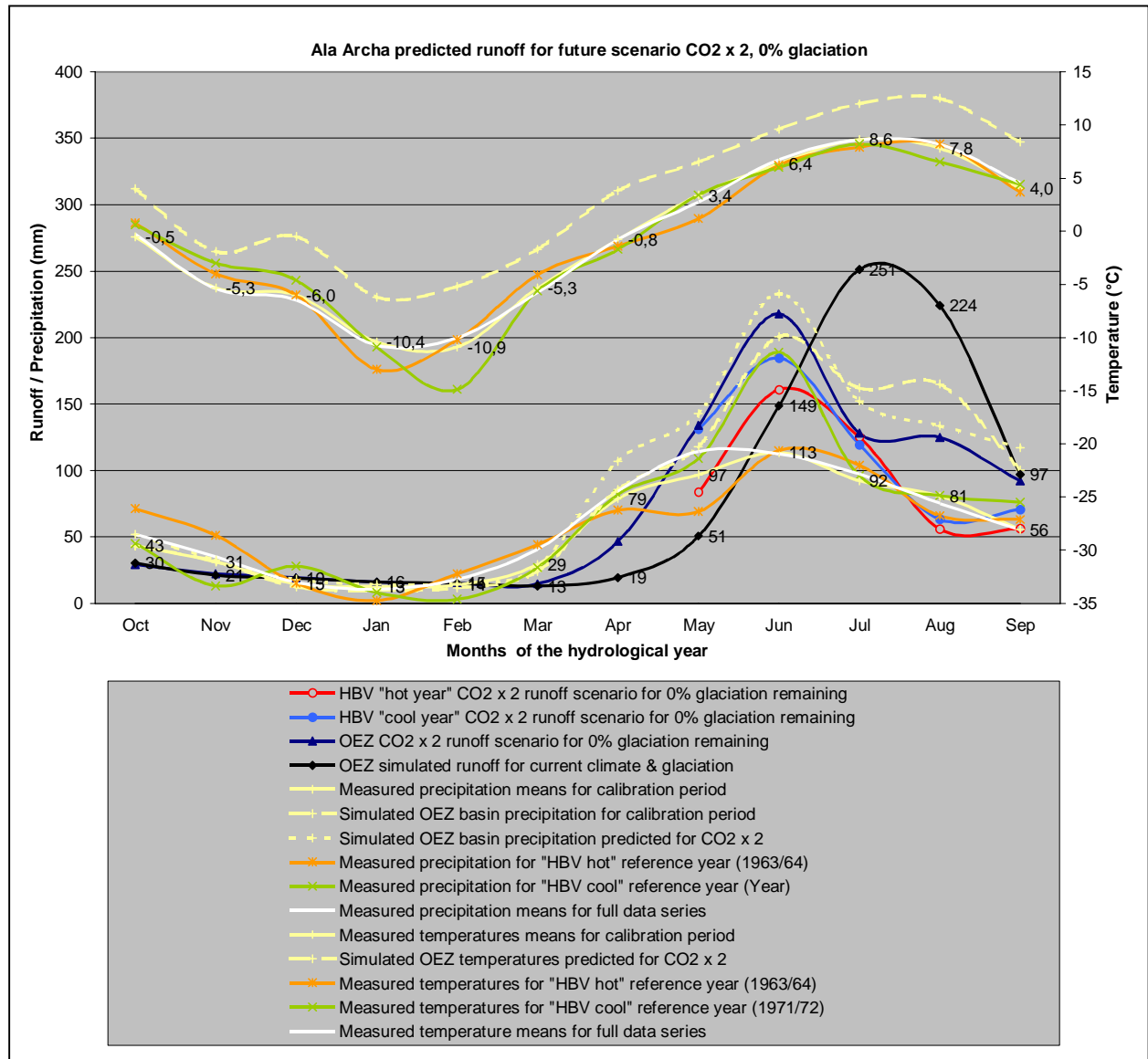


Table G4 Ala Archa: Data displayed by Fig G3

	Oct	Nov	Dec	Jan	Feb	Mar	Apr	May	Jun	Jul	Aug	Sep	Oct - Apr	May - Sep	Jul - Aug	Year
OEZ simulated current runoff	30	21	19	16	15	13	19	54	147	247	226	93	134	767	473	901
OEZ CO ₂ x 2 runoff scenario	29	22	19	16	15	15	46	134	218	128	125	92	163	696	253	859
HBV "hot year" CO ₂ x 2 runoff scenario								84	161	125	56	56		482	181	
HBV "cool year" CO ₂ x 2 runoff scenario								131	184	120	63	71		569	183	
P meas: mean total data series	52	35	16	11	18	41	85	114	112	97	75	55	256	454	172	710
P meas: calibration period mean	43	31	15	13	14	29	79	97	113	92	81	56	223	438	173	662
P sim: OEZ P-basin for calibration period	43	32	12	10	11	24	85	118	201	162	165	100	218	746	327	964
P sim: OEZ P-basin predicted for CO ₂ x 2	52	32	18	14	15	27	107	143	233	152	134	117	265	779	286	1044
P meas: HBV hot ref year (1963/64)	71	51	15	2	22	44	70	69	115	104	66	63	275	417	170	692
P meas: HBV cool ref year (1971/72)	45	13	28	8	3	27	82	109	189	96	81	76	206	551	177	757
T meas: mean total data series	-0,3	-5,4	-6,5	-10,7	-10,0	-5,7	-0,8	2,7	6,7	8,6	8,2	4,6	-5,6	6,2	8,4	-0,7
T meas: calibration period mean	-0,5	-5,3	-6,0	-10,4	-10,9	-5,3	-0,8	3,4	6,4	8,6	7,8	4,0	-5,6	6,0	8,2	-0,8
T sim: OEZ predicted for CO ₂ x 2	4,0	-1,9	-0,5	-6,2	-5,2	-1,7	3,8	6,5	9,6	12,0	12,5	8,4	-1,1	9,8	12,3	3,4
T meas: HBV hot ref year (1963/64)	0,8	-4,0	-6,0	-13,0	-10,2	-4,1	-1,4	1,2	6,2	7,9	8,2	3,7	-5,4	5,4	8,1	-0,9
T meas: HBV cool ref year (1971/72)	0,6	-3,0	-4,6	-10,9	-14,9	-5,6	-1,7	3,4	6,0	8,2	6,5	4,4	-5,7	5,7	7,4	-1,0

P = Precipitation
 T = Temperature
 Meas = Measured
 Sim = Simulated

Fig G5 Abramov: Meteorological context of HBV & OEZ runoff curves

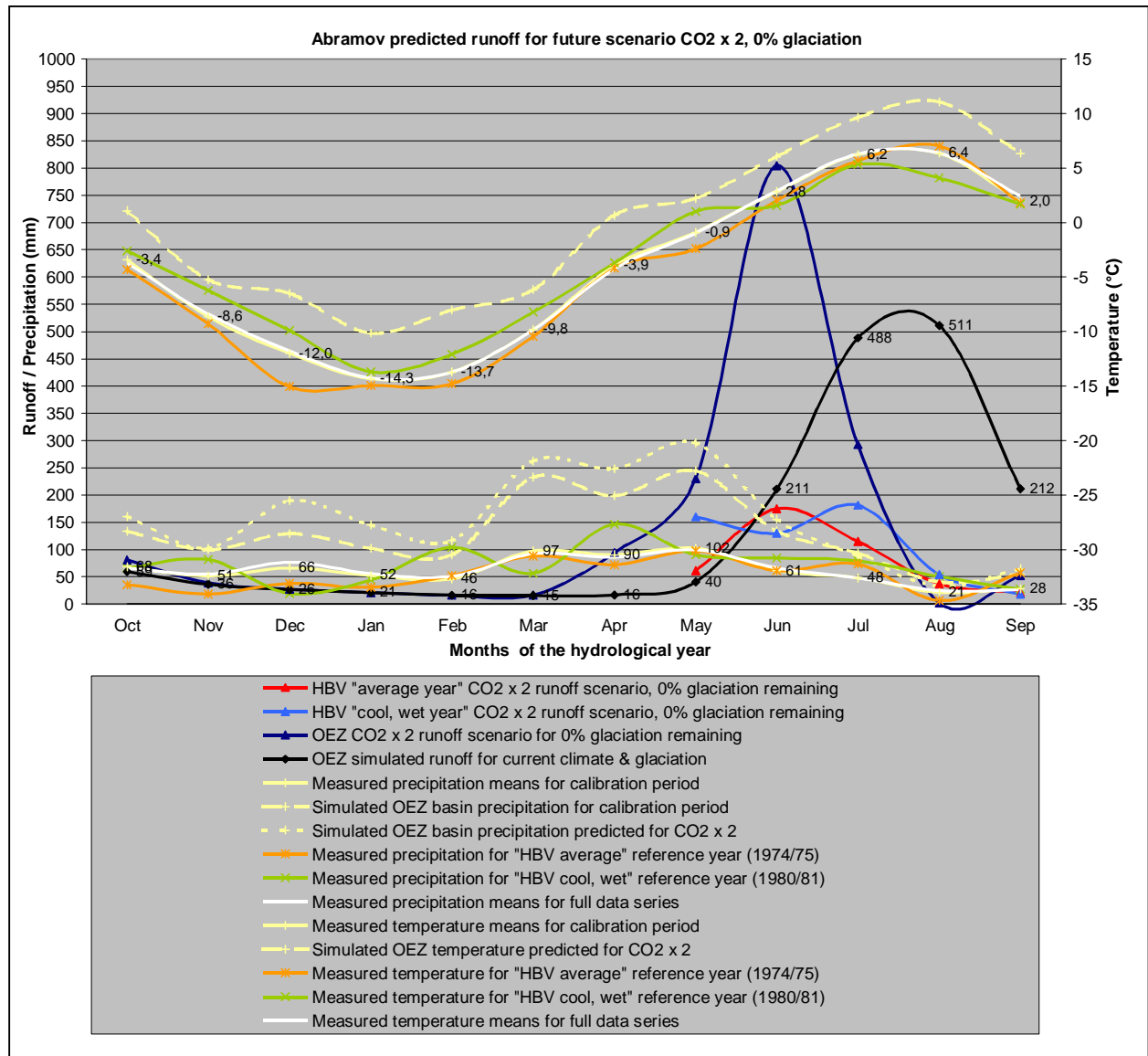


Table G6 Abramov: Data displayed by Fig F5

	Oct	Nov	Dec	Jan	Feb	Mar	Apr	May	Jun	Jul	Aug	Sep	Oct - Apr	May - Sep	Jul - Aug	Year
OEZ simulated current runoff	59	36	26	21	16	15	16	41	203	484	511	224	189	1463	995	1653
OEZ CO ₂ x 2 runoff scenario	81	38	27	21	16	16	94	230	805	292	1	52	294	1381	294	1675
HBV "hot year" CO ₂ x 2 runoff scenario								61	175	115	37	21		408	151	
HBV "cool year" CO ₂ x 2 runoff scenario								160	129	181	54	18		542	235	
P meas: mean total data series	66	54	76	55	50	92	86	100	66	48	24	26	480	263	72	744
P meas: calibration period mean	68	51	66	52	46	97	90	102	61	48	21	28	471	260	69	730
P sim: OEZ P-basin for calibration period	133	99	129	102	90	232	198	244	134	93	40	55	984	567	134	1551
P sim: OEZ P-basin predicted for CO ₂ x 2	160	102	190	145	116	262	248	296	155	88	33	64	1223	636	121	1859
P meas: HBV average ref year (1974/75)	35	18	38	30	52	88	72	97	61	73	6	57	333	294	79	627
P meas: HBV cool ref year (1980/81)	66	81	19	44	104	56	146	90	84	79	50	27	516	330	129	846
T meas: mean total data series	-3,7	-8,4	-11,8	-14,3	-13,7	-9,8	-4,3	-1,0	2,9	6,3	6,4	2,4	-9,4	3,4	6,3	-4,1
T meas: calibration period mean	-3,4	-8,6	-12,0	-14,3	-13,7	-9,8	-3,9	-0,9	2,8	6,2	6,4	2,0	-9,4	3,3	6,3	-4,1
T sim: OEZ predicted for CO ₂ x 2	1,1	-5,2	-6,5	-10,1	-8,0	-6,2	0,7	2,2	6,0	9,6	11,1	6,4	-4,9	7,1	10,4	0,1
T meas: HBV hot ref year (1974/75)	-4,3	-9,3	-15,1	-15,0	-14,8	-10,4	-4,2	-2,4	2,1	5,7	7,0	1,8	-10,4	2,8	6,4	-4,9
T meas: HBV cool ref year (1980/81)	-2,6	-6,2	-9,9	-13,7	-12,1	-8,2	-3,7	1,0	1,5	5,3	4,1	1,7	-8,1	2,7	4,7	-3,6

P = Precipitation
T = Temperature
Meas = Measured
Sim = Simulated

Declaration of Originality

I declare that this thesis is my own work and that, to the best of my knowledge, it contains no material previously published, or substantially overlapping with material submitted for the award of any other degree at any institution, except where due acknowledgement is made in the text.

Thomas Nesgaard